National Library of Canada
Bibliothèque nationale du Canada

Canadian Theses Service
Services des thèses canadiennes

Ottawa, Canada
K1A 0N4

CANADIAN THESES

THÈSES CANADIENNES

NOTICE

The quality of this microfiche is heavily dependent upon the quality of the original thesis submitted for microfilming. Every effort has been made to ensure the highest quality of reproduction possible.

If pages are missing, contact the university which granted the degree.

Some pages may have indistinct print especially if the original pages were typed with a poor typewriter ribbon or if the university sent us an inferior photocopy.

Previously copyrighted materials (journal articles, published tests, etc.) are not filmed.

Reproduction in full or in part of this film is governed by the Canadian Copyright Act, R.S.C. 1970, c. C-30. Please read the authorization forms which accompany this thesis.

AVIS

La qualité de cette microfiche dépend grandement de la qualité de la thèse soumise au microfilmage. Nous avons tout fait pour assurer une qualité supérieure de reproduction.

S'il manque des pages, veuillez communiquer avec l'université qui a conféré le grade.

La qualité d'impression de certaines pages peut laisser à désirer, surtout si les pages originales ont été dactylographiées à l'aide d'un ruban usé ou si l'université nous a fait parvenir une photocopie de qualité inférieure.

Les documents qui font déjà l'objet d'un droit d'auteur (articles de revue, examens publiés, etc.) ne sont pas microfilmés.

La reproduction, même partielle, de ce microfilm est soumise à la Loi canadienne sur le droit d'auteur, SRC 1970, c. C-30. Veuillez prendre connaissance des formules d'autorisation qui accompagnent cette thèse.

THIS DISSERTATION
HAS BEEN MICROFILMED
EXACTLY AS RECEIVED

LA THÈSE A ÉTÉ
MICROFILMÉE TELLE QUE
NOUS L'AVONS REÇUE

NL 339 (r. 86/01)

Canada

National Library of Canada
Canadian Theses Division
Ottawa, Canada
K1A 0N4

Bibliothèque nationale du Canada
Division des thèses canadiennes

0-315-24807-6

PERMISSION TO MICROFILM — AUTORISATION DE MICROFILMER

• Please print or type — Écrire en lettres moulées ou dactylographier

Full Name of Author — Nom complet de l'auteur

MING-CHUN CHAU

Date of Birth — Date de naissance

AUGUST 20, 1955

Country of Birth — Lieu de naissance

HONG KONG

Permanent Address — Résidence fixe

606, GLADIOLUS HOUSE, SO UK ESTATE, KOWLOON, HONG KONG

Title of Thesis — Titre de la thèse

Microprocessor-Controlled ANN System for De-embedding FET Parameters

University — Université

UNIVERSITY OF ALBERTA

Degree for which thesis was presented — Grade pour lequel cette thèse fut présentée

MASTER OF SCIENCE

Year this degree conferred — Année d'obtention de ce grade

1984

Name of Supervisor — Nom du directeur de thèse

W. R. Tinga
J. F. Vanderkooi

Permission is hereby granted to the NATIONAL LIBRARY OF CANADA to microfilm this thesis and to lend or sell copies of the film.

The author reserves other publication rights, and neither the thesis nor extensive extracts from it may be printed or otherwise reproduced without the author's written permission.

L'autorisation est, par la présente, accordée à la BIBLIOTHÈQUE NATIONALE DU CANADA de microfilmer cette thèse et de prêter ou de vendre des exemplaires du film.

L'auteur se réserve les autres droits de publication; ni la thèse ni de longs extraits de celle-ci ne doivent être imprimés ou autrement reproduits sans l'autorisation écrite de l'auteur.

Date

Oct. 3rd, 84

Signature

Ming-Chun Chau

NL-91 (4/77)

THE UNIVERSITY OF ALBERTA

Microprocessor-Controlled ANA System for De-Embedding FET Parameters

by

Ming-Chun Chau

(C)

A THESIS

SUBMITTED TO THE FACULTY OF GRADUATE STUDIES AND RESEARCH

IN PARTIAL FULFILMENT OF THE REQUIREMENTS FOR THE DEGREE

OF Master of Science

Department of Electrical Engineering

EDMONTON, ALBERTA

Fall 1984

THE UNIVERSITY OF ALBERTA

RELEASE FORM

NAME OF AUTHOR Ming-Chun Chau

TITLE OF THESIS Microprocessor-Controlled ANA System for De-Embedding FET Parameters

DEGREE FOR WHICH THESIS WAS PRESENTED Master of Science

YEAR THIS DEGREE GRANTED Fall 1984

Permission is hereby granted to THE UNIVERSITY OF ALBERTA LIBRARY to reproduce single copies of this thesis and to lend or sell such copies for private, scholarly or scientific research purposes only.

The author reserves other publication rights, and neither the thesis nor extensive extracts from it may be printed or otherwise reproduced without the author's written permission.

(SIGNED) Chan Ming Chun

PERMANENT ADDRESS:

606, GLADIOLUS HOUSE,
SO UK ESTATE, KOWLOON,
HONG KONG

DATED Oct. 3rd 1984

THE UNIVERSITY OF ALBERTA

FACULTY OF GRADUATE STUDIES AND RESEARCH

The undersigned certify that they have read, and recommend to the Faculty of Graduate Studies and Research, for acceptance, a thesis entitled Microprocessor-Controlled ANA System for De-Embedding FET Parameters submitted by Ming-Chun Chau in partial fulfilment of the requirements for the degree of Master of science.

.....

Co-Supervisor

.....

Co-Supervisor

.....

.....

Date.....

ABSTRACT

An HP8410A conventional network analyser was modified and converted into an Automatic Network Analyser (ANA) with an external HP-85 desktop computer as the controller. The HP-85 computer, in co-operating with the custom-designed Microprocessor-Controlled Data Acquisition System (MCDAS), is able to remotely control all the instruments of the modified network analyser system. A self-prompting measurement system program was developed for measurement sequence automation, data acquisition, error correction and Field-Effect-Transistor (FET) parameters characterization. The automatic control of the simplified measurement procedure has made the S-parameter measurement much easier and ten times faster than the measurement using the conventional point-to-point technique. Furthermore, the developed software using the 12-term error model is able to correct all the internal systematic errors and hence give the best measurement accuracy. The performance of the developed ANA was verified by measuring a few standard devices such as a direct short, an offset short, an HP 30 dB attenuator and a through-connection cable.

The developed ANA was used to characterize FET parameters with the FET embedded in an HP11608A test fixture. The FET parameters were obtained by subtracting the effects of the test fixture from the measured parameters. Thus, the equivalent circuit model of the HP test fixture

was first found with the help of a computer network analysis program named COMPACT. The de-embedding technique used for extracting the FET parameters from the modelled test fixture was based on the signal flowgraph so that the previously written error correction program could also be used for de-embedding purposes. As a result, the de-embedding program has become very simple. Finally, the performance of the developed ANA in characterizing FET parameters using the developed de-embedding software was verified by comparing the measured S-parameters of three commercial FETs with the typical S-parameters given by the manufacturers.

With the success of this project, the modified conventional network analyser has become a very useful system in the laboratory. Thus a designer is now able to characterize any two-port network or FET device by its S-parameters, which is an important factor for the successful design of any advanced microwave circuits.

ACKNOWLEDGEMENT

The author wishes to express his sincere thanks to his supervisor Dr. W. R. Tinga and Dr. J. F. Vaneldik for their interest, financial support, advice and encouragement throughout the project. The author is also thankful to Dr. D. Routledge and Dr. E. Karpinski for serving on the examining committee.

The author owes a special thanks to Dr. G. Walker for his help, advice and contribution in developing the hardware of the interface system and in modifying the conventional network analyser. To Mr. M. Locker, the author is thankful for his help in many ways in the laboratory. Thanks must also be given to the Department of Electrical Engineering for the financial support.

The author wishes to express thanks to his fiancee K. Y. Chui for her help in preparing most of the diagrams in this manuscript. The author is also grateful to Y. Ung for his time to proof read this manuscript.

The author sincerely thanks his parents, teachers and all those whose direct and indirect interaction with him has resulted in the research work reported in this thesis. The author is also thankful to all the prayer support from the members of the E.C.C. Fellowship. Finally, the author wishes to express thanks to GOD for His strength and His wisdom.

Table of Contents

Chapter		Page
1.	INTRODUCTION	1
	1.1 Historical Background of the Automatic Network Analyser	1
	1.2 The Objectives and Merits of the Modified ANA	4
	1.3 The Content of the Thesis	6
2.	DESCRIPTION OF THE MICROPROCESSOR-CONTROLLED ANA SYSTEM	8
	2.1 Description Of the Microprocessor-Controlled Data Acquisition System (MCDAS) Hardware Design	10
	2.2 Modification of the Network Analyser System	30
	2.3 Operation of the ANA System	35
3.	ERROR CORRECTION MODEL FOR TWO-PORT MEASUREMENT	38
	3.1 Introduction	38
	3.2 Sources of Measurement Errors	40
	3.3 System Error Model	42
	3.4 Calibration Techniques	47
	3.5 Derivation of Error Equations	52
	3.6 Error Correction Methods	59
4.	THE ANA SYSTEM SOFTWARE FOR S-PARAMETER MEASUREMENT	60
	4.1 Structure of the Measurement System Program	61
	4.2 Software Techniques For Improving Measurement Accuracy	71
	4.3 Other Errors Affecting the Measurement Accuracy	77
	4.4 Performance and Measurement Accuracy of the ANA System	79
5.	CHARACTERIZATION OF LOW-NOISE FET PARAMETERS	86
	5.1 Methods for Characterization of FET Parameters	87
	5.2 Fixture Modelling	91

5.2.1 Network Topology For Modelling the Test Fixture 91

5.2.2 Calculation of the Initial Values of Elements 93

5.2.3 Actual Model of the Test Fixture 98

5.3 De-Embedding Techniques 100

5.4 Experimental Results 103

6. SUMMARY AND CONCLUSIONS 110

6.1 Summary and Conclusions 110

6.2 Recommendations for Further Research 112

REFERENCES 114

APPENDIX I-A The Schematic Diagram of the Digital Attenuator 120

APPENDIX I-B The Modifications of the Connection Inside the Mainframe of the Netwrok Analyser 121

APPENDIX II S-parameter Measurement Instruction Manual ..122

APPENDIX III Explicit Solution for 12-Term Error Model ..129

APPENDIX IV The Flow Chart of the Developed ANA System Program for S-parameter Measurement 134

APPENDIX V An Efficient Circle Fitting Method 138

List of Tables

Tables	Description	page
2.1	List of the External I/O Decoded Addresses From the On-board Decoder of the K-8073 With the Corresponding Peripheral Devices.	15
4.1	The Reflection Measurement Errors of a Direct Short Device at 1-2 GHz and 8-12 GHz.	80
4.2	The Reflection Measurement Errors of an Offset Short Device at 1-2 GHz and 8-12 GHz.	80
4.3	The Transmission Measurement Errors of a Through-Line Connector at 1-2 GHz and 8-12 GHz.	82
4.4	The Measurement Errors of an HP 30 dB Attenuator at 1-2 GHz and 8-12 GHz.	82
5.1	The Insertion Loss Per Unit Length of the Input and Output Lines of the Test Fixture, as a Function of Frequency.	96
5.2	The Launcher Equivalent Circuit Parameters For Various Substrates at 10 GHz.	97
5.3	Final Modelled Values of Elements in the Overall Fixture Model Network.	101
5.4	The Measurement Results of a Through-Connection Insert After De-embedding From an HP Test Fixture.	104
5.5	The Measurement Results and the Given Typical S-Parameters of an AT-8110 FET.	106
5.6	The Measurement Results and the Given Typical S-Parameters of a NE-218 FET.	108
5.7	The Measurement Results and the Given Typical S-Parameters of a MGF-1412 FET.	109

List of Figures

Figure		page
1.1	Two-port Network Showing Incident (a_1, a_2) and Reflected (b_1, b_2) Waves used in S-parameter Definition.	2
2.1	Block Diagram of the Automatic Network Analyser (ANA) System.	9
2.2	Description of the MCDAS Front Panel a)Locations of all the LED Indicators, the A/D and D/A Channels. b)Circuit Diagram of the LED Indicators.	11
2.3	Wiring Diagram of the Standard (STD) Bus Connectors at the Back Plane of the Card Cage.	13
2.4	The Physical System Package of the Microprocessor-Controlled Data Acquisition System (MCDAS).	14
2.5a	Wiring Diagram of the Interconnections of the I/O Ports of the 8255 PPI With the Network Analyser, the Test Set and the Polar Display.	17
2.5b	Description of the Pin Functions of the 8255 PPI, the 36 Pin and 14 Pin Connectors.	18
2.6	The Schematic Diagram of the GPIO-STD Module.	21
2.7	The Schematic Diagram of the 12-bit A/D Module.	22
2.8	The Schematic Diagram of the 14-bit D/A Module.	25
2.9	The Schematic Diagram of the 8-bit D/A Module.	28
2.10	The Circuit Diagram of the HP8620A Sweeper Modification.	31
2.11	The Diagram of the Modification of the HP8410A Network Analyser.	32

2.12 The Circuit Diagram of the Added TTL-driver Between the Digital Input and the Relay Switch of the HP8414A Polar Display Unit. 34

3.1 Signal Flowgraph Showing the Directivity Error. 42

3.2 Signal Flowgraph Showing the Source Match Error. 43

3.3 Signal Flowgraph Showing the Frequency Tracking Error. 43

3.4 Signal Flowgraph Showing the Directivity Error Source Match Error, Frequency Tracking Error of a Two-port Error Model. 44

3.5 Signal Flowgraph Showing the Load Match Error. 45

3.6 Signal Flowgraph Showing the Isolation Error. 46

3.7 Signal Flowgraph of a 12-term Transmission and Reflection Error Model. 47

4.1 Block Diagram Outline of the Measurement System Program. 61

4.2 The Variation of the Horizontal and Vertical D.C. Offset Voltages With Time. 68

4.3 S_{11} Measurement Results Using Different Modelled Fringing Capacitance of an Open-Circuit Calibrator at 1-2 GHz. 75

4.4 S_{11} Measurement Results Using Different Modelled Fringing Capacitance of an Open-Circuit Calibrator at 8-12 GHz. 75

4.5 S_{21} Measurement Error of a Through-Line Connector at 1-2 GHz. 83

4.6 S_{21} Measurement Error of a Through-Line Connector at 8-12 GHz. 83

4.7 Simplified Smith Chart Plotted With Corrected Measured S_{21}, Uncorrected Measured S_{21} and Calculated S_{21} of a Through-Line Connector at 1-2 GHz. 84

4.8 Simplified Smith Chart Plotted With Corrected Measured S_{21}, Uncorrected Measured S_{21} and Calculated S_{21} of a Through-Line Connector at 8-12 GHz. 84

5.1 Network Model of a Device Embedded in a Test Fixture. 86

5.2 The Signal Flowgraph of a Device Embedded in a Test Fixture. 90

5.3 Network Topology For Modelling the Test Fixture
a)With a Short Circuit Calibrator Inserted.
b)With a Through-Line Calibrator Inserted. 92

5.4 Equivalent Circuit of the Input Connector With a Through-Line Calibrator Inserted in the HP Test Fixture. 95

List of Abbreviations

Abbreviations	Description
ANA	Automatic Network Analyser
FET	Field-Effect Transistor
HP	Hewlett Packard
MCDAS	Microprocessor-Controlled Data Acquisition System
RF	Radio Frequency
GPIO	General Purpose Input Output
LED	Light-Emitter-Diode
EPROM	Electrically Programmable Read-Only-Memory
V	Voltage
STD	Standard
RAM	Random-Access-Memory
A/D	Analog-to-Digital
D/A	Digital-to-Analog
EEPROM	Electrically Erasable Programmable Read-Only-Memory
I/O	Input/Output
PPI	Programmable Peripheral Interface
I.F.	Intermediate Frequency
HP-IB	Hewlett Packard Interface Bus
AIS	Analog Input Section
ADC	Analog-Digital Converter
VSWR	Voltage Standing Wave Ratio
GHz	Gigahertz

KHz	Kilohertz
APU	Arithmetic Processor Unit
RLC	Resistor-Inductor-Capacitor
CRT	Cathode-Ray-Tube
DUT	Device Under Test
BASIC	Beginners All-purpose Symbolic Instruction Code
TTL	Transistor-Transistor-Logic

1. INTRODUCTION

1.1 Historical Background of the Automatic Network Analyser

One of the most important trends in microwave technology today is the increasing sophistication and accuracy in advanced circuit design. Due to this trend, it is necessary to completely and accurately characterize components and network devices at microwave frequencies. In order for the measuring system to accomplish this, it must have the capability to make precise measurements rapidly, require minimal operating skill, and be able to display measured parameters in their most descriptive form.

By far the most useful and conveniently measured set of two-port parameters for any network are the scatterring parameters (S-parameters). The S-parameters of a two-port network as shown in Figure 1.1 are defined analytically by:

$$b_1 = S_{11}a_1 + S_{12}a_2 \qquad (1.1)$$

$$b_2 = S_{21}a_1 + S_{22}a_2 \qquad (1.2)$$

where

a_1 = normalized complex voltage wave incident on port 1

b_1 = normalized complex voltage wave reflected from port 1

a_2 = normalized complex voltage wave incident on port 2

b_2 = normalized complex voltage wave reflected from port 2

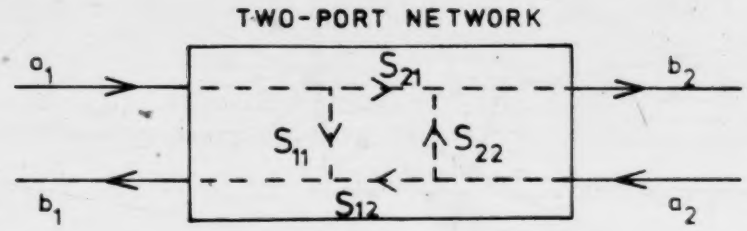

Figure 1.1 Two-port Network Showing Incident (a_1,a_2) and Reflected (b_1,b_2) Waves Used in S-parameter Definition.

Scattering parameters are being used more and more in microwave design because they are easier to measure and work with at higher frequencies than other kinds of parameters. As dimensionless expressions of gain and reflection, S-parameters are conceptually simple, analytically convenient, and capable of giving a clear and meaningful physical interpretation of the network performance. Anderson [1], Weinert [2], and Fredricks [3] give good discussions on how to use S-parameter techniques for faster and more accurate microwave network design.

A Microwave Network Analyser is a swept or stepped frequency instrument that measures all four S-parameters of any active or passive device. This analyser has been

commercially available since 1967, but it was limited to some extent by mismatch, tracking, isolation, and directivity errors which gave an overall accuracy of about ±10 %. This led to the introduction of the concept of error modelling and error correction by using the computer as an integral part of the measurement system. The internal systematic errors were first measured at each frequency by connecting various standard calibrators to the equipment under the guidance of a computer program. Then, the computer corrected errors in the raw measured data of a device under test and printed out the result. More details in describing how an HP network analyser was connected to a minicomputer to achieve error correction were provided by Hackborn [4] and Adam [5].

Since the first commercial Automatic Network Analyser (ANA) system was introduced in the early seventies, the hardware of the ANA system and software program for error correction has been undergoing constant development. The hardware, such as the test set, sweeper and controller has been improved and upgraded. The 12-term error model accuracy enhancement program [6-7], was able to provide full directivity, source match, load match and frequency tracking vector error correction for transmission and reflection measurement of two-port devices and hence gave the best magnitude and phase measurement accuracy.

As a result of the improvement in speed and accuracy, the ANA system has become an important tool for the

characterizaton of any component or network device. In the past fifteen years, the ANA system has completely revolutionized the microwave measurement field as shown by the fact that most manufacturers of high-frequency transistors and solid-state devices have specified their products in terms of S-parameters measured in this way. During this time, many papers have been written on the subject of the Automatic Network Analysers and most of these papers are found in the bibliographies of three excellent references written by Adam [8], Beatty [9] and Warner [10].

1.2 The Objectives and Merits of the Modified ANA

The main objective of this project is to convert a conventional network analyser into an Automatic Network Analyser. It is necessary to have an Automatic Network Analyser measurement system in the microwave research laboratory to characterize any component or network device accurately in order to design advanced circuits at microwave frequencies. Two complete ANA systems ready for hook-up and immediate use, the HP4809B/C by Hewlett Packard' were offered on the market in the price range of $60,000 to $151,000 in 1980-1981, but they are too expensive for most university laboratories. In addition to the high cost, the disadvantage of purchasing a new system is that it would make an existing conventional manual-control network analyser system in the laboratory redundant. Therefore, to

---

' HP 4809B/C will be replaced by a new ANA system - HP8510 in late 1984 with a price of $250,000.

fully ultilize the existing hardware, this project involved designing a microprocessor ANA interface system, modifying the manual-control network analyser system to operate under remote control and developing a software program for both data acquisition and error correction. The total cost for completing this project was approximately $3,000[2] which is less than one twentieth of the cost of the cheapest version of a commercial ANA system. Though the accuracy and speed of the developed ANA system are not as great as that of the commercial ANA system which employs a more powerful desktop computer and a phase-locked subsystem[3], they are much improved as compared with the conventional system. The automatic control of the simplified measurement procedure has made the measurement using an ANA system much easier and ten times faster than the measurement using the conventional point-by-point technique. The developed software using the 12-term error model is able to correct all the internal systematic errors and hence good measurement accuracy can be achieved.

The other important objective of this project was to develop the de-embedding software in addition to the ANA system program for accurately characterizing low-noise Field-Effect-Transistor (FET) parameters which are important for the development of low-noise amplifiers at microwave

---

[2] This figure does not include the cost of an HP-85 desktop computer, an HP82901M disc drive, an HP7470A printer, the conventional HP8410A network analyser and an EIP575 frequency counter.

[3] The phase-locked subsystem provides accurate frequencies with excellent repeatability.

frequencies. In characterizing the FET parameters, the FET is usually mounted in a microstrip test fixture. Therefore, the S-parameters of the FET must be de-embedded by modelling the test fixture and subtracting the effects of the modelled test fixture from the measured parameters. The de-embedding technique used in this project is based on the signal flowgraph so that the de-embedding software can be simplified by making use of the previously written error correction subprogram for extracting the FET parameters from the modelled test fixture.

1.3 The Content of the Thesis

The conversion of a conventional network analyser into an Automatic Network Analyser and the application of the modified ANA in characterizing FET parameters are described in this thesis. In chapter two, the design of all the interface modules in the microprocessor ANA interface system, the modifications of an old but still useful network analyser into a computer-controlled network analyser and the interconnections and operation of the instruments in the developed ANA system are described so that this ANA system can be reproduced in other laboratories. In chapter three, all the errors inherent in the measuring system and the procedure for deriving the 12-term error model including the error and S-parameter correction equations are discussed. The software design of this project is described in chapter four. This includes the structure of a program for data

acquisition and 12-term model error correction, some techniques used for improving accuracy and the development of the simplified ANA calibration procedure which make the measurement much easier and more accurate. In order to test the system's performance and accuracy, a few standard test devices were measured with the results presented in this thesis. After the ANA system had been developed, it was used for characterizing FET parameters. The techniques for modelling an HP11608A test fixture and de-embedding the FET parameters from the modelled fixture are developed and presented in chapter five. Finally, in chapter six, the important conclusions of this research are summarized and some recommendations are made for further research.

2. DESCRIPTION OF THE MICROPROCESSOR-CONTROLLED ANA SYSTEM

INTRODUCTION

A general overview of the complete Automatic Network Analyser (ANA) system and the interconnections of all the instruments are shown in Figure 2.1. The hardware external to the network analyser consists of an interface system called Microprocessor-Controlled Data Acquisition System (MCDAS). The MCDAS with the external HP-85 as the controller is used to control all the measuring instruments of the network analyser system through the Input/Output peripheral interface, to acquire data from the A/D converter, to calculate and correct the internal systematic errors and to display the required results on the appropriate peripheral devices. The conventional network analyser system being converted into the ANA is composed of the following instruments: an HP8620A sweeper with various RF sections, an HP8746B test set, an HP8410A network analyser, an HP8411A harmonic frequency converter, an HP8414A polar display and an EIP575 source locking microwave counter (option[4]). Some of these instruments had to be modified so that they could be fully automatically controlled by the MCDAS. The total cost required for designing the MCDAS and modifying the network

---

[4] If the EIP575 source locking counter is used to set the desired RF frequency, accurate frequency and better repeatability can be achieved.

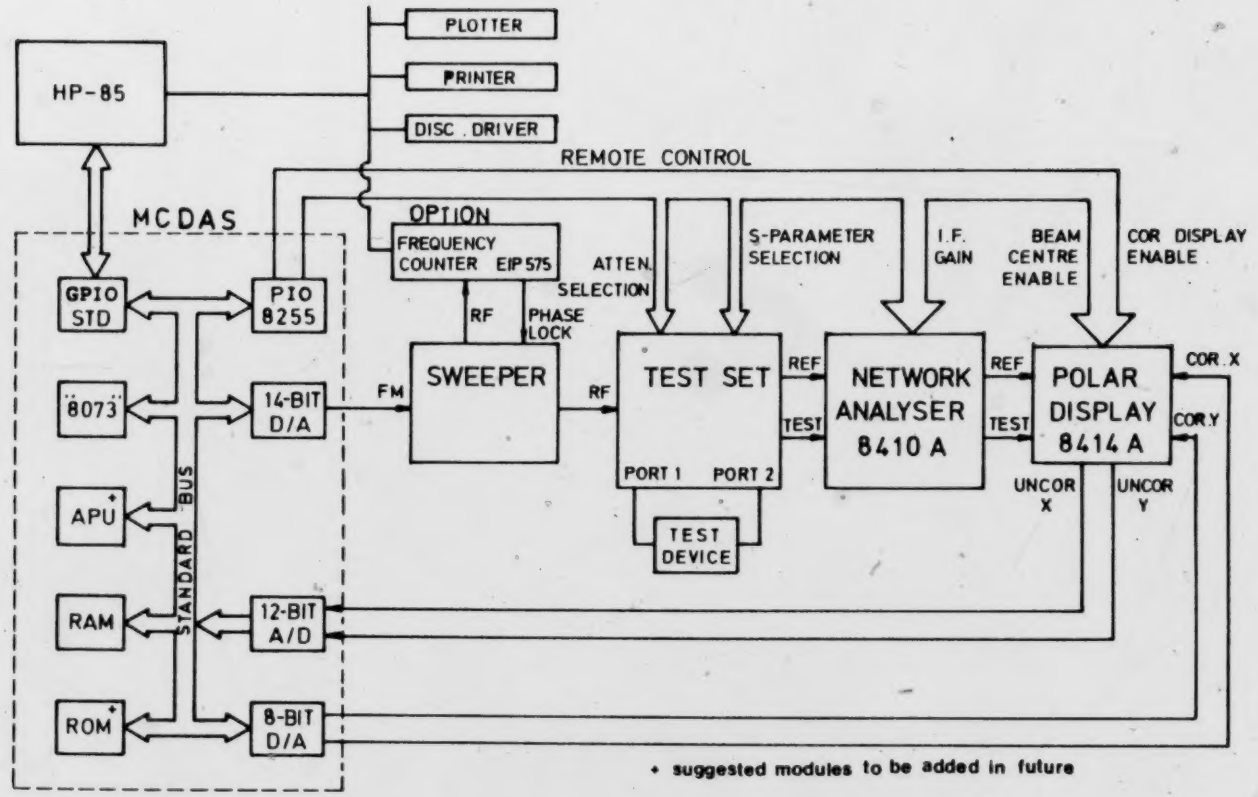

Figure 2.1 Block Diagram of the Automatic Network Analyser (ANA) System.

analyser is approximately $3,000 which is less than one twentieth of the cost of the cheapest version of the HP ANA system. Details of the hardware design of the MCDAS, the modifications of the network analyser system and the operation of the complete ANA system under remote control will be described in the following sections.

2.1 Description Of the Microprocessor-Controlled Data Acquisition System (MCDAS) Hardware Design

The MCDAS contains a power supply unit[5], a K-8073[6] single-board microcomputer[11], several interface modules, and the necessary interface connectors which are all housed in a cabinet of size 20" X 13" X 6.5". Mounted on the rear panel of the cabinet are the power supply unit, a 50 pin connector for connecting to the General Purpose Input Output (GPIO) interface module of an HP-85 desktop computer, a power ON/OFF switch and an input for an external EPROM 25 V programming supply. The front panel holds all the BNC connectors of the inputs and output of the A/D and D/A converters, a 36 pin connector for connecting the remote control cable and several light-emitting-diode (LED) indicators. The operator is able to determine from the LED indicators which controller (K-8073 or HP-85) and which interface is active. Details of the front panel and the diagram of the LED circuit are shown in Figure 2.2.

---

[5] Model HCAA-60W-A from POWER-ONE INC.
[6] The 8073 microprocessor is fully described in the manual from Transwave.

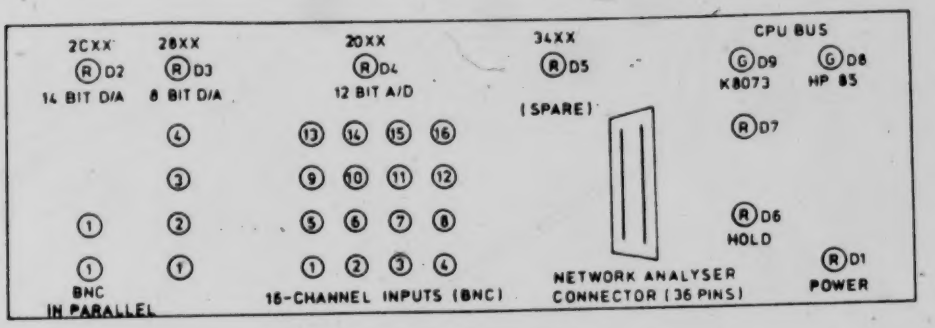

(a)

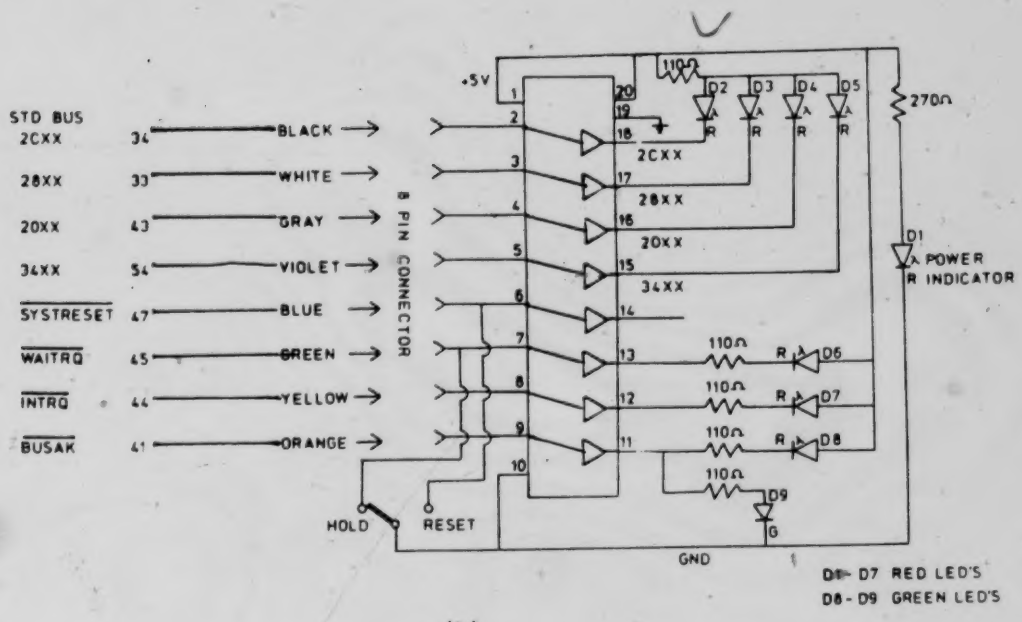

(b)

Figure 2.2 Description of the MCDAS Front Panel

a) Locations of all the LED Indicators, the A/D and D/A Channels.

b) Circuit Diagram of the LED Indicators.

Inside the cabinet, there is a 56 pin Standard (STD) Bus[7] card cage which accommodates up to a maximium of ten cards. At present, eight slots have been assigned to specific modules but only six of them have been built. These are: a K-8073 microcomputer board, a General Purpose Input Output to Standard Bus (GPIO-STD) interface module, a 12-bit A/D module, an 8-bit D/A module, a 14-bit D/A module and an expanded 16K RAM memory module. The MCDAS, with these six modules plugged in, together with an external HP-85 desktop computer, is more than sufficient to control the ANA system and give accurate measurement results. The other two suggested modules which will be added to the MCDAS in the future in order to further improve the speed and the performance of the MCDAS are an Arithmetic Processing Unit and an Electrically Erasable Programmable Read-Only-Memory (EEPROM).

Details of the wiring diagram of the Standard bus connectors at the back plane of the card and the physical location of the cards are shown in Figure 2.3 and Figure 2.4 respectively. The function of each module and the corresponding subroutines of the S-parameter measurement software program will be described subsequently.

a) The K-8073 Microcomputer Board

A Transwave K-8073 single-board microcomputer has complete control of the STD bus when there is no

---

[7] A detailed description of the pin functions are presented by Cummings [12].

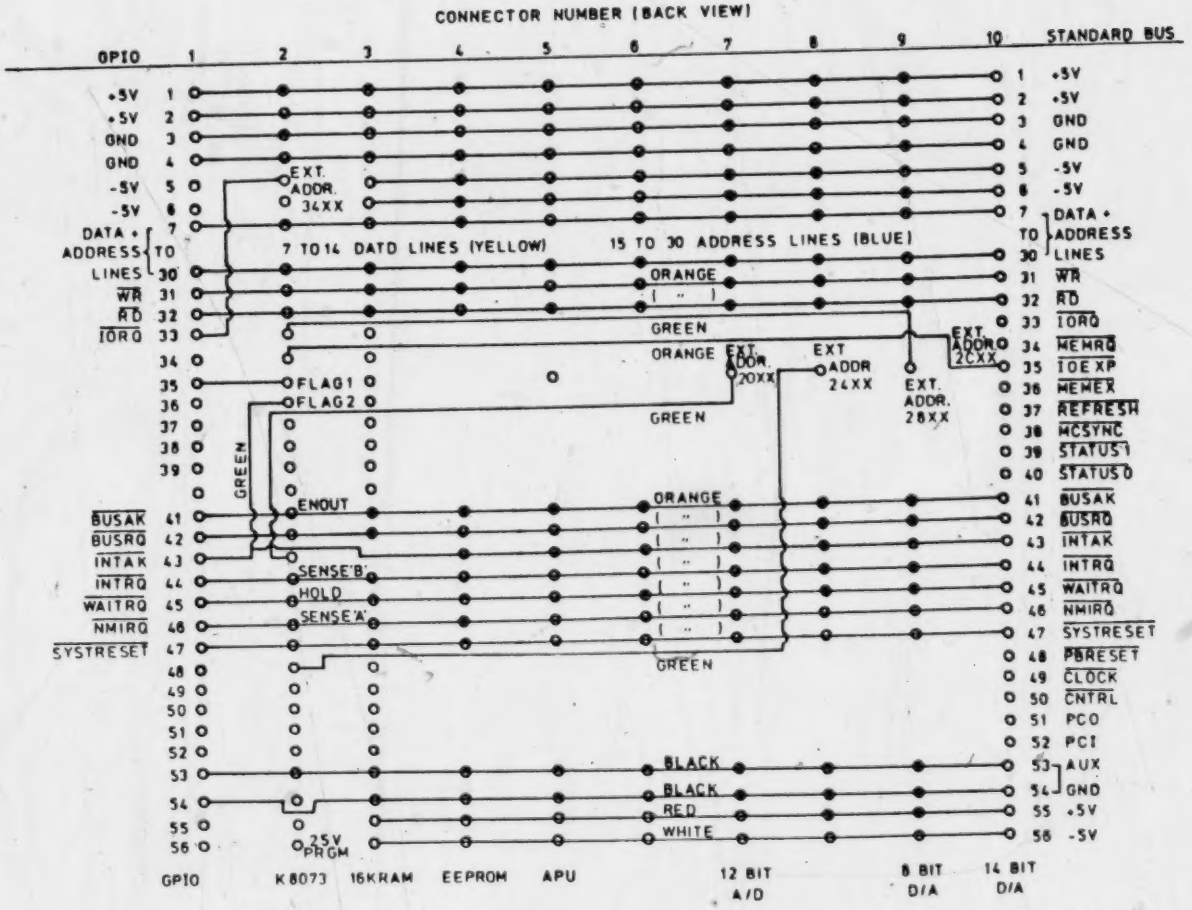

Figure 2.3 Wiring Diagram of the Standard (STD) Bus Connectors at the Back Plane of the Card Cage

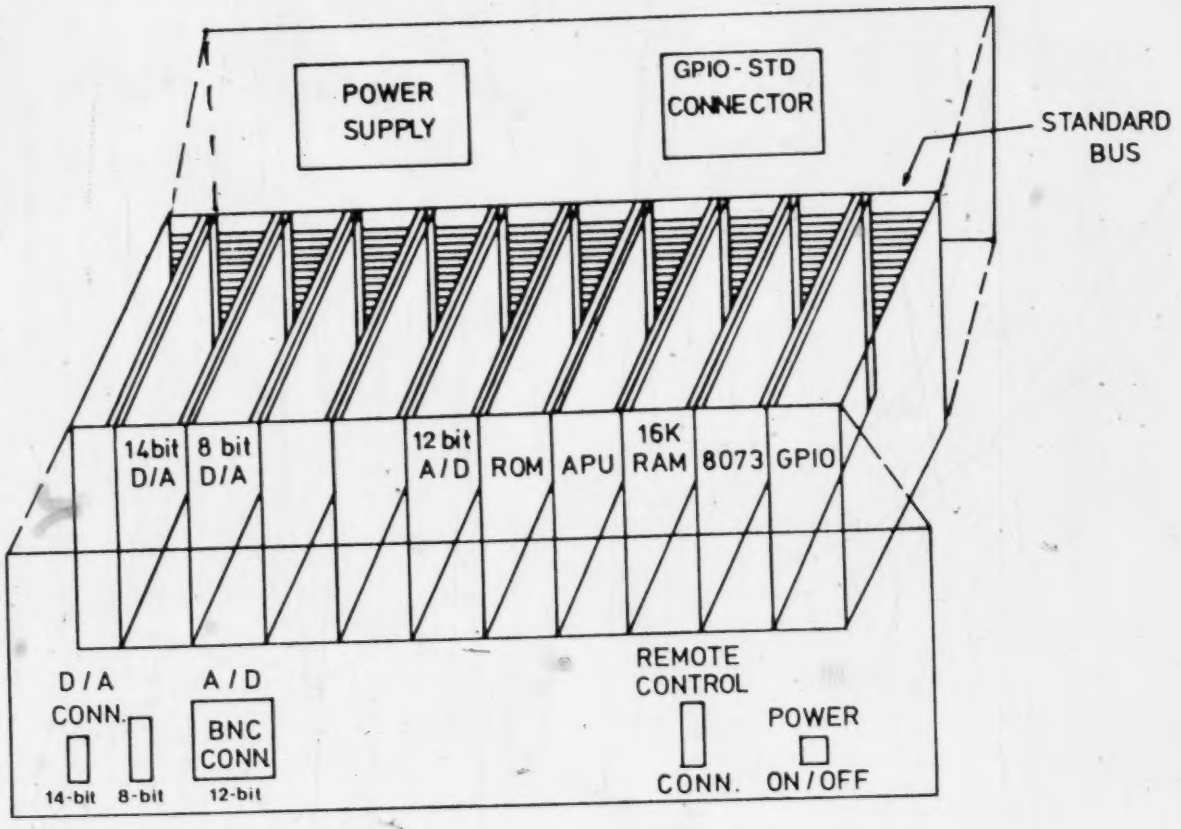

Figure 2.4 The Physical System Package of the Microprocessor-Controlled Data Acquisition System (MCDAS)

communication between the external HP-85 compatible desktop computer or any interrupt request from the peripheral device. It can be operated in a stand-alone mode by storing a program for a particular measurement in an on-board 8K EPROM. The program will be executed automatically on Power On or upon resetting of the MCDAS. The K-8073 is also able to access the external HP-85 computer for I/O operation through the GPIO-STD interface*.

The on-board 74LS138 decoder decodes external I/O addresses for enabling of the peripheral interfaces. The following table lists the peripheral interface devices with their corresponding decoded addresses.

Ext.Decoded Addresses	Slot No.	Peripheral Devices
# 2000	# 7	12-bit A/D
# 2400	# 8	spare
# 2800	# 9	8-bit D/A
# 2C00	# 10	14-bit D/A
# 3000	# 1	GPIO-STD
# 3400	# 5	spare
# 3800	NC	NC

Table 2.1 List of the External I/O Decoded Addresses From the On-board Decoder of the K-8073 With the Corresponding Peripheral Device

---

* This feature is presently not being used.

Furthermore, the on-board 8255 programmable peripheral interface (PPI) provides 24 bi-directional lines to interface with the user's system. For S-parameter measurement, the 8255 PPI is configured to be operated in the output mode (mode 0) and is used to control the I.F. gain of the network analyser, the beam centering enable, the corrected display enable of the polar display and the input attenuation and S-parameter switches of the test set. Figure 2.5a and Figure 2.5b show the wiring diagram of the interconnection of the I/O ports of the 8255 PPI with the network analyser, the test set and the polar display.

Although either a K-8073 single-board microcomputer or an HP-85 computer can be the controller of the MCDAS, the HP-85 has been chosen particularly in S-parameter measurement for three reasons. Firstly, the EIP575 source locking counter is employed in the network analyser system for controlling the RF frequency of the sweeper. If the HP-85 is the controller, it will be easy and direct for it to talk to the counter through the Hewlett Packard Interface Bus (HP-IB)* Secondly, the controller must be able to store or load the program for both data acquisition and error correction to and from a disc drive into the RAM for further modification. It is easier and more convenient for the HP-85 than for the K-8073 computer to do that. Thirdly, the RAM

---

* IEEE standard-488 Interface Bus = HP-IB

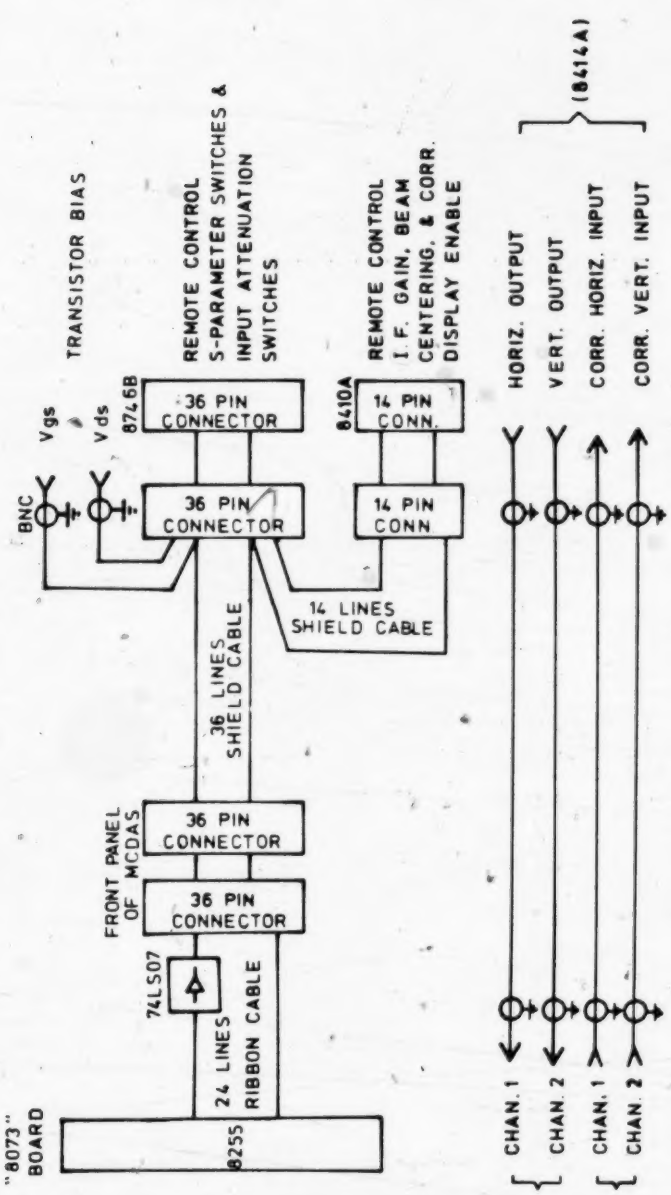

Figure 2.5a Wiring Diagram of the Interconnections of the I/O Ports of the 8255 PPI With the Network Analyser, the Test Set and the Polar Display.

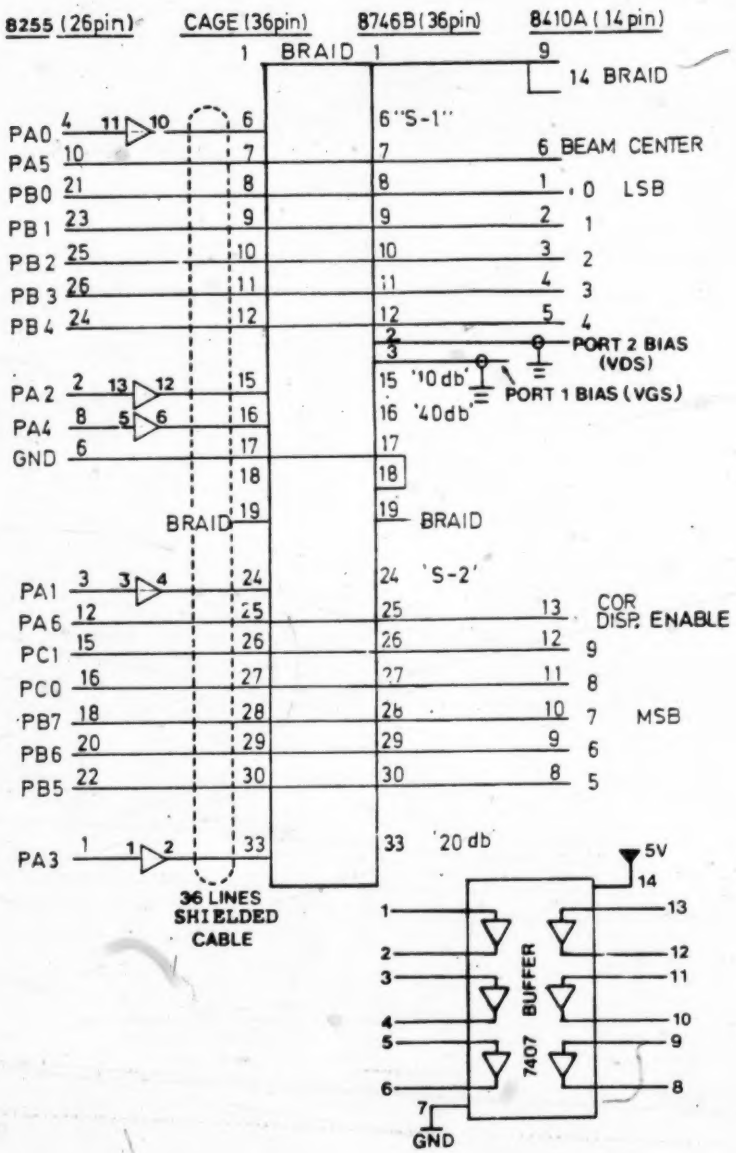

Figure 2.5b Description of Pin Functions of the 8255 PPI, the 36 Pin and 14 Pin Connectors.

and EPROM memory in the present MCDAS is not large enough to contain and execute the entire program'* for data acquisition and error correction.

The HP-85 takes control of the MCDAS's bus and all the I/O modules. It is also capable of monitoring and controlling the remote instruments through the 8255 PPI interface on the K-8073 board. Details of how the HP-85 requests control of the MCDAS bus will be described in the next section.

b) The GPIO-STD Interface Module

The General Purpose Input Output to Standard Bus (GPIO-STD) interface is designed to interface the Standard Bus of the MCDAS to the HP's General Purpose Input Output (HP-GPIO) interface so that the external HP-85 computer is able to communicate with the K-8073 microcomputer or vice versa. With the GPIO-STD interface module inserted in the MCDAS, the K-8073 microcomputer is able to have access to the HP-85 computer for I/O operation. In this way, the HP-85 acts as either a terminal or as an interface to HP-IB equipped instruments. The other way of communication is to let the HP-85 act as the controller of the MCDAS and to let it have direct access to I/O peripheral devices (such as the A/D or D/A converter) to the system memory on STD bus

---

'* The execution of the system program requires a 32K system memory of the computer.

and to the programmable peripheral interface on the K-8073 board. The schematic diagram of the module is shown in Figure 2.6.

The HP-85 requests the bus of the MCDAS by setting the control line CTL0 high while the Flip Flop latches the $\overline{\text{BUSRQ}}$ line low. The K-8073 releases the bus and sends the acknowledge signal by setting the $\overline{\text{BUSAK}}$ line low. These two lines are connected to the input of an OR gate which enables the buffers on the data and address lines. After the port B output has been enabled and the strobe-handshake mode has been selected, the HP-85 is then able to read from or write to the memory location specified by the 16-bit address from Port C and D of the HP-GPIO interface. The corresponding routine in the software program for the HP-85 to request the bus, to enable output from port B and to select the strobe-handshake mode is called " *INITIAL-S ".

c) The 12-bit A/D Module

The 12-bit A/D module was built to convert the analog voltage of the horizontal and vertical outputs of the polar display unit to digital inputs for the MCDAS. The module consists of an 8255 Programmable Peripheral Interface (PPI), interfacing the A/D to the Standard bus, and an AD363 12-bit A/D converter. The schematic diagram of the module is shown in Figure 2.7. The AD363 D/A is composed of an analog input section (AIS) incorporating a 16-channel multiplexer with a sample/hold and a 12-bit successive approximation

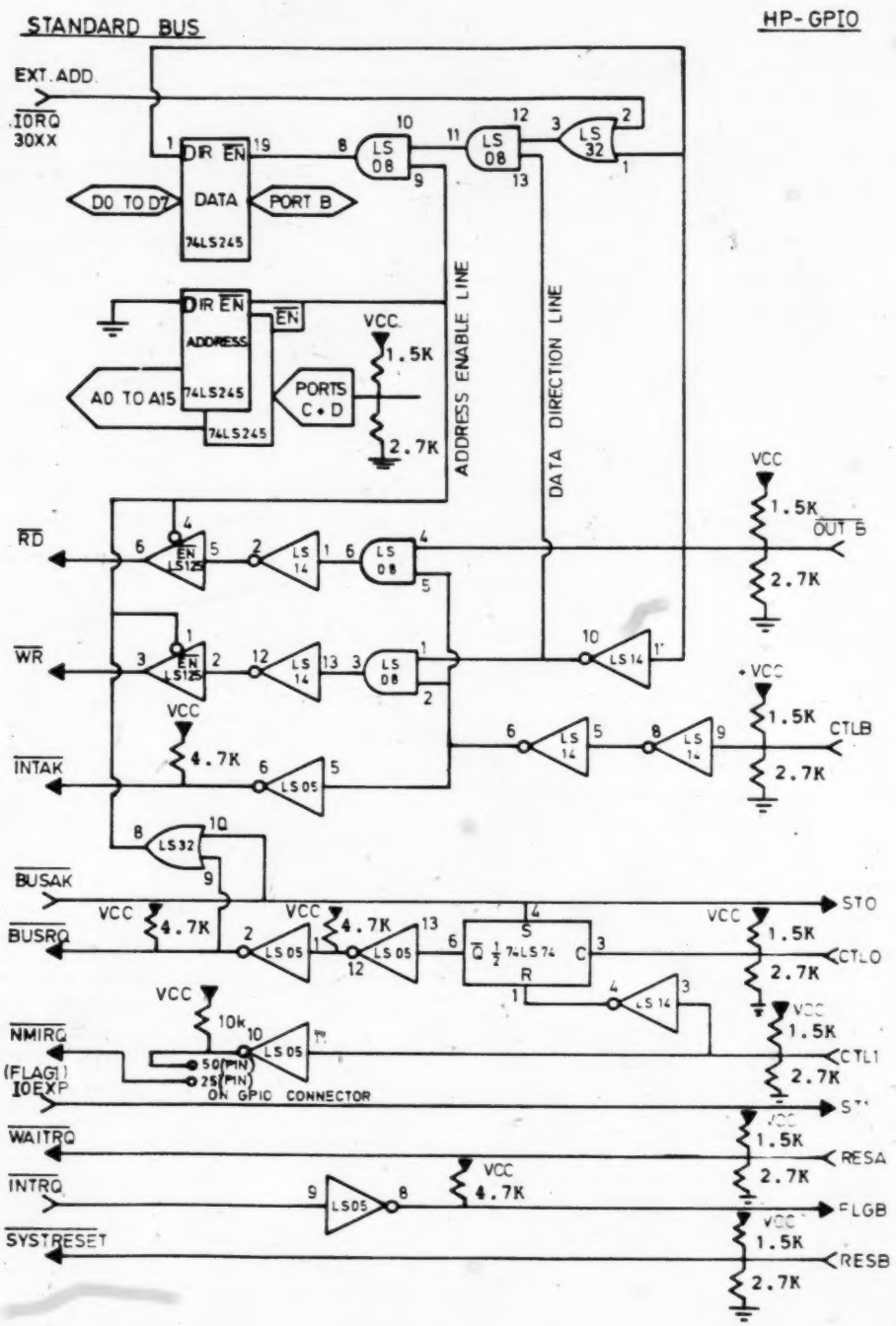

Figure 2.6 The Schematic Diagram of the GPIO-STD Module

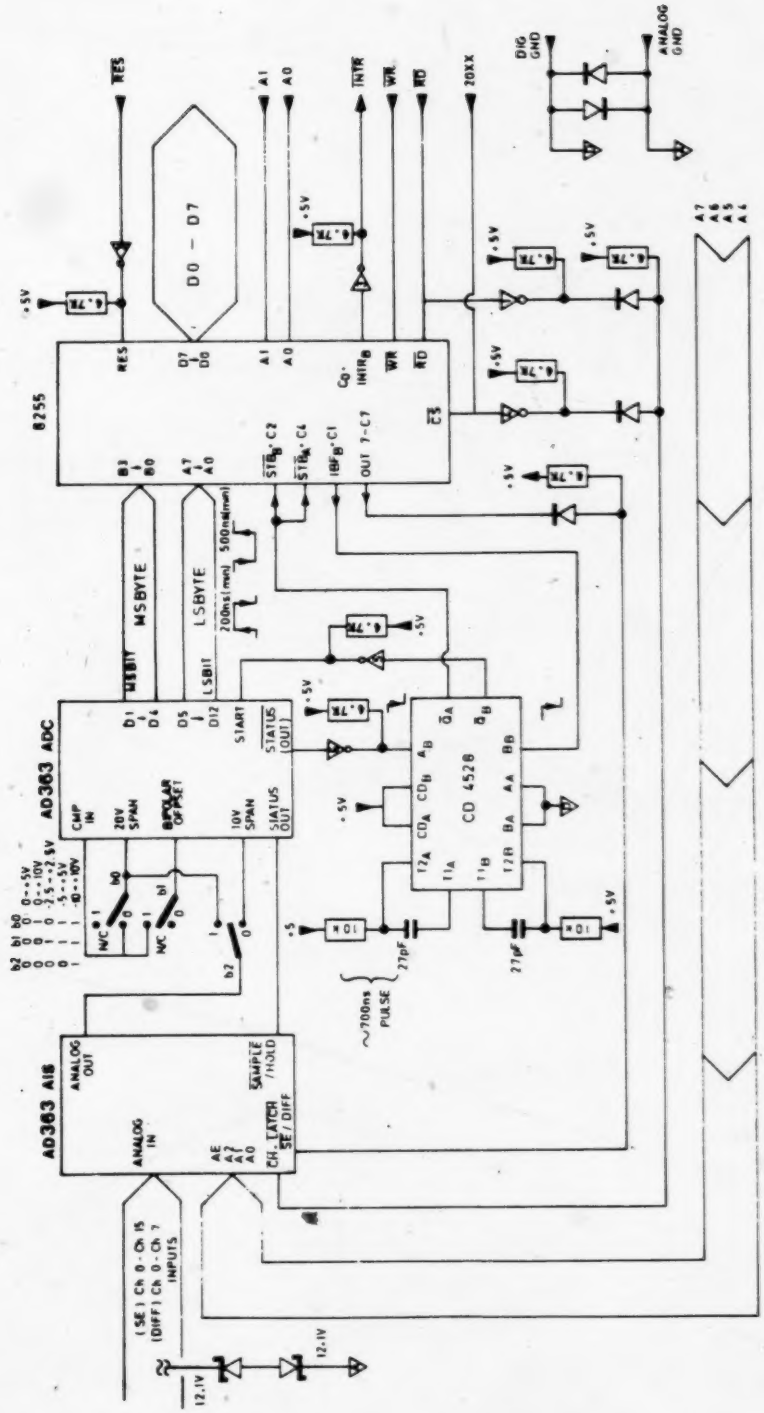

Figure 2.7 The Schematic Diagram of the 12-Bit A/D Module

analog-to-digital converter(ADC). The input voltage ranges available are: ±2.5 V, ±5 V, ±10 V, 0 to 5 V and 0 to 10 V selectable by a DIP switch. Inputs may be configured as 16 single-ended inputs or 8 differential inputs by resetting or setting of Bit 7 on Port C of the 8255 PPI. A read from address #20NX specifies channel N where N may be 0 to F in hexadecimal. The channel is latched till another read occurs. The output of the selected channel goes to the input of the analog-to-digital conversion section.

The A/D has to be initialized by setting the operation mode of the 8255 PPI to strobe-handshake input mode (mode 1) and by setting the input channels of the A/D converter to single-ended input mode. The input voltage range of ±2.5 V is set for both channels so that better resolution can be obtained. The conversion is initiated by a dummy read from Port B which resets the input buffer full line (C_1) of the 8255 PPI. The high to low transition on line C_1 triggers one half of a dual monostable to send a start pulse to the ADC thus causing its status to go high, and making it hold the output from the AIS. After a maximum of 25 μs, the status line goes low again indicating valid data is on the A/D output lines. On a high to low status transition, the other half of the monostable is triggered causing it to send a strobe pulse to the lines C_2 and C_4 (handshake lines). Line C_0 is set low to indicate to the Standard (STD) Bus that data is on Port A and B of 8255 PPI. The 8255 PPI is configured to operate in mode 1. The 8 lines of Port A read

the lowest 8 significant bits and lines 0 to 3 of Port B read the remaining four bits while lines on Port C are used for handshaking between the A/D and the STD Bus. The corresponding subroutines in the software program are listed below :

" *ADINIT-S " -- initialize the 12-bit A/D module
" *ADLSB-S " -- read the least significant byte (LSB)
" *ADMSB-S " -- dummy read for initiating conversion,
read the most significant byte (MSB)

The first two A/D converter channels have been assigned to S-parameter measurement while the rest of the channels can be connected to other instruments and can be used for other measurements such as resonant frequency and Q factor measurements of resonant circuits [13], wide-range dynamic complex dielectric constant measurements [14] and precision measurement of high VSWR'S [15].

d) The 14-bit D/A Module

The 14-bit D/A module is used for providing an output voltage of 0-10 V to control the RF frequency of the sweeper. It consists of an Intersil 7134 14-bit D/A converter, a 74LS04 inverter and an 8255 Programmable Peripheral Interface (PPI), plus three low noise, low voltage offset operational amplifiers. The schematic diagram of the module is shown in Figure 2.8. The 8255 PPI is

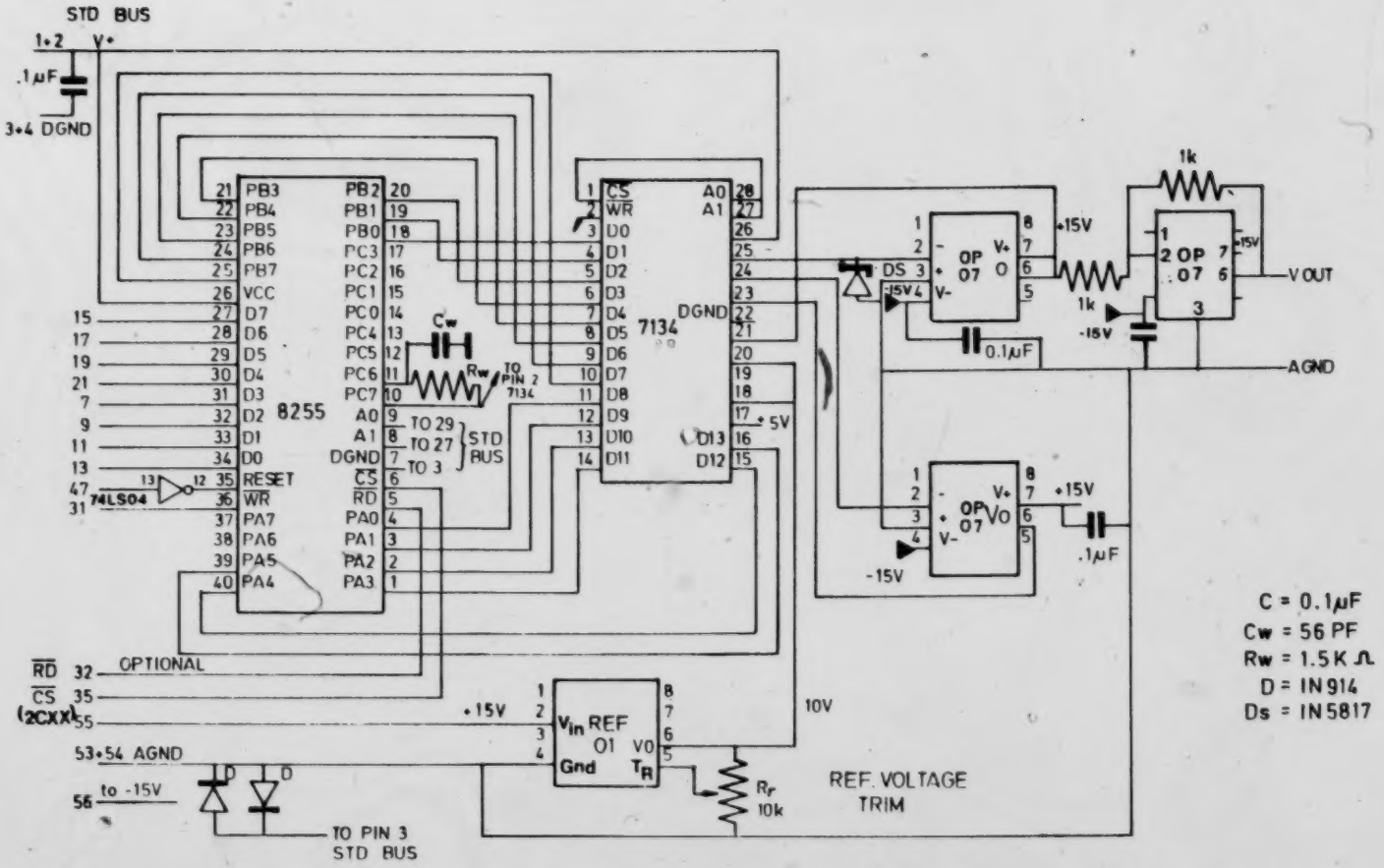

Figure 2.8 The Schematic Diagram of the 14-Bit D/A Module

configured to operate in strobe-handshake output mode (mode 1). The 8 output lines of Port B are connected to the lowest 8 bit data inputs of the 7134 (D_0-D_7) and 6 output lines of Port A (A_0-A_5) are connected to the most significant bits (D_8-D_{13}). Two lines of Port C (PC_6-PC_7) are used as handshaking lines to indicate to the 7134 D/A converter when valid data is present on Port A and B. The input reference is a REF01'', 10 V reference and the output is the product of the reference and the digital input. The output current is then converted to voltage output by an OP07'' and this voltage is further inverted by another OP07 for providing a positive output in the range of 0 to 10 V. The purpose of the third OP07 is to correct any analog ground offsets.

With the 14-bit D/A module plugged into the MCDAS, the RF frequency of the sweeper can be controlled by the digital output of the 14-bit D/A converter. However, there are two disadvantages which result from using this module to control the sweeper. Firstly, it can only set the sweeper to the desired RF frequency within ±10 MHz and secondly, the frequency may not be repeatable. Since there was an EIP 575 counter with a phase-locking feature in the laboratory which provided better frequency repeatability and which allowed frequency settings within ±10 KHz over the 1-12 GHz range, this counter was used for controlling the RF frequency of the sweeper in the ANA system. Although the 14-bit D/A

'' A +10v precision voltage reference manufactured by Precision Monolithics Incorp (PMI).
'' An ultra-low offset voltage operational amplifier manufactured by PMI.

module remains presently idle, it can be used for controlling the sweeper whenever the counter is not available or is used for other measurements as a high resolution DC voltage source.

e) The 8-bit D/A Module

The 8-bit D/A module was built for displaying the corrected parameters on the polar display unit. There are four MC6890, self-contained, bus-compatible, 8-bit D/A converters on a board located at decoded address #2800 to #2804 to provide four analog outputs. The output voltage ranges available for each channel are: ±2.5 V, ±5 V, 0 to 5 V, 0 to 10 V, and 0 to 20 V selectable by simply changing the positions of the jumpers on the board. The current output is converted to a voltage output by a 741 operational amplifier. The schematic diagram is shown in Figure 2.9.

Although the first two channels have been assigned for displaying the corrected parameters on the polar display, the speed using the strobe-handshake mode for transferring data is not fast enough to give a continuous display over the selected frequency band. Morever, the polar display needs a horizontal input and a vertical input to display a dot. If either one of these inputs changes before the other, an ambiguous dot will appear on the display. As a result, a pair of true and false dots can be seen on the display. Therefore, instead of displaying the corrected parameters on the polar display unit, the parameters are plotted on a

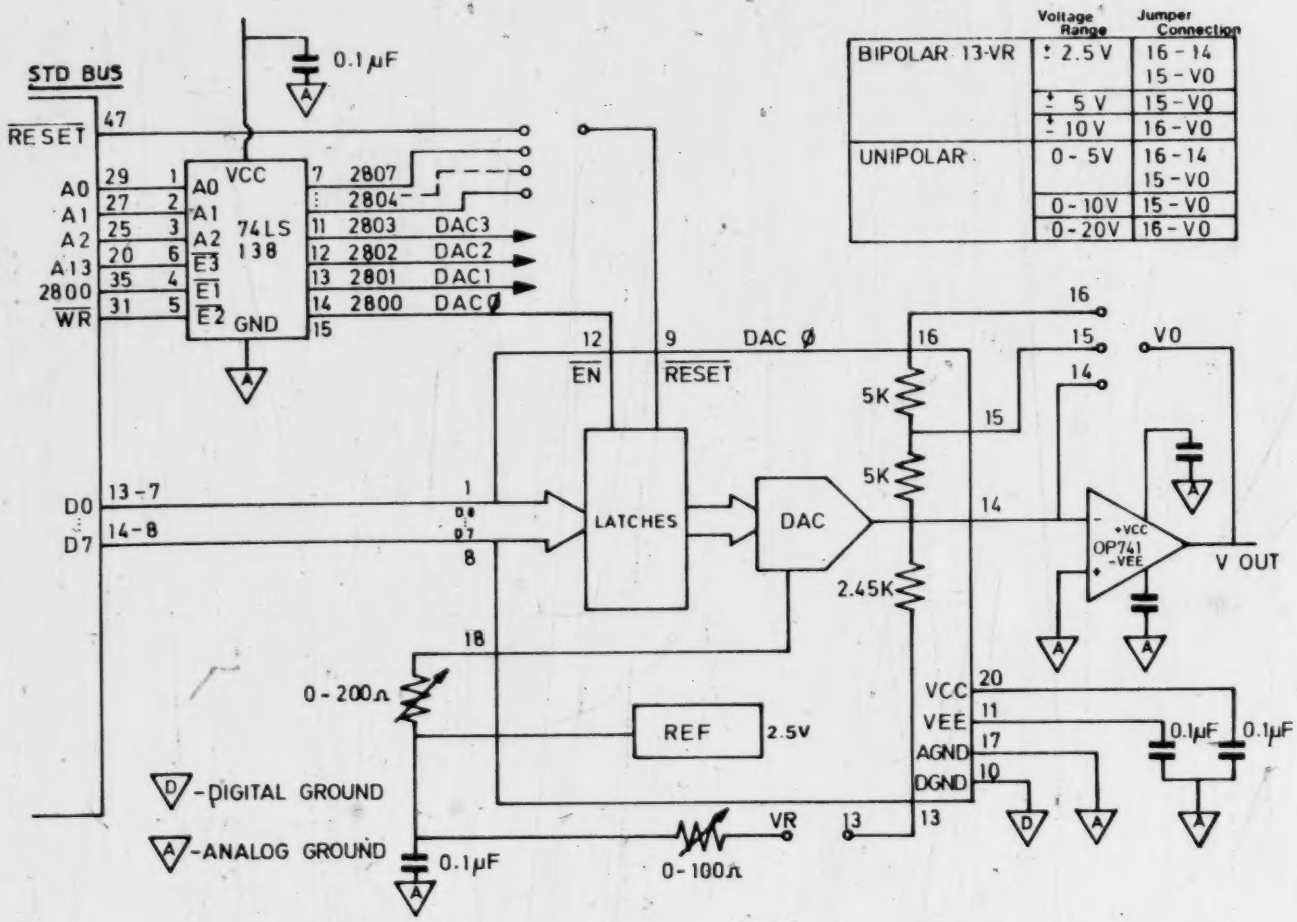

Figure 2.9 The Schematic Diagram of the 8-Bit D/A Module

simplified Smith Chart by a plotter. A subprogram named "SMITH-S" was written for plotting any one of the four parameters onto an HP plotter. At present, the 8-bit D/A module is idle.

f) A 16K RAM Memory Module

The external 16K RAM is located in the memory address range from #4000 to #7FFF. This memory board is not used presently for S-parameter measurement. However, if the K-8073 microcomputer is used in a stand-alone mode for other measurements, this board will be used for storing the measured data.

g) Other Modules

The other two suggested modules that can be added to the MCDAS in the future are an ISBX 331 Arithmetic Processing Unit and an expanded 12K EEPROM memory module. The ISBX 331 board contains an 8231 Arithmetic Processing Unit (APU) which accepts data and commands from the MCDAS controller and provides high performance single or double precision or fixed point arithmetic operations. It is able to perform a repertoire of 43 floating point and fixed point commands an order of magnitude faster than is possible through conventional programming routines. Therefore, if an 8231 APU is employed in performing error correction in S-parameter measurements, the accuracy and measurement time will be improved. The expanded EEPROM memory board not only

provides extra memory to the MCDAS, it also makes the MCDAS more convenient and flexible for modification of the program and storage in the EPROM by the programmer.

The designed MCDAS is significant for its versatility, flexibility, low-cost, compatibility and its capability to perform the desired functions simply by changing software. It is not difficult to upgrade the system in the future either by adding more modules or by replacing a module with an upgraded one. The system also has the potential to be operated in multiprocessing applications.

2.2 Modification of the Network Analyser System

Three instruments had to be modified before the conventional network analyser can be used under remote control. These instruments are the HP8620A sweeper, the HP8410A network analyser and the HP8414A polar display. Figure 2.10 shows a toggling switch added between the internal sweep circuitry and the ramp amplifier in the mainframe of the 8620A sweeper.

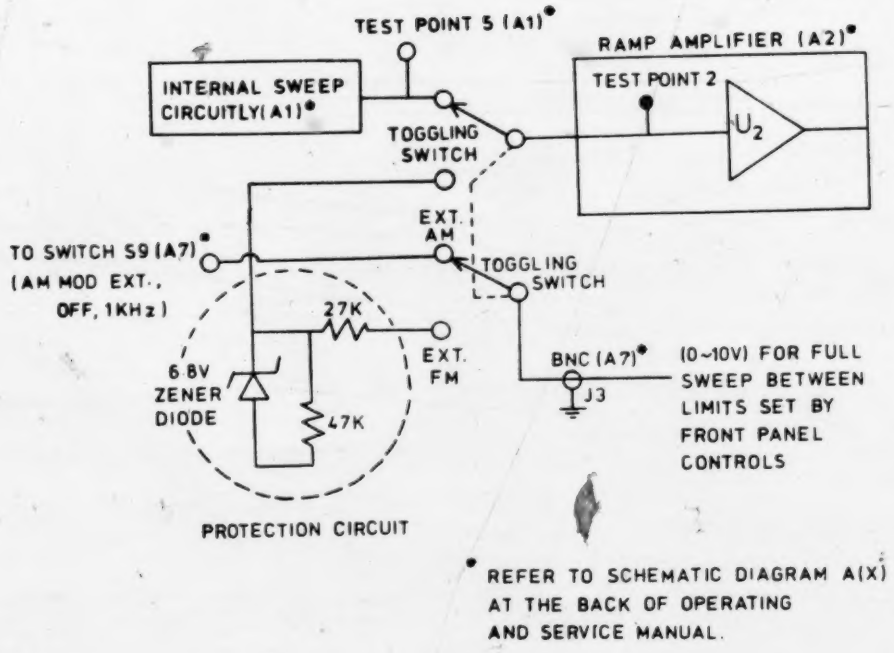

Figure 2.10 The Circuit Diagram of the HP8620A Sweeper Modification

The BNC connector on the rear panel becomes either the existing external AM input or an external FM input depending on the position of the switch. The external FM input voltage of 0-10 V originates either from the EIP575 frequency counter or the 14-bit D/A converter and sets the desired RF frequency between the frequency band limits as determined by the front panel controls. Further details of the circuit diagram of each block are shown in the Sweeper Oscillator

Operating and Service Manual [16].

The HP8410A network analyser also needed to be modified so that the I.F. gain could be controlled automatically by the computer through the 8255 PPI interface. The I.F. gain of the test channel of this model is normally within a range of 69 dB in 10- and 1- dB steps set by two knobs on the front panel. It was necessary to insert a digital attenuator to allow the computer to have control over the I.F. gain. Thus, an 8-bit digital attenuator was inserted in parallel with the mechanical attenuator in the 8410A mainframe as shown in Figure 2.11.

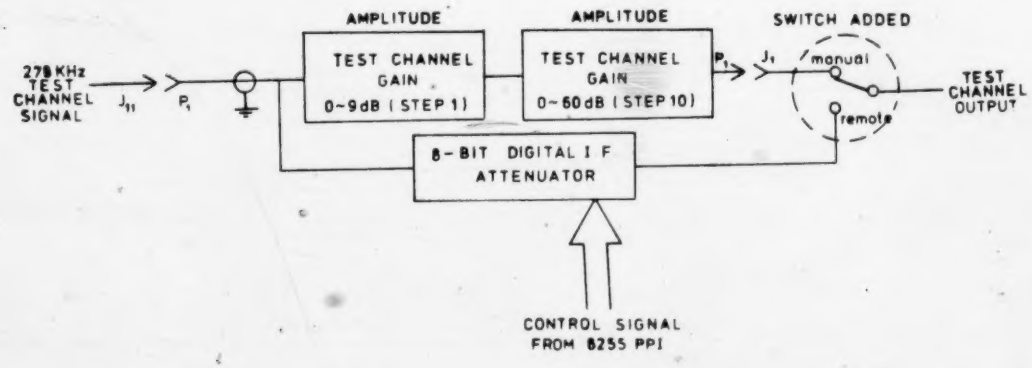

Figure 2.11 The Diagram of the Modification of the HP8410A Network Analyser

The inputs of these two attenuators are connected to a two-way switch at the rear panel so that either pathway can be selected. Moreover, the digital attenuator circuit board is installed in a shielded box to avoid interference which might upset the performance of the analyser. The board consists of an ICL7523 D/A converter, an LF351 and an LM318 operational amplifier, a 78L15 voltage regulator, and an RLC-filter. Since the maximum range of attenuation available from the 8-bit D/A attenuator is 54 dB and the optimal I.F. gain setting for a 50 ohm calibrator is 60 dB, the dynamic range of the I.F. gain was made adjustable between 18 dB and 65 dB limits, corresponding to 53 dB and 0 dB attenuation, respectively, of the digital attenuator. The schematic diagram of the digital attenuator and the diagram of the modifications of the connection inside the analyser mainframe are shown in Appendix I. Further details of the circuit diagram of the mechanical attenuator are shown in the Network Analyser Operating and Service Manual [17].

With the insertion of the auto-beam centering enable circuit[13] in the display unit and the modification of the interconnection between the network analyser and the display unit, the beam centering enable can be activated by a digital signal from the I/O ports of the 8255 PPI interface using the remote control cable. To enable the corrected display input of the polar display with a digital signal instead of a conventional analog signal, a TTL-driver for

---

[13] The circuit is shown in Figure 8-18 of the HP Polar Display Operating and Service Manual [18].

providing enough driving current was added between the digital input and the relay switch, as shown in Figure 2.12.

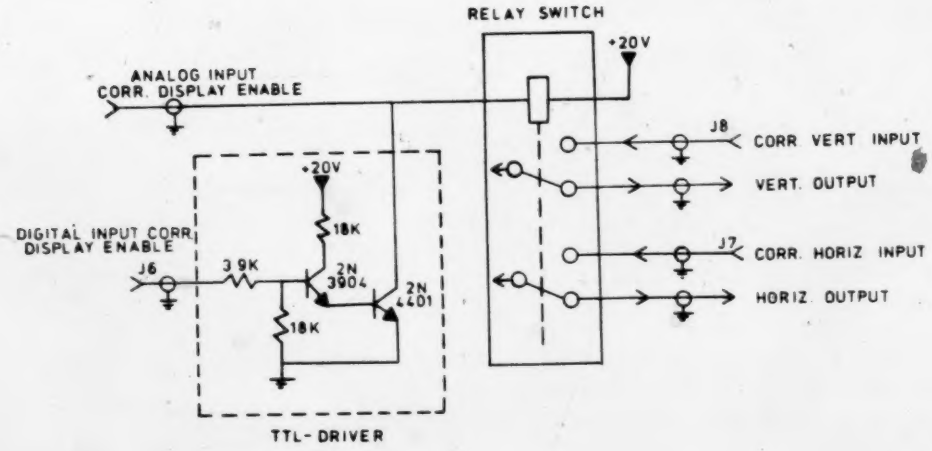

Figure 2.12 The Circuit Diagram of the Added TTL-driver Between the Digital Input and the Relay Switch of the HP8414A Polar Display Unit

As a result of these modifications, both the beam centering enable and the corrected display enable can be controlled by the MCDAS through the 8255 PPI interface.

2.3 Operation of the ANA System

With the modified network analyser, the S-parameters of any device can be measured under manual or auto-remote control. The HP-85 requests control of the MCDAS bus from the K-8073 microcomputer and initializes the I/O interfaces of the A/D module, the D/A modules and the 8255 PPI on the K-8073 board. A subprogram named "*ACQDA-S" is called for controlling the measurement sequence and for acquiring data. The DC offset voltages of the polar display output amplifiers are first measured with the beam centering enable being activated. These voltages will be subtracted from all the measured data later in error vector calculations. The sequence for calibrating the 12-term error model of the ANA system is set in the program. The instructions for connecting the appropriate calibrator are displayed on the CRT of the HP-85 computer, one at a time. If the remote-control mode is selected, the HP-85 controls the I.F. gain, S-parameter switches and input attenuation switches'• through the I/O ports of the 8255 PPI. The operator is required to respond by simply connecting the appropriate calibrator to the test set. Thus, no special skill or knowledge is required for calibrating the system error model. When calibration is done, a device under test (DUT) is then connected to the test set. The computer searches for the optimal I.F. gain over the entire frequency band for

---

'• The switching of the input attenuation in the test set causes phase shifts of 5° to 15° in the measured data. Therefore, the input attenuation is set to 0 dB which remains unchanged throughout the measurement.

each parameter. All four S-parameters of the DUT are measured completely without requiring any further attention from the operator. For each measurement, the HP-85 reads the voltage from the horizontal and vertical output of the display unit through channels 1 and 2 of the 12-bit A/D converter. Each final data point is the result of averaging 20 measurements at each frequency. The calibration data and measured parameters of the DUT are stored in arrays A and C respectively. After all the measured data have been acquired, the error correction subprograms[18] are called to calculate the internal systematic errors and correct the measured four parameters of the DUT. The results are then stored, printed or can be plotted on a simplified Smith Chart.

In measuring an active device or component with gain greater than 6 dB, the manual mode for the I.F. gain setting has to be selected because the dynamic range of the digital attenuator is not wide enough. When a short is connected to one port of the test set with 24 dB I.F. gain, the dot appears at the circular edge of the display. When an active device with a gain greater than 6 dB is measured, the I.F. gain needs to be set lower than 18 dB in order for the dot to appear within the display region. However, the digital attenuator cannot be set lower than 18 dB. As a result of this, the horizontal or vertical output voltages of the

---

[18] *NORM-s - normalize I.F. gain and subtract DC offset ; *12ERROR-s - calculate 12 error vectors ; *12CORR-s - correct raw measured data explicitly.

display unit may exceed ±2.5 v which is the upper limit set for the 12-bit A/D converter. The dot may not be seen on the display and the measured data may be incorrect. Therefore, the manual mode with a wider dynamic range (0-69 dB) has to be used. If the manual mode is selected, the operator sets the I.F. gain manually for each calibration according to the table in the System Operating Manual (Appendix II). When measuring the parameters of a DUT, the operator searches for the optimal I.F. gain manually for each parameter and then enters the optimal value obtained into the program which is required later for error correction. Although the measurement using the manual-control mode requires more work, the accuracy of the measurement result can be as good as that using the remote-control.

However, the fully automatic control of the measurement procedure developed in this project has made the S-parameter measurement much easier and ten times faster than point-by-point measurement techniques. As a result, a minimal amount of technical skill or knowledge is required for characterizing any two-port device with reasonably good accuracy and speed.

3. ERROR CORRECTION MODEL FOR TWO-PORT MEASUREMENT

3.1 Introduction

All network analysers introduce error to the measurement results. These errors can be separated into two categories: random errors and system errors. The latter category is usually the most significant source of error in measurements at microwave frequencies.

Several methods have been used for removing system errors occuring in the measurement of linear two-ports. The approach used by Evans [19] consists of measuring the S-parameters of the unknown device normalized to the actual test set impedance. The test set impedance is established using measurements performed with standard terminations. The measured two-port S-parameters are then transformed to the desired reference impedance using a general transformation. A more direct method using the network analyser was presented in the mid-60's by Hackborn [4], and then Hand [20]. The error signals introduced at the input and output measuring ports are obtained from measurements using standard terminations. These errors are then removed by solving a set of four coupled equations using an iterative procedure. Although the iterative algorithm converges quickly, the process must be repeated at each frequency point. Later Kruppa and Sodomsky [21], and Rehnmark [22] showed that explicit solutions are possible, thereby reducing the calculation time significantly. Rehnmark solved

the 10-term error vector model explicitly while Gelnovatch [6-7] explicitly solved the 12-term error vector model.

The 12-term error model provides full directivity, isolation, source match, load match, and frequency response vector error correction for transmission and reflection measurements of two-port devices. This model provides the best magnitude and phase measurement accuracy. Therefore, in this project, a 12-term error model is chosen in order to achieve the best measurement accuracy.

To characterize all the error terms in the error model, there are a few techniques using different sets of calibrators. For these techniques, the error equations derived are different from one another because the measurement procedures are different. Therefore, the accuracy enhancement program designed for one particular set of calibrators may not be suitable for another set of calibrators. However, the system program developed in this project allows two sets of calibrators to be used for error model calibration. For reflection calibration, the calibrators (a short, an APC-7 open and a 50 ohm load) used in this project are the same for both sets. However, the through-connection calibrator used for transmission calibration can be either a flexible cable or a custom-made semi-rigid cable. The following discussion describes the error vectors in greater detail and explains how they can be characterized and derived using both sets of calibrators. The derivation of the explicit solutions of the unknown

S-parameters of a device under test is also presented in this chapter.

3.2 Sources of Measurement Errors

Any measurement result is the vector sum of the actual test device response plus all error terms. The precise effect of each error term depends on its magnitude and phase relationship to the actual test device response. The error terms can be separated into 2 categories : random errors and system errors. Random errors are non-repeatable measurement variations due to noise, connector interface uncertainty, instrument linearity, inaccurate logarithmic conversion, temperature drift and other physical variations in the setup. These errors cannot be precisely quantified, so they cause ambiguity in the measured data. However the systematic category of repeatable, measureable error terms is the most significant source of measurement uncertainty. Since each of these errors produces a predictable effect upon the measured data, the effects can be removed to obtain corrected values for the measurement. These systematic errors are quantified as directivity, source match, load match, isolation, and tracking (frequency response) errors.

Directivity Error - This error is due to the inability of the couplers or bridges to absolutely separate incident and reflected waves to the residual reflections of test cables and adapters. Directivity has its most profound effect on low reflection (high return loss) measurements.

It produces the major ambiguity in a reflection measurement.

Source Match Error - When the test port characteristic impedance is not exactly 50 ohms, multiple reflections can occur causing measurement error. This error is a problem particularly when measuring very high or low impedance(large mismatch). When measuring the reflection coefficient of a direct short device using the HP 8410A network analyser, this leads to a potential ± 0.11 reflection coefficient error in magnitude. It is a factor in both transmission and reflection measurement.

Frequency Tracking Error - The variation in frequency response is typically less than ± 0.5 dB and 5° over a 1 -12 GHz frequency range. However, these variations can be removed automatically with the accuracy enhancement program. It is a factor in both transmission and reflection measurement.

Load Match Error - This error is due to the effects of impedance mismatches between the test device output port and the receiver test input. Since the test setup transmission return port is not exactly the characteristic impedance (normally 50 ohms), some of the transmitted signal is reflected from the return port to port 2. A portion of this wave may be re-reflected at port 2, thus affecting the S_{21} measurement or part may be transmitted to appear at port 1, thus affecting the S_{11} measurement. It is a factor in both transmission and reflection measurements. The effect will produce a major transmission measurement error for a test

device whose output port is highly reflective.

Isolation Error - This error is the vector sum of signals appearing at the receiver detectors resulting from crosstalk between the reference and test signal paths, including signal leakage across test switches and within both the RF and IF sections of the receiver. The uncertainty contributed by lack of isolation is a factor in high loss transmission measurements.

3.3 System Error Model

Consider the measurement of the reflection coefficient of an unknown one-port device, in the forward direction.

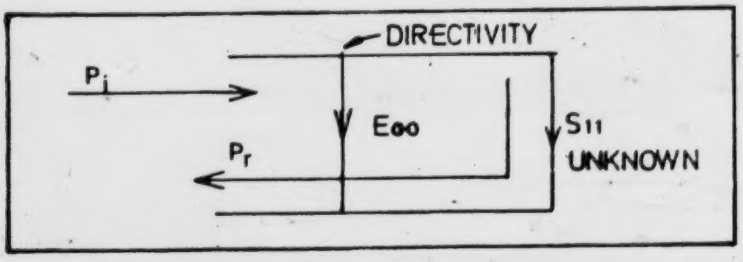

Figure 3.1 Signal Flowgraph Showing the Directivity Error

Reflection coefficients are measured by taking the ratio of the incident power P_i to the reflected power P_r. However, not all the incident power reaches the unknown. Some power may bounce back due to an imperfect bridge and less than perfect adapters and couplers. This is called

"Directivity Error", E_{oo} as shown in Figure 3.1.

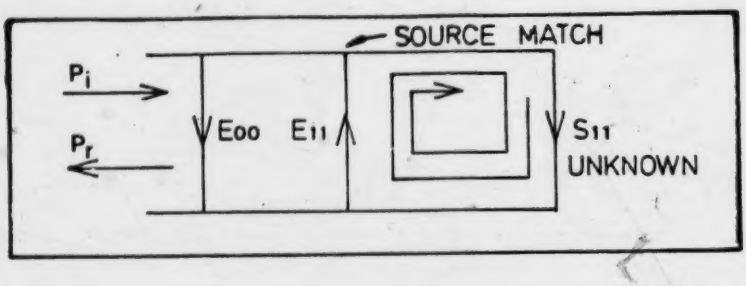

Figure 3.2 Signal Flowgraph Showing the Source Match Error

Since the measurement system test port is never exactly the characteristic impedance, some of the reflected signal bounces off the test port and back to the unknown adding to the incident signal P_i. This is called "Source Match Error", E_{11} as shown in Figure 3.2.

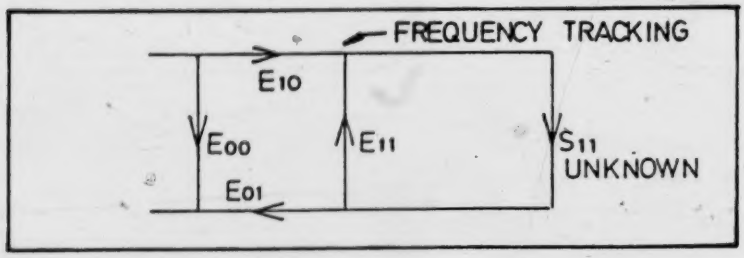

Figure 3.3 Signal Flowgraph Showing the Frequency Tracking Error

A frequency tracking error, $E_{10}E_{01}$ (usually expressed as a product of two terms) is caused by small variations in magnitude and phase flatness versus frequency of the test and reference channel signal due to imperfectly matched cables, differences between incident and test couplers and in the frequency converter.

Similarly, in the reverse direction, directivity error, source match error and frequency tracking error are labeled E_{33}, E_{22}, and $E_{32}E_{23}$ respectively. The signal flowgraph of Figure 3.4 shows the 6 error terms of a two-port error model.

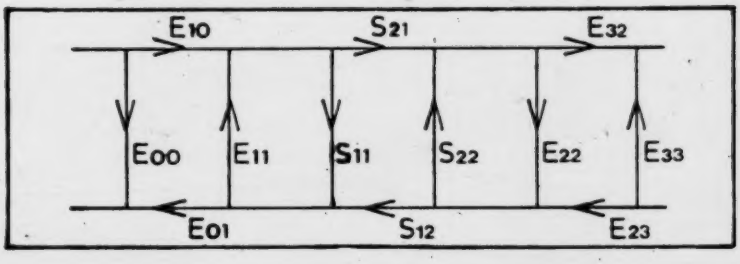

Figure 3.4 Signal Flowgraph Showing the Directivity Error, Source Match Error, and Frequency Tracking Error of a Two-port Error Model

When the transmission coefficient of an unknown two-port device is measured, the HP8746B test set is operated in the transmission configuration with a through connection. The transmission frequency tracking error is denoted as $E_{32}E_{10}$ for the forward direction and $E_{23}E_{01}$ for

the reverse direction.

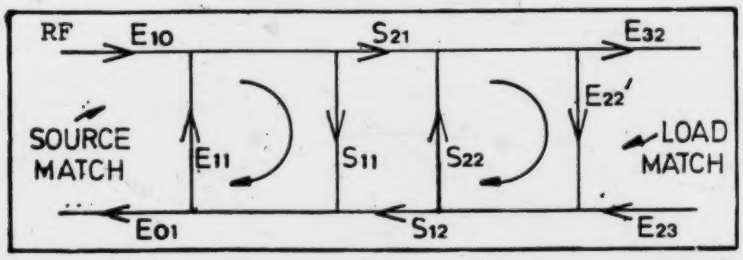

Figure 3.5 Signal Flowgraph Showing the Load Match Error

As in the reflection model, source match can cause incident power to vary as a function of test device S_{11}. Some of the transmitted signal returns to port 2 because the transmission return port is never exactly the characteristic impedance. A portion of this wave may be re-reflected at port 2 or part may be transmitted to appear at port 1. This is called "Load Match Error" E_{22}' as shown in Figure 3.5 which causes the magnitude and phase of the actual transmitted signal to vary as a function of S_{22} of the test device. In the reverse direction, the load match error is E_{11}'

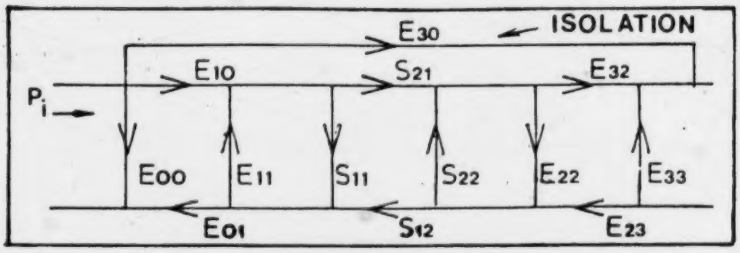

Figure 3.6 Signal Flowgraph Showing the Isolation Error

Isolation, E_{30}, represents the part of the incident wave that appears at the receiver detectors without actually passing through the test device. Isolation is measured with the test set in the transmission configuration.

The HP8745A test set can measure both the forward and reverse characteristics of the test device without any need of physically removing and reversing it. The comprehensive 12-term transmission and reflection error model is shown in Figure 3.7. There are two sets of error terms, forward and reverse, with each set consisting of six error terms. It includes terms for directivity E_{00} (forward) and E_{33} (reverse), Isolation E_{30} and E_{03}, Source match E_{11} and E_{22}, Load match E_{22}' and E_{11}', reflection tracking $E_{10}E_{01}$ and

$E_{32}E_{23}$, and transmission tracking $E_{32}E_{10}$ and $E_{23}E_{01}$.

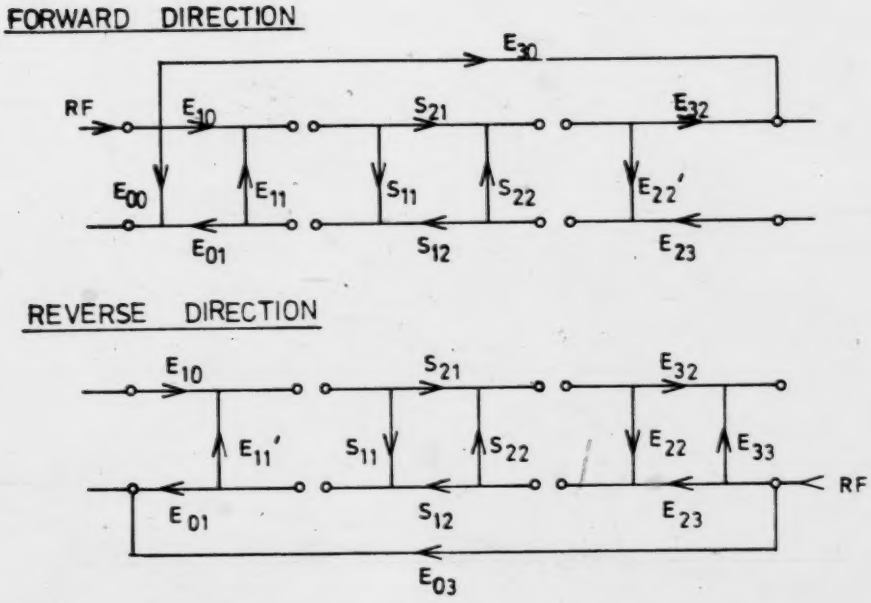

Figure 3.7 Signal Flowgraph of a 12-term Transmission and Reflection Error Model

3.4 Calibration Techniques

All the error vectors in the error model can be characterized using different calibration techniques. There are four common techniques used for the reflection measurement calibration. They are:

a. a direct short and two offset shorts

b. a direct short, an offset short and a sliding match

c. a direct short, an open circuit, and a sliding match

d. a direct short and two different sliding load, one with high and one with low reflection coefficient

Method (a) was proposed by Silver and McPhun [23]. It permits better phase resolution, better signal/noise ratio and low variance. Thus it provides an optimum solution in terms of measurement uncertainty for low loss two-port devices. However, the frequency and the offset length must be known accurately and precisely. The phase of the offset short is frequency sensitive. Therefore, care must be taken to avoid lengths that are multiples of a half-wavelength, or the offset short will not be unique.

Method (b) was used by Hackborn [4], Hand [20], Rehnmark [22] and Adam [5] and is applied in Hewlett Packard's computer-based, automatic network analysers. It requires a series of offset shorts over the frequency range in order to approximate an open circuit. The offset shorts are not broadband devices. Again, the frequency and offset length must be known accurately.

Method (c) is very similiar to Method (b), but it replaces the offset shorts with an open circuit. This technique was described by Cobb [24], Gelnovatch [6-7] and Krupa and Sodomsky [21] and appeared in Hewlett Packard application notes [25-26]. The fringing capacitance of the open circuit needs to be modelled very precisely as a function of frequency in order to achieve good measurement accuracy.

The approach of method (d) is the most mathematically involved, but has the potential of achieving the best performance. This method was devised by Kasa [27].

Method (c) was chosen to be used in this project for calibrating the error model of the reflection measurement for the following reasons. The calibrators available in the laboratory when the project started were a 50 ohm load, a 50 ohm sliding load, a direct short and an open circuit. It was found that using a 50 ohm (sliding or standard) load for calibration considerably simplified the equations for the calculation of the error vectors. The high variance in the measured signal due to low signal/noise ratios was improved by connecting a low-pass filter'' at the input of the A/D converter and by introducing a data averaging [24] routine in the software. Moreover, the open circuit fringing capacitance was modelled accurately as a function of frequency by Rytting [28]. This capacitance error was included in the error vector equations and the error in measuring the reflection coefficient of an APC-7 offset short device was reduced significantly.

To calibrate the transmission measurement errors, a through-connection cable is required to be connected between test ports 1 and 2. Two through-connection calibrators used in this project were a flexible cable (flexible arm or flexible coaxial cable) and a custom-made semi-rigid cable.

'' A low-pass filter was made of a 270 ohm resistor and a 0.1μF capacitor with cut-off frequency at 5.9 KHz. It is used to filter most of the noise at 8 KHz frequency.

The flexible cable is used for characterizing any device which requires a cable to connect one end of the test device to the other end of the test port. The custom-made cable is used particularly for characterizing FET parameters. When a flexible cable is used as a through-connection calibrator,it is connected to the test set for both calibration and device measurements. The calibrator is treated as a zero length cable in error vector calculations. The transmission error in device measurement caused by the extra length of the calibrator can be eliminated after error correction. The error equations obtained using this calibration technique were presented by Gelnovatch [6] and Hand [20].

However, the ANA will be used for characterizing FET parameters which are embedded in an HP11608A test fixture or similar fixture. The HP fixture is designed in such a way that it is connected directly to both ends of the test ports. There is no room left for connecting a through-connection calibrator in between the fixture and test ports. Therefore, the calibrator has to be removed when the calibration is done. The length of the calibrator can no longer be treated as a zero length cable, but as a cable with transmission coefficient equal to $\alpha\angle\gamma$, where α is the magnitude and γ is the phase. Although a flexible arm can be used as the calibrator, a cable with shorter length is preferable since its transmission coefficient can be characterized more accurately. Therefore, a short semi-rigid

cable with known characteristics'' was made particularly for characterizing FET parameters. The error equations obtained using this semi-rigid cable calibrator are more complex. However, these equations can be reduced to the same error equations obtained previously by simply setting the transmission coefficient α/γ to $1/0$. Details of the derivation of the error equations using the second set of calibrators are described in the following section.

'' The cable was made of BA50250 Solid Dielectric Cable of 19.74 cm in length and with two APC-7 connectors at both ends.

3.5 Derivation of Error Equations

The ratio between any two complex wave amplitudes can be obtained as an expression involving the parameters of a signal flowgraph by making use of a general formula known as Mason's non-touching loop rule [10]. The ratio is given by the following expression :

$$R = \frac{P_1(1-\Sigma' L_1+\Sigma' L_2-\ldots)+P_2(1-\Sigma^2 L_1+\Sigma^2 L_2-\ldots)+\ldots}{1-\Sigma L_1+\Sigma L_2-\ldots} \qquad (3.0)$$

Where

P_1 is one path from X to Y

P_2 is a different path from X to Y etc..

ΣL_1 is the sum of all 1st order loops

ΣL_2 is the sum of all 2nd order loops

$\Sigma' L_1$ is the sum of all 1st order loops not touching P_1

$\Sigma' L_2$ is the sum of all 2nd order loops not touching P_1

$\Sigma^2 L_1$ is the sum of all 1st order loops not touching P_2

$\Sigma^2 L_2$ is the sum of all 2nd order loops not touching P_2

Consider the signal flowgraph in Figure 3.7. The ratio between the incident wave and reflected wave at port one is the reflection coefficient M_o

$P_1 : E_{oo}$

$P_2 : E_{10}S_{11}E_{01}$

$P_3 : E_{10}S_{21}E_{22}'S_{12}E_{01}$

ΣL_1 : $E_{11}S_{11}+S_{22}E_{22}'+E_{11}S_{21}E_{22}'S_{12}$

ΣL_2 : $E_{11}S_{11}S_{22}E_{22}'$

$\Sigma' L_1$: $E_{11}S_{11}+S_{22}E_{22}'+E_{11}S_{21}E_{22}'S_{12}$

$\Sigma' L_2$: $E_{11}S_{11}S_{22}E_{22}'$

$\Sigma^2 L_1$: $S_{22}E_{22}'$

Therefore, by substituting the above expressions into the general equation,

$$M_0 = E_{00} + \frac{S_{11}E_{10}E_{01}(1-S_{22}E_{22}') + S_{21}S_{12}E_{10}E_{01}E_{22}'}{1-S_{11}E_{11}-S_{22}E_{22}'-S_{21}S_{12}E_{11}E_{22}' + S_{11}S_{22}E_{11}E_{22}'} \qquad (3.1)$$

Using the same rule, the other three equations can be obtained and listed below :

$$M_3 = E_{30} + \frac{S_{21}E_{10}E_{22}}{1-S_{11}E_{11}-S_{22}E_{22}'-S_{21}S_{12}E_{11}E_{22}' + S_{11}S_{22}E_{11}E_{22}'} \qquad (3.2)$$

$$M_0' = E_{33} + \frac{S_{12}E_{32}E_{23}(1-S_{11}E_{11}') + S_{21}S_{12}E_{32}E_{23}E_{11}'}{1-S_{11}E_{11}'-S_{22}E_{22}-S_{21}S_{12}E_{11}'E_{22} + S_{11}S_{22}E_{11}'E_{22}} \qquad (3.3)$$

$$M_3' = E_{03} + \frac{S_{12}E_{23}E_{01}}{1-S_{11}E_{11}'-S_{22}E_{22}-S_{21}E_{12}E_{11}'E_{22} + S_{11}S_{22}E_{11}'E_{22}} \qquad (3.4)$$

Where

M_o = reflection coefficient for forward direction

M'_o = reflection coefficient for reverse direction

M_s = transmission coefficient for forward direction

M'_s = transmission coefficient for reverse direction

With 12 different calibrations, the error equations can be derived from equations (3.1) to (3.4). The following steps show how the error equations can be expressed in terms of the calibration data.

1) Reflection

For Port 1 and from equation (3.1):
Using a matched load for which $S_{21}=S_{12}=S_{22}=0$, $S_{11}=0$ gives

$$M_{om} = E_{oo} \tag{3.5}$$

Using the short with $S_{11}=-1$ gives

$$M_{os} = E_{oo} - \frac{E_{10}E_{01}}{1 + E_{11}} \tag{3.6}$$

and using the open with $S_{11}=\exp(-j2\beta)$ gives

$$M_{oo} = E_{oo} + \frac{E_{10}E_{01}\exp(-j2\beta)}{1 - E_{11}\exp(-j2\beta)} \tag{3.7}$$

For Port 2 and from equation (3.3):

Similarly, using a matched load, short and open for which $S_{22}=0$; $S_{22}=-1$; $S_{22}=\exp(-j2\beta)$ respectively, produces:

$$M'_{om} = E_{33} \tag{3.8}$$

$$M'_{o.} = E_{33} - \frac{E_{32}E_{23}}{1 + E_{22}} \tag{3.9}$$

$$M'_{oo} = E_{33} + \frac{E_{32}E_{23}\exp(-j2\beta)}{1 - E_{22}\exp(-j2\beta)} \tag{3.10}$$

2) Isolation

For Ports 1 & 2 and from equation (3.2) & (3.3)

Using the matched load for which $S_{21}=S_{12}=S_{11}=S_{22}=0$ results in:

$$M_{3m} = E_{30} \tag{3.11}$$

$$M'_{3m} = E_{03} \tag{3.12}$$

3) Transmission tracking

Using a semi-rigid cable connected between ports 1 & 2 for which $S_{22}=S_{11}=0$, $S_{21}=S_{12}=\alpha\exp(-j\gamma)$

From equation (3.2):

The reflection at port 1 is given by

$$M_{01} = E_{00} + \frac{E_{10}E_{01}E_{22}'\alpha^2\exp(-j2\gamma)}{1- E_{11}E_{22}'\alpha^2\exp(-j2\gamma)} \qquad (3.13)$$

For the reflection at port 2:

$$M'_{01} = E_{33} + \frac{E_{32}E_{23}E_{11}'\alpha^2\exp(-j2\gamma)}{1 - E_{11}'E_{22}\alpha^2\exp(-j2\gamma)} \qquad (3.14)$$

For the transmission at port 1:

$$M_{31} = E_{30} + \frac{E_{32}E_{10}\alpha\exp(-j\gamma)}{1 - E_{11}E_{22}'\alpha^2\exp(-j2\gamma)} \qquad (3.15)$$

Finally, for the transmission at port 2:

$$M'_{31} = E_{03} + \frac{E_{23}E_{01}\alpha\exp(-j\gamma)}{1 - E_{11}'E_{22}\alpha^2\exp(-j2\gamma)} \qquad (3.16)$$

From equations (3.5) to (3.16), the error vector equations in terms of the measured parameters can be obtained. By substituting (3.5) into (3.6) & (3.7) and solving these two equations,

$$E_{11} = \frac{\exp(j2\beta)(M_{00}-M_{0m})(M_{0m}-M_{01})}{(M_{00}-M_{01})} \qquad (3.17)$$

$$E_{10}E_{01} = (1+E_{11})(M_{0m}-M_{01}) \qquad (3.18)$$

Similarily, by substituting (3.8) into (3.9) & (3.10) and solving these two equations,

$$E_{22} = \frac{\exp(j2\beta)(M'_{00}-M'_{0m})(M'_{0m}-M'_{0s})}{(M'_{00}-M'_{0s})} \qquad (3.19)$$

$$E_{32}E_{23} = (1+E_{22})(M'_{0m}-M'_{0s}) \qquad (3.20)$$

By rearranging (3.13) & (3.14),

$$E_{22}' = \frac{(M_{01}-E_{00})}{((M_{01}-E_{00})E_{11}+E_{10}E_{01})\alpha^2\exp(-j2\gamma)} \qquad (3.21)$$

$$E_{11}' = \frac{(M'_{01}-E_{33})}{((M'_{01}-E_{33})E_{22}+E_{32}E_{23})\alpha^2\exp(-j2\gamma)} \qquad (3.22)$$

By substituting (3.11) into (3.15), (3.12) into (3.16) and rearranging the equations,

$$E_{32}E_{10} = \frac{(M_{31}-M_{3m})(1-E_{11}E_{22}'\alpha^2\exp(-j2\gamma))}{\alpha\exp(-j\gamma)} \qquad (3.23)$$

$$E_{23}E_{01} = \frac{(M'_{31}-M'_{3m})\ (1-E_{11}'E_{22}\alpha^2\exp(-j2\gamma))}{\alpha\exp(-j\gamma)} \qquad (3.24)$$

Therefore, the equations of the 12 error terms can be summarized as below.

$$E_{00} = M_{0m} \tag{3.5}$$

$$E_{11} = \frac{\exp(j2\beta)(M_{00}-M_{0m})-(M_{0m}-M_{0s})}{(M_{00}-M_{0s})} \tag{3.17}$$

$$E_{10}E_{01} = (1+E_{11})(M_{0m}-M_{0s}) \tag{3.18}$$

$$E_{30} = M_{3m} \tag{3.11}$$

$$E_{22}' = \frac{(M_{01}-E_{00})}{((M_{01}-E_{00})E_{11}+E_{10}E_{01})\alpha^2\exp(-j2\gamma)} \tag{3.21}$$

$$E_{32}E_{10} = \frac{(M_{31}-M_{3m})(1-E_{11}E_{22}'\alpha^2\exp(-j2\gamma))}{\alpha\exp(-j\gamma))} \tag{3.23}$$

$$E_{33} = M'_{0m} \tag{3.8}$$

$$E_{22} = \frac{\exp(j2\beta)(M'_{00}-M'_{0m})-(M'_{0m}-M'_{0s})}{(M'_{00}-M'_{0s})} \tag{3.19}$$

$$E_{32}E_{23} = (1+E_{22})(M'_{0m}-M'_{0s}) \tag{3.20}$$

$$E_{03} = M'_{3m} \tag{3.12}$$

$$E_{11}' = \frac{(M'_{01}-E_{33})}{((M'_{01}-E_{33})E_{22}+E_{32}E_{23})\alpha^2\exp(-j2\gamma)} \tag{3.22}$$

$$E_{23}E_{01} = \frac{(M'_{31}-M'_{3m})(1-E_{11}'E_{22}\alpha^2\exp(-j2\gamma))}{\alpha\exp(-j\gamma))} \tag{3.24}$$

If the values of α and γ of the above equations are set to 1 and 0 respectively, these equations are the same set of equations presented by Gelnovatch [6].

3.6 Error Correction Methods

The unknown S-parameters of a device under test embedded in the error model can be obtained either explicitly or by solving four coupled equations (3.1) to (3.4) using an iterative method. In this project, the former method is used. The four unknown parameters are expressed in terms of error vectors and measured parameters as below:

$$S_{11} = \frac{\left(\frac{S_{11m} - E_{00}}{E_{10}\,E_{01}}\right)\left[1 + \frac{E_{22}\,(S_{22m} - E_{33})}{E_{32}\,E_{23}}\right] - E_{22}'\left(\frac{S_{21m} - E_{30}}{E_{32}\,E_{10}}\right)\left(\frac{S_{12m} - E_{03}}{E_{01}\,E_{23}}\right)}{D} \qquad (3.25)$$

$$S_{22} = \frac{\left(\frac{S_{22m} - E_{33}}{E_{32}\,E_{23}}\right)\left[1 + \frac{E_{11}\,(S_{11m} - E_{00})}{E_{10}\,E_{01}}\right] - E_{11}'\left(\frac{S_{21m} - E_{30}}{E_{32}\,E_{10}}\right)\left(\frac{S_{12m} - E_{03}}{E_{01}\,E_{23}}\right)}{D} \qquad (3.26)$$

$$S_{21} = \frac{\left[1 + \frac{(S_{22m} - E_{33})(E_{22} - E_{22}')}{E_{32}\,E_{23}}\right]\left[\frac{S_{21m} - E_{30}}{E_{32}\,E_{10}}\right]}{D} \qquad (3.27)$$

$$S_{12} = \frac{\left[1 + \frac{(S_{11m} - E_{00})(E_{11} - E_{11}')}{E_{10}\,E_{01}}\right]\left[\frac{S_{12m} - E_{03}}{E_{01}\,E_{23}}\right]}{D} \qquad (3.28)$$

WHERE

$$D = \left[1 + \frac{E_{11}\,(S_{11m} - E_{00})}{E_{10}\,E_{01}}\right]\left[1 + \frac{E_{22}\,(S_{22m} - E_{33})}{E_{32}\,E_{23}}\right] - E_{11}'\,E_{22}'\left(\frac{S_{21m} - E_{30}}{E_{32}\,E_{10}}\right)\left(\frac{S_{12m} - E_{03}}{E_{01}\,E_{23}}\right)$$

Details of the derivation of the four S-parameter equations are shown in Appendix III. By solving the equations explicitly, the time required to calculate the solutions is reduced significantly. Furthermore, equations (3.25) to (3.28) will also be used later for de-embedding FET parammeters from the test fixture.

4. THE ANA SYSTEM SOFTWARE FOR S-PARAMETER MEASUREMENT

INTRODUCTION

Most of the software for this project involved the design of a self prompting measurement system program for accurately characterizing any network device or microwave Field-Effect-Transistor. The developed system program is composed of various subprograms. Each subprogram is used for performing various functions such as initialization, data acquisition, error correction and de-embedding. The most significant feature of the program is that the developed data acquisition subprogram with the auto-remote control function has made the S-parameter measurement simpler and easier. As a result, minimal skill or knowledge is required to be able to accurately characterize any test device.

The structure of the system program and the function of the various subprograms will be described in the first section of this chapter. Several special techniques used for improving the measurement accuracy and the remaining unsolved errors due to the hardware limitations of the present modified ANA system will also be discussed. Finally, the performance and accuracy of this system in the reflection and transmission measurements of a few standard devices such as a short, an offset short, a through-line connector and an HP 30 dB attenuator will be presented.

4.1 Structure of the Measurement System Program

The measurement system program is written in BASIC for running on an HP-85 or HP-85 compatible desktop computer. Figure 4.1 shows how the program is divided into five sections. These are : Initialization and Selection, Data Acquisition, Error Correction, Measurement Results and De-embedding.

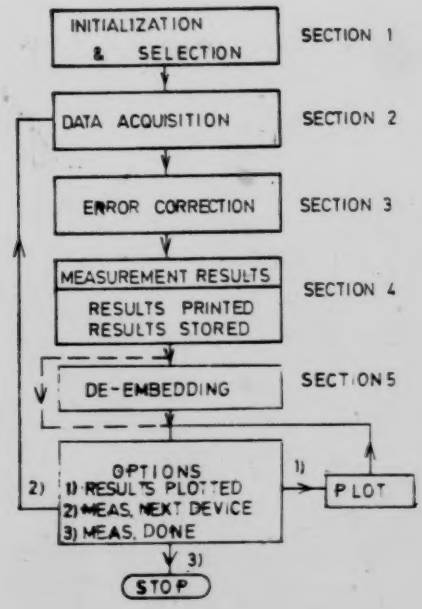

Figure 4.1 Block Diagram Outline of the Measurement System Program.

At the beginning of the system program, a subprogram named "*INITIAL-S" is called to allow the HP-85 to request the access to the Standard bus from the K-8073 microcomputer and to initialize the operation mode of all the I/O interfaces and the EIP575 frequency counter. Then, the

computer prompts the operator to enter various selections such as frequency range, one or two port measurement, sliding matched or standard-matched load and others. A data acquisition subprogram named "*ACQDA-S" is called to control all the instruments and acquire the calibration data and the parameters of a device under test (DUT). After all the data have been acquired, three subprograms'' are called to normalize the measurement data, calculate the error vectors and correct the four parameters explicitly. The measurement results are then stored and printed on the appropriate peripheral devices through the HP-IB bus. If the device under test is embedded in an HP11608A test fixture, a subprogram named "*DE-EMB-S" is called to de-embed the FET parameters from the fixture model. The flow chart of the complete system program is shown in Appendix IV and the details of each section are described as below.

a. Initialization and Selection

The HP-85 computer must first request the bus and set the operation mode of all the I/O interfaces before taking any measurements. The HP-85 requests the bus by toggling control line CTL0 of the HP-GPIO interface. Then, it enables output port B and sets the strobe-handshake mode for data transfer. The EIP575 frequency counter is also set by the HP-85 to 1-18 GHz range through the HP-IB bus. Before acquiring data, various subprograms are called for setting

---

'' "*NORM-S", "*12ERROR-S" and "*12CORR-S"

the operation mode of the 8255 Programmable Peripheral Interface (PPI) on the I/O peripheral modules. The "*INITRE-S" subprogram is called to set the 8255 PPI on the K-8073 board to the output mode for remote control of all the instruments. The "*14INIT-S" subprogram is called to set the 8255 PPI on the 14-bit D/A board to strobe-handshake output mode for controlling the RF frequency of the sweeper. The initialization is done after the "*ADINIT-S" subprogram is called to set the 8255 PPI to strobe-handshake input mode on the 12-bit A/D board for acquiring the horizontal and vertical outputs of the polar display.

After the initialization, the program outputs the instructions and the prompts on the CRT for the operator to make various selections. The operator is allowed to enter the desired start frequency, number of steps and step frequency. However, on account of the specified dimension of arrays in the program[1], the number of steps over the selected band must not exceed 11. If de-embedding is required to extract the FET parameters from the test fixture, the operator has to enter the step frequency for each band which is specified in the program and displayed on the CRT. The selected step frequency must be the same as when the parameters of the fixture model are calculated and stored[2]. The computer then prompts the operator to select, in sequence, the datafile for storing error vectors and

---

[1] The dimension of the arrays is limited by the size of the system memory.
[2] The details will be discussed in chapter 5.

measurement results, auto-remote or manual mode, one or two port measurement, flexible or semi-rigid through-connection calibrator, calibration done or not and sliding matched or standard-matched load. When "Calibration Done" is selected, the stored error vectors will automatically be loaded from the disc memory into the HP-85 system memory. Thus, no calibration is required in this case.

b. Data Acquisition

The "*ACQDA-S" subprogram is written for acquiring data through the I/O interfaces of the MCDAS. The D.C. offset is first measured and stored in array B before calibrating the error model of the ANA system and acquiring data for a device under test (DUT). The operating sequence for the ANA system error model calibration is displayed, one item at a time, on the CRT and the operator follows the instructions and connects the appropriate calibrator. If the "Auto-Remote" mode is selected, the I.F. gain setting, input attenuation switches, S-parameter switches and RF frequencies are operated under remote control. Thus, device under test can be fully characterized automatically.

For characterizing any two-port device, 12 calibrations are required to calculate the full (12 terms) error vectors of the ANA system. However, only 3 calibrations (match, short, open) are sufficient to characterize any one-port device accurately. The calibrators used for calibrating a two-port measurement are a short, an open, a

standard-matched or a sliding matched load and a through-connection cable. Since it is difficult to provide a high quality fixed coaxial 50 ohm termination, a sliding matched load is used to separate the reflection of a somewhat imperfect termination from the actual effective directivity so that better measurement accuracy can be obtained. At each frequency, moving the sliding matched load with respect to the measurement plane produces a complete circle when the load is displayed over one-half wavelength at the test frequency. The measured effective directivity is the vector sum of the actual reflection coefficient (radius) and the actual effective directivity (center) of the sliding matched load. Therefore, an additional subroutine using matrix operations[21] is invoked to compute the center of the circle. The latter requires measuring the sliding matched load at 6 positions at each test frequency.

Each data point, being the averaged result of 20 individual data points, is a complex number whose real and imaginary parts are the X and Y output of the polar display respectively. The speed of the data acquisition in the ANA system is slow compared with that of the commercial system because of the slow strobe-handshake mode used for transferring data from the A/D converter to the HP-85 computer. Nevertheless, it is still ten times faster than using the conventional point-by-point technique. All the data acquired including the D.C. offset, the calibration

---

[21] The equations for calculating the center of the circle are presented in Appendix V.

data and the raw measured S-parameters of an unknown device are stored in arrays B, A, and C respectively. When the calibration is finished, a flag is set to indicate that no further calibration is required for measurement on the next device.

c. Error Correction

A subprogram named "*NORM-S" is called to subtract the D.C. offset error from the measured data and to normalize the data to the reference I.F. gain. Each measured data point is the sum of the actual data and the D.C. offset error. Therefore, the D.C. offset error has to be subtracted from the measured data. The setting of the I.F. gain is varied from time to time during each calibration and device measurement in order to have the dot appear as close as possible to the outer edge of the polar display. In this manner, optimal sensitivity of measurement is achieved. In practice, usually a reference value[22] of 24 dB I.F. gain is taken, and all the subsequent measurements will be referenced to this gain.

After correction for the D.C. offset error and following normalizing of all measured data, a subprogram named "*12ERROR-S" is called to calculate the error vectors of the ANA system by solving the 12 error vector equations (found in chapter 3). If a flexible-cable through calibrator is selected at the beginning of the program, the magnitude

---

[22] The reference gain is the I.F. gain set for a short circiut calibrator.

and phase of the transmission coefficient of the calibrator in the error vector equations will automatically be set to 1 and 0 respectively. The calculated error vectors are then stored on disc and can be retrieved at any time for entry into the HP-85 system memory. However, the temperature in the ANA system and the A/D converter may be different between the time one does the calibration and the time one does the measurement on the unknown devices. This difference may degrade the measurement accuracy. Figure 4.2 shows how the D.C. offset voltage acquired by the 12-bit A/D converter varies with time following the application of power to the ANA system. The curve is almost flat after two hours. Therefore, the ANA system has to be turned on for two or three hours prior to any calibration so that there is enough time for the equipment to reach a steady state temperature.

Having calculated and stored the error vectors, a subprogram named "*12CORR-S" is called to solve equations (3.25)-(3.28). The explicit solutions obtained are the corrected S-parameters of the device under test.

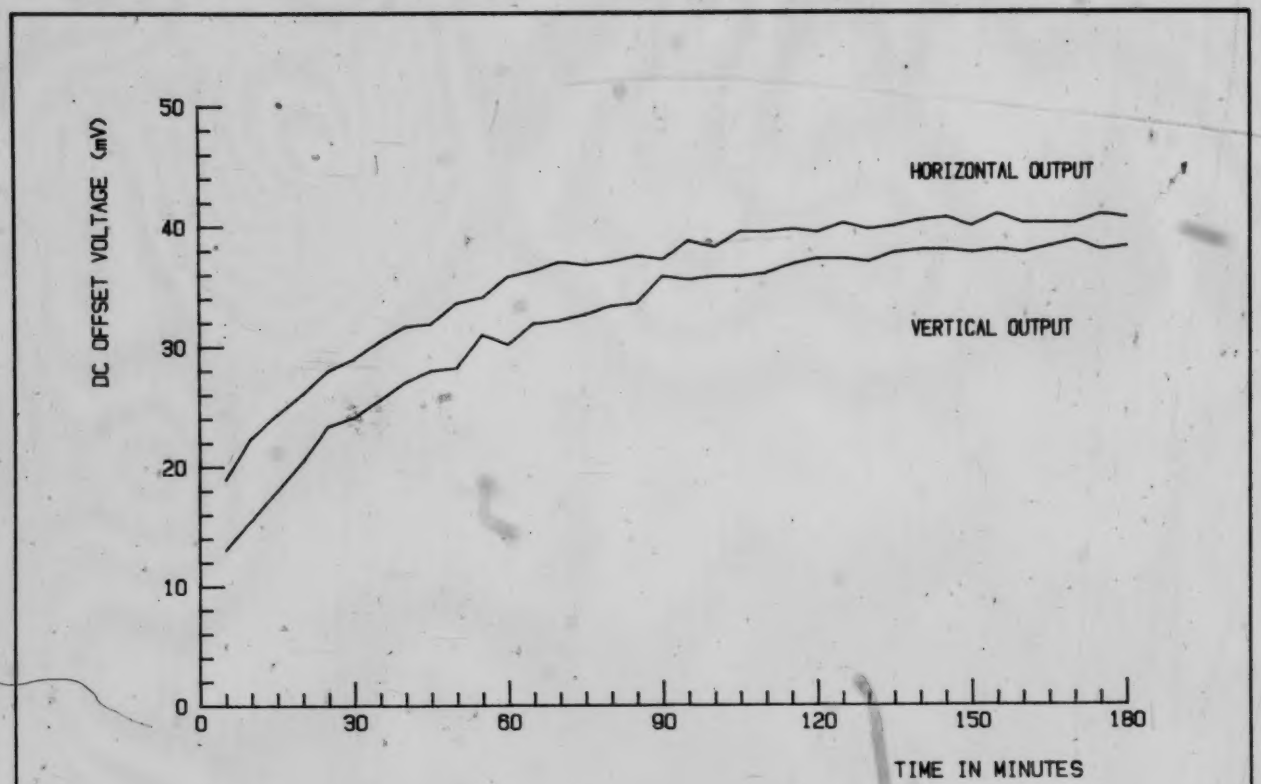

FIG 4.2 The Variation of the Horizontal and Vertical DC Offset Voltages With Time

d. Measurement Results

When the measurement of the first device under test is done, the error vector data are stored in the file named "CXERRDAT" where CX is selected by the operator at the beginning of the program and X varies from 1 to 10. If the error vectors have, in fact, been stored, no further calibration is required for subsequent measurements on an unknown device. The resulting corrected S-parameters for each unknown device, relating to the same set of calibration data, is stored in a datafile named "CXYRESDAT" in an ascending order where Y varies from 1 to 10. Thus, the maximum number of datafiles for storing the corrected results is 10 which is usually more than sufficient. When the value of Y reaches 10, it will reset to 1 automatically. If there are more than 10 devices to be measured, the result of the eleventh and subsequent devices will be stored in a datafile with Y starting over again beginning with 1. The previously stored results will be overwritten. After the corrected results for each device have been stored, the HP-85 prompts the operator to enter the title for the result and then to print the results on an external printer[23].

e. De-embedding

The parameters of an HP11608A test fixture modelled in three discrete frequency bands (1-2 GHz, 2-4 GHz and 8-12 GHz) are stored in the disc memory. When de-embedding is

---

[23] The printer used is an HP82905B Printer.

required for extracting FET parameters from the test fixture, a subprogram named "*DE-EMB-S" is called. The fixture parameters and the measured embedded parameters are loaded into the arrays E and C respectively from the disc memory. Then, a simplified version of the 12-term error correction subprogram named "*10CORR-S" is called to obtain the solution explicitly. Details of the de-embedding technique and procedure are described in the next chapter.

At the end of the measurement, three options are displayed on the CRT from which the operator is allowed to select one by simply pushing one of the special keys K1, K2 or K3. This corresponds to instructing the computer (1) to plot the results on a Smith Chart, (2) to measure the next device, or (3) to end the measurement. When the plotting command is selected, a subprogram named "SMITH-S" is called which is able to plot any one of the four parameters of a measured device on a simplified Smith chart. After the results have been plotted, three options are displayed again on the CRT so that the operator is allowed to either plot other results or go on measuring the next test device. Although the developed system program is not listed in the thesis, a copy of the complete program is available (if requested) from the Microwave Power Laboratory, Electrical Engineering Department, University of Alberta.

4.2 Software Techniques For Improving Measurement Accuracy

Although all the internal systematic errors are corrected using the 12-term error model, there are other sources of error which affect the absolute accuracy of the measurement result. These errors are: Noise error, Fringing Capacitance Error of an Open Circuit, System Calibration Error, Harmonic Skip Error, Quadrature Error, Error in Standard Calibration, Resonance Error and Random Errors. The effects of the first three errors on the measurement can be reduced significantly by using some special software techniques. The software actually applied to correction of these errors is described below.

a. Noise Error

Over the frequency range (1-18 GHz) of a sliding matched load[24], the reflection coefficient in terms of system signal/noise ratio can vary from 20 dB to as low as 3 dB. The signal/noise ratio decreases further if the I.F. gain control is set to the remote mode because of the additional noise introduced by the insertion of a digital attenuator in the network analyser. This error can be over 100% in S_{11} the reflection coefficient measurement. Moreover, by inspection of the solutions of the corrected S-parameter, it can be seen that the term S_{11} appears in all four equations[25]. Thus, the noise in the measured S_{11} will be tranferred to the other measured S-parameters also. In

---

[24] HP 907A coaxial sliding load.
[25] Equation (3.25) to (3.28)

addition, it can have a serious effect on the insertion loss measurement. Therefore, the use of software averaging plus a low-pass filter[24] become essential to define a reasonably invariant result.

Hand [20] and Cobb [24] have made a detailed study of the noise error. Some measurements have been carried out by Cobb to evaluate the variance of the sampled value. Useful results were presented by Cobb showing that the variance is inversely proportional to the square root of the number of samples acquired. If the number of samples acquired is doubled, the measurement time will be doubled too. However, the measurement accuracy will not be improved by a factor of two. Therefore, the amount of data acquired for averaging has to be optimized.

When a matched load is connected to the test set, a dot of approximately 8 dB signal/noise ratio is displayed on the polar display unit. With this signal/noise ratio, the number of samples required for less than 5% variance is in the region of 15 or 16[27]. In this project, more data samples are acquired in order to achieve better measurement accuracy. However, the speed of data transfer using the strobe-handshake mode of the HP-GPIO interface is slow. Therefore, there is a limit on the number of data samples that the ANA system can acquire for data averaging purposes. The reflection measurement results of a direct short device

---

[24] A filter with 5.9 KHz cut off frequency which by-passes most of the noise at 8 KHz.
[27] Refer to the Figure given by Cobb in [24]

using 10, 20, 30 and 40 data samples for averaging, together with the calculated standard deviation were obtained. These results showed that 20 data samples for averaging was a good compromise as far as speed and accuracy were concerned. When 20 was chosen to be the number of samples acquired for data averaging, the operator was able to finish 12 calibrations within one hour and to measure all parameters of each test device every 15 to 20 minutes.

b. Fringing Capacitance Error of an Open-Circuit

An open-circuit is used as one of the calibrators for obtaining the error model of the ANA system. In practice, an open-circuit has an associated fringing capacitance. This capacitance has to be known and must be included in the program for calculating the error vectors. The incorrectly specified capacitance of an open-circuit causes the measured reflection coefficient of an unknown device to be in error both in magnitude and phase by an amount that is independent of the network analyser error model.

The incorrect calibration of the ANA system caused by using the wrong value of capacitance has been studied by Rytting from Hewlett Packard [28] and Ambrose [29]. Rytting modelled this capacitance as a power series of frequency as given by:

$$Cf = 0.079 + 0.00004*f*f \text{ pF/GHz}^2$$

However, Ambrose modelled this capacitance as a linear frequency dependent value as represented by the expression:

$$Cf = 0.06 + 0.002*f \text{ pF/GHz}$$

By modelling the capacitance either as a power series of frequency, or as a linear function of frequency, the error was reduced to less than 0.3 dB peak-to-peak. Figure 4.3 and Figure 4.4 show the results obtained from measuring the reflection coefficient of a 10.38 cm offset short device with various values of modelled open-circuit fringing capacitance in the 1-2 GHz and 8-12 GHz frequency ranges respectively. It was found from the results that using the Rytting capacitance model was more satisfactory.

c. Calibration Error

The conventional method for calibrating the analyser described in HP Application Note 117-1 [30] has the disadvantage of being used to measure both the reflection and transmission coefficient of an unknown device. The reasons for considering this a disadvantage are given below.

Since the frequency vector ratio voltmeter of the network analyser measures the amplitude ratio and phase difference between the reference and test channels, the test set has to be calibrated prior to any measurement by connecting the appropriate reference line at the rear panel and adjusting the Reference Plane Extension on the front

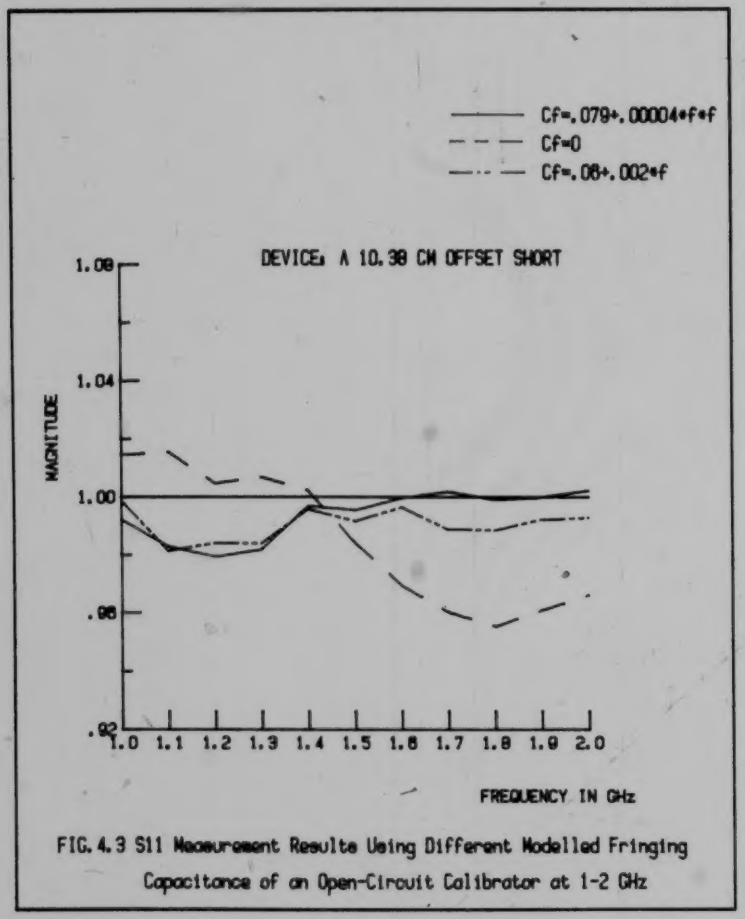

FIG. 4.3 S11 Measurement Results Using Different Modelled Fringing Capacitance of an Open-Circuit Calibrator at 1-2 GHz

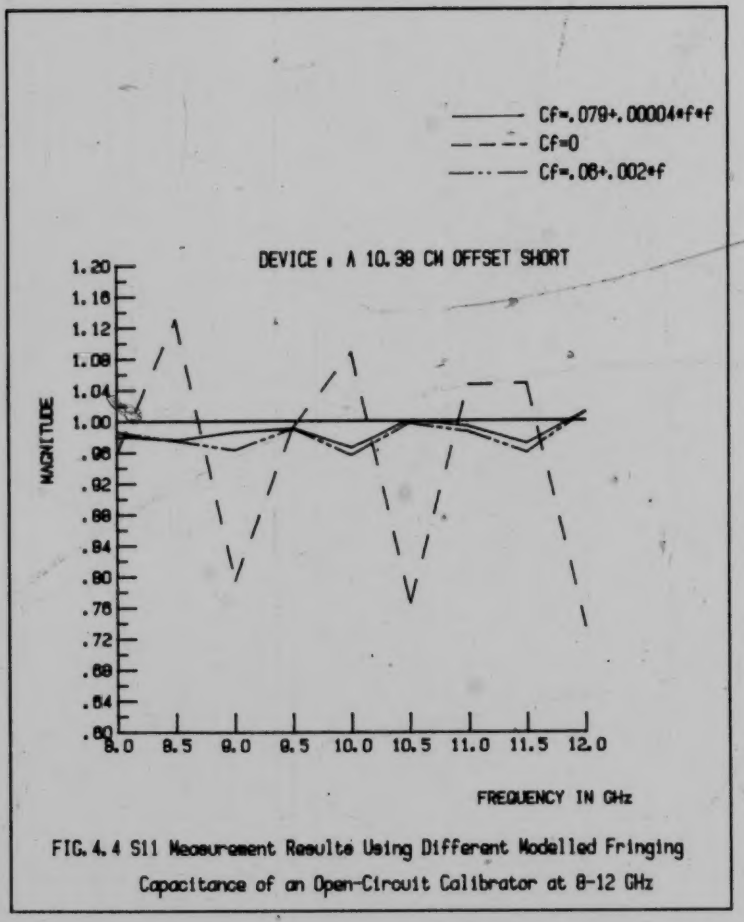

FIG. 4.4 S11 Measurement Results Using Different Modelled Fringing Capacitance of an Open-Circuit Calibrator at 8-12 GHz

panel to achieve equal path lengths in both channels. However, the path lengths of the test channel are different for reflection and transmission measurements. Therefore, the calibration of the test set for the two measurements is not the same. Consequently, every time the system is switched from reflection to transmission measurement or vice versa, a different reference line has to be connected at the rear panel and the Reference Plane Extension has to be reset. Every time the Reference Plane Extension is reset, an error of 0.1-0.3 mm in electrical length occurs. This error becomes more significant at or above 8-12 GHz. Besides introducing error in measuring the S-parameters, this method is undesirable because of its inconvenience.

With the enhancement program in the ANA system program, it is no longer necessary to calibrate the test set before measurement. During the calibration and device measurements, the path lengths of the test and reference channels may not be equal. As a result, the readings from the frequency vector ratio voltmeter of the network analyser are uncorrected. However, such errors are taken into account in the 12-term error and they will be fully corrected in the enhancement program. Thus, the new calibration procedure for the operation of the ANA system is simplified and the additional errors caused by setting and resetting the Reference Plane Extension are eliminated.

4.3 Other Errors Affecting the Measurement Accuracy

The remaining errors mentioned in section 4.2 are caused by technical limitations of the equipment of the present ANA system. The first error is called Harmonic Skip Error. The phase lock circuitry of the HP 8410A network analyser essentially tunes the frequency of a 65-150 MHz oscillator in the HP 8411A harmonic frequency converter until some harmonic of this oscillator beats in a mixer with the unknown reference input microwave signal to produce a 20.278 MHz I.F. gain signal. However, Harmonic Skip Error can occur when the receiver selects a different harmonic for the same R.F. frequency in going from the calibration procedure to the measurement procedure. The power of the local oscillator in the harmonic frequency converter varies from one harmonic to another. This causes ± 0.25 dB and 2° variation in the measurements[2*]. This error can be eliminated if a source phase-lock subsystem is added to the ANA system. The subsystem basically consists of a synthesizer and a synchronizer. Details of the differences in measurement uncertainties using the ANA system with and without the phase-lock subsystem including the equations and results, are described by Adam [8].

The second error is called Quadrature Error of the polar display. In the present ANA system, the magnitude and the angle of the measured data are taken from the outputs of the 8414A polar display. As a result of test-to-reference

---

[2*] These figures are given in HP Application Note 221[25].

channel leakage within the polar display, the actually displayed magnitude of a constant magnitude varying phase dot changes by as much as ±0.25 dB as a function of phase. An HP 8412A rectangular display unit does not exhibit this problem. If it were added to the ANA system to provide the magnitude data, the measurement accuracy could be further improved. Although a rectangular display unit is available in the laboratory, an additional HP8418 auxillary display holder is needed to house the rectangular display. The cost for purchasing this unit is approximately $6,000.

The third error called "Error in Standard Calibration" is described by Adam [5,8]. Experimentally he found the errors caused by imperfections of the standard calibrators (matched load, open, short) used in reflection coefficient measurements to be less than 0.009 in magnitude. Thus, this error is negligible in comparison with the previous two errors.

The fourth error is introduced as the result of the resonance of the ANA system at certain test frequencies when a DUT is connected. This error may cause high measurement uncertainties at certain frequencies. Although these four errors plus the Random Errors described in chapter three remain in the present ANA system, the measurement accuracy in characterizing a two-port device is found to be satisfactory, based on measurement results obtained for some standard devices. The performance and accuracy of the system will be discussed in more detail in the following section.

4.4 Performance and Measurement Accuracy of the ANA System

The performance of the system hardware and software can be verified by measuring various types of standard test devices. In this project, a direct short and a 10.38 cm offset short were chosen as the standard test devices for one-port measurement. The 10.38 cm offset short was composed of an HP 10.38 cm air-line terminated with a direct short at one end. For two-port measurements, a modified HP reference line coaxial cable[2] and an HP 30 dB attenuator were used to test the accuracy of the ANA system for measuring devices with high transmission coefficients and high return losses respectively. The measurement errors were obtained by comparing the measured data with either the calculated data, or with the specifications of the standard devices. From these results, the performance and accuracy of the ANA system can, thus, be derived.

For one-port measurements, the accuracy of the ANA system was tested by measuring the reflection coefficients of two standard devices: a direct short and a 10.38 cm offset short. With the assumption that the two devices were lossless and the offset short was exactly 10.38 cm in electrical length, the reference data of the two devices were calculated. Hence, the measurement error estimates were obtained by comparing the measured data with the calculated data. The measured data of the two devices together with the calculated data and errors are listed in Table 4.1

---

[2] An HP model 11604-20021 reference line cable was bent to fit the test ports of the test set.

Device : A direct short circuit							
Freq (GHz)	measurement result S_{11} Mag	Ang	calculation result S_{11} Mag	Ang	error magnitude in %	dB	phase in degree
1.00	1.000	-179.9	1.00	-180.0	0.0	0.00	0.1
1.10	1.011	-179.9	1.00	-180.0	1.1	0.09	0.1
1.20	1.001	-179.9	1.00	-180.0	0.1	0.00	0.1
1.30	1.001	-179.9	1.00	-180.0	0.1	0.00	0.1
1.40	1.000	-179.9	1.00	-180.0	0.0	0.00	0.1
1.50	1.007	-179.6	1.00	-180.0	0.7	0.06	0.4
1.60	0.999	-179.9	1.00	-180.0	0.1	0.00	0.1
1.70	1.001	-179.9	1.00	-180.0	0.1	0.00	0.1
1.80	1.001	-179.9	1.00	-180.0	0.1	0.00	0.1
1.90	1.000	-179.9	1.00	-180.0	0.0	0.00	0.1
2.00	1.001	-179.9	1.00	-180.0	0.1	0.00	0.1
8.00	0.997	-180.0	1.00	-180.0	0.3	0.03	0.0
8.50	1.000	180.0	1.00	-180.0	0.0	0.00	0.0
9.00	0.997	-179.9	1.00	-180.0	0.3	0.03	0.1
9.50	1.002	179.9	1.00	-180.0	0.2	0.02	0.1
10.0	0.998	-180.0	1.00	-180.0	0.2	0.02	0.0
10.5	1.001	180.0	1.00	-180.0	0.1	0.00	0.0
11.0	0.999	-180.0	1.00	-180.0	0.1	0.00	0.0
11.5	1.001	-180.0	1.00	-180.0	0.1	0.00	0.0
12.0	0.999	-179.9	1.00	-180.0	0.1	0.00	0.1

Table 4.1 The Reflection Measurement Errors of a Direct Short Device at 1-2 GHz and 8-12 GHz.

Device : A 10.38 cm air-line terminated with a short							
Freq (GHz)	measurement result S_{11} Mag	Ang	calculation result S_{11} Mag	Ang	error magnitude in %	dB	phase in degree
1.00	0.993	-68.2	1.00	-69.1	0.7	0.06	0.9
1.10	0.994	-92.8	1.00	-94.0	0.6	0.05	1.3
1.20	0.979	-118.4	1.00	-118.9	2.1	0.18	0.6
1.30	0.987	-141.8	1.00	-143.9	1.3	0.11	2.0
1.40	0.994	-168.0	1.00	-168.8	0.6	0.05	0.7
1.50	0.998	166.2	1.00	166.3	0.2	0.02	0.1
1.60	0.987	140.8	1.00	141.4	1.3	0.11	0.6
1.70	0.996	115.9	1.00	116.5	0.4	0.04	0.6
1.80	0.994	90.5	1.00	91.6	0.6	0.05	1.1
1.90	0.996	65.0	1.00	66.7	0.4	0.04	1.7
2.00	0.999	40.4	1.00	41.8	0.1	0.01	1.4
8.00	0.989	-15.5	1.00	-13.0	1.1	0.10	2.5
8.50	0.980	-139.4	1.00	-137.5	2.0	0.18	1.9
9.00	0.985	98.4	1.00	97.9	1.5	0.13	0.5
9.50	0.988	-29.4	1.00	-26.6	1.2	0.11	2.8
10.0	0.963	-153.2	1.00	-151.2	3.7	0.33	2.0
10.5	1.027	84.1	1.00	84.2	2.7	0.23	0.2
11.0	0.987	-42.7	1.00	-40.3	1.3	0.11	2.4
11.5	0.966	-166.1	1.00	-164.9	3.4	0.30	1.2
12.0	1.007	69.1	1.00	70.6	0.7	0.06	1.5

Table 4.2 The Reflection Measurement Errors of an Offset Short Device at 1-2 GHz and 8-12 GHz.

and Table 4.2. From these results, the error for one-port measurements was found to be within ±3.7 % in magnitude and ±2.8° in phase over 8 to 12 GHz frequency range.

The measurement accuracy of the ANA system was further tested by performing some two-port measurements on a modified HP reference line and an HP 30 dB attenuator. Based on the known characteristics of the reference line, the transmission coefficients (magnitude and phase) were computed for purposes of comparison to measured values and hence the errors were known. The measurement errors over the 1-2 GHz and 8-12 GHz frequency ranges are not only listed in Table 4.3 but are also plotted as shown in Figure 4.5 and Figure 4.6. From these figures, the transmission measurement error was found to be within ±2.2 % in magnitude and ±2° in phase over 8 to 12 GHz frequency range. To test the accuracy of the system in measuring a high trasnsmission loss device, an HP 30 dB standard attenuator was used as the test device. The measurement results are listed in Table 4.4. By comparing the measured results with the specified attenuation of the test device, the error found was within ±0.46 dB over the 1-2 GHz and 8-12 GHz frequency ranges.

Furthermore, the improvement of the measurement accuracy using the ANA system with the enhancement program operative is illustrated in Figure 4.7 and Figure 4.8. The corrected measured data, the uncorrected measured data and the calculated reference data of the modified HP reference line were plotted on a simplified Smith Chart. If the

Device : A through-line connector with electrical length equal to 56.44 cm							
Freq (GHz)	measurement result S_{21} Mag	Ang	calculation result S_{21} Mag	Ang	error in magnitude %	dB	phase degree
1.00	0.989	42.2	.9897	42.7	0.1	0.01	0.6
1.10	0.996	-25.6	.9891	-25.0	0.7	0.06	0.6
1.20	0.987	-93.5	.9887	-92.7	0.2	0.02	0.8
1.30	0.992	-161.4	.9882	-160.5	0.4	0.03	0.9
1.40	0.994	131.7	.9876	131.8	0.6	0.06	0.1
1.50	0.986	63.3	.9871	64.0	0.1	0.01	0.7
1.60	0.990	-3.8	.9866	-3.7	0.3	0.03	0.1
1.70	0.996	-70.0	.9861	-71.4	1.0	0.09	1.3
1.80	0.974	-138.4	.9855	-139.1	1.2	0.10	0.7
1.90	0.979	153.2	.9851	153.2	0.6	0.05	0.0
2.00	0.978	84.4	.9845	85.4	0.7	0.06	1.0
8.00	0.978	-20.2	.9647	-18.2	1.4	0.12	1.9
8.50	0.962	2.6	.9633	3.1	0.1	0.01	0.5
9.00	0.969	22.5	.9618	24.5	0.7	0.07	2.0
9.50	0.966	45.5	.9604	45.8	0.6	0.05	0.4
10.0	0.968	65.5	.9590	67.2	0.9	0.08	2.0
10.5	0.956	88.0	.9575	88.6	0.2	0.01	0.6
11.0	0.962	108.5	.9560	109.9	0.6	0.05	1.4
11.5	0.952	131.2	.9547	131.3	0.3	0.03	0.1
12.0	0.973	152.1	.9532	152.6	2.2	0.18	0.6

Table 4.3 The Transmission Measurement Errors of a Through-Line Connector at 1-2 GHz and 8-12 GHz.

Device: An HP 30 dB Attenuator				
Freq GHz	Measured Attenuation (Mag)	(dB)	Measurement Errors in (dB)	Specifications Given by HP in (dB)
1.0	0.031	30.17		
1.1	0.030	30.46		
1.2	0.030	30.46		
1.3	0.031	30.17		
1.4	0.030	30.46	30 + 0.46 dB	30 ± 1 dB
1.5	0.031	30.17		
1.6	0.030	30.46		
1.7	0.030	30.46		
1.8	0.031	30.17		
1.9	0.031	30.17		
2.0	0.031	30.17		
8.0	0.032	29.90		
8.5	0.032	29.90		
9.0	0.032	29.90		
9.5	0.031	30.17		
10.0	0.031	30.17	30 + 0.46 dB	30 ± 1 dB
10.5	0.031	30.17	- 0.10 dB	
11.0	0.030	30.46		
11.5	0.032	29.90		
12.0	0.032	29.90		

Table 4.4 The Measurement Errors of an Hp 30 dB Attenuator at 1-2 GHz and 8-12 GHz.

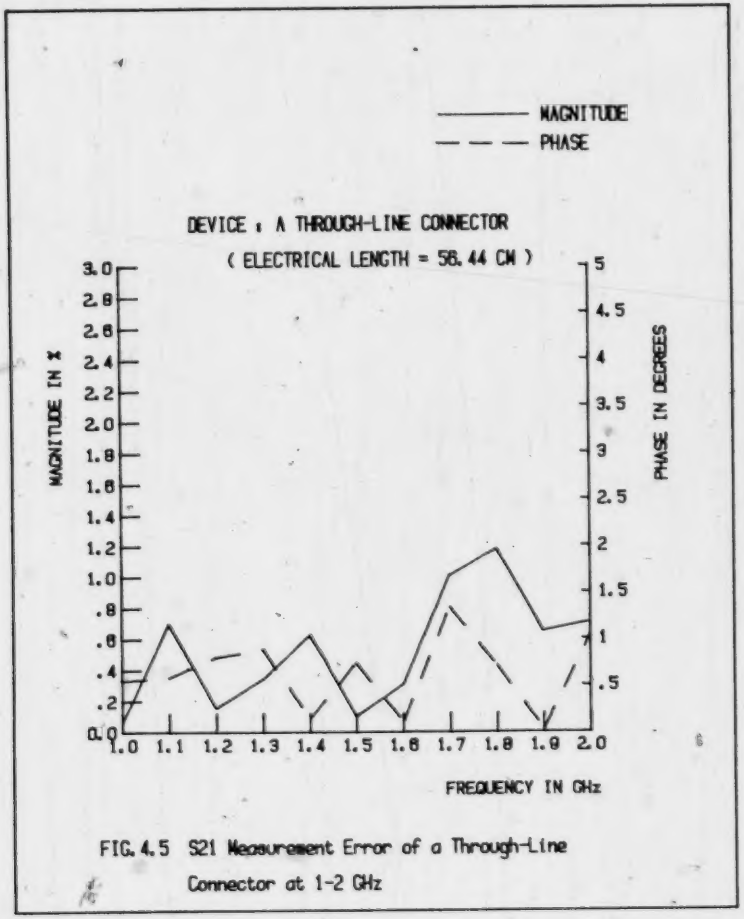

FIG. 4.5 S21 Measurement Error of a Through-Line Connector at 1-2 GHz

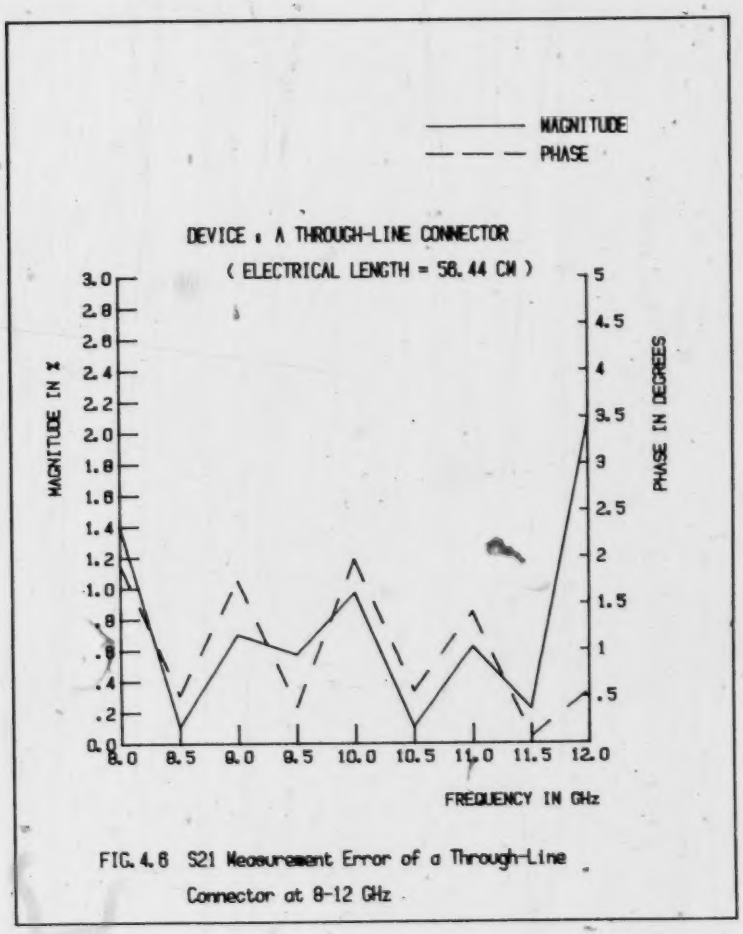

FIG. 4.6 S21 Measurement Error of a Through-Line Connector at 8-12 GHz

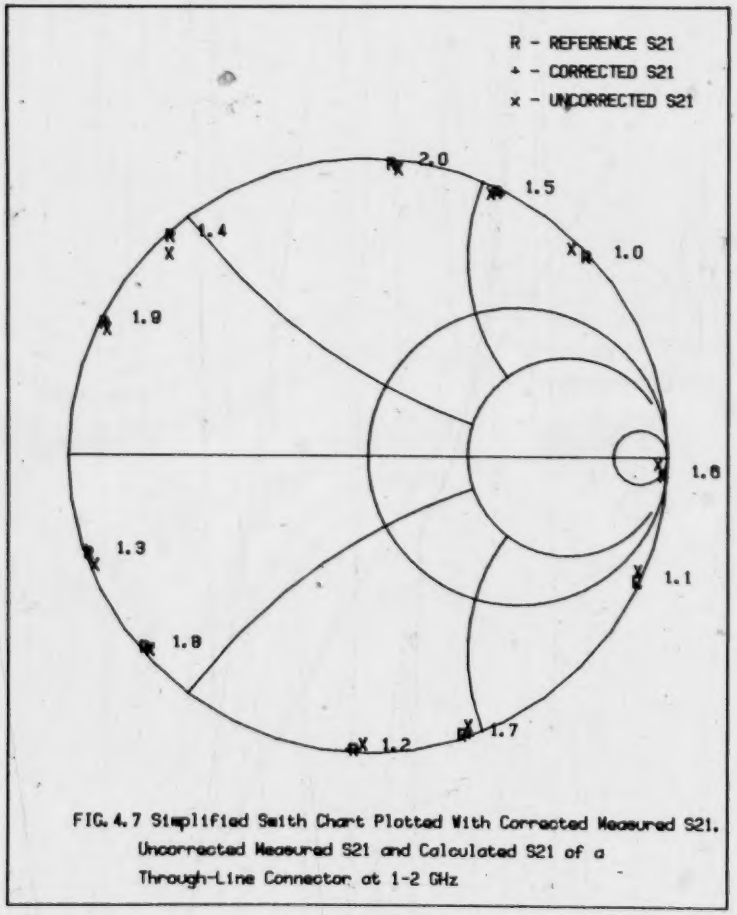

FIG. 4.7 Simplified Smith Chart Plotted With Corrected Measured S21. Uncorrected Measured S21 and Calculated S21 of a Through-Line Connector at 1-2 GHz

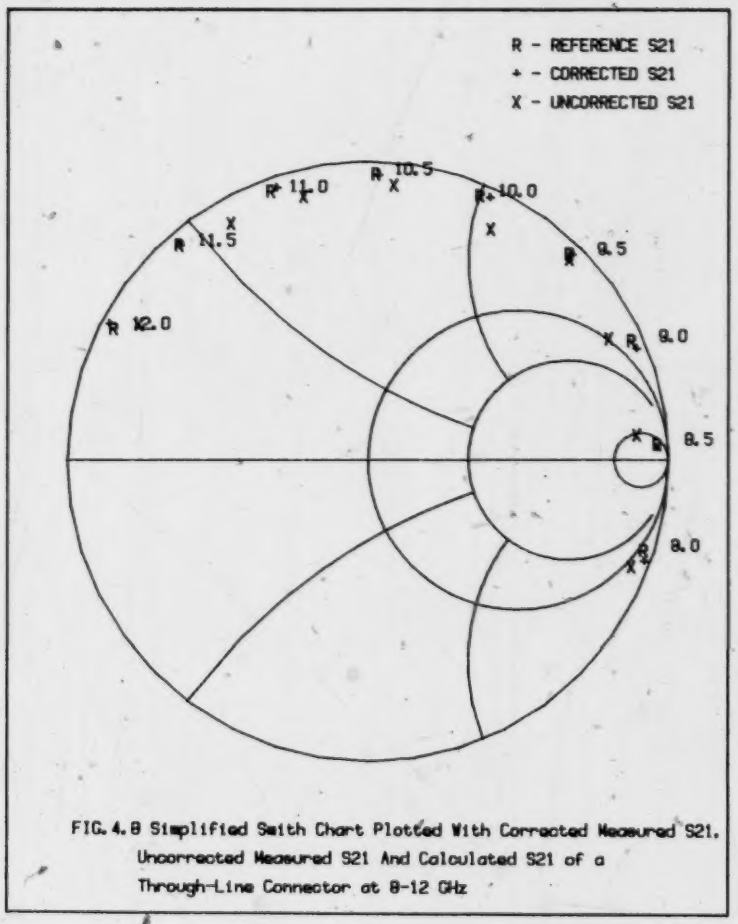

FIG. 4.8 Simplified Smith Chart Plotted With Corrected Measured S21. Uncorrected Measured S21 And Calculated S21 of a Through-Line Connector at 8-12 GHz

measured values are correct, the measured data should coincide with the reference data. These figures readily demonstrate that the enhancement program significantly improves accuracy.

However, it should be pointed out that the comparisons made on a limited number of components do not define the absolute measurement accuracy of the ANA for all possible networks. It merely provides an indication of the accuracy that may be expected. A complete study of the accuracy obtainable was deemed to be beyond the scope of the present project.

5. CHARACTERIZATION OF LOW-NOISE FET PARAMETERS

INTRODUCTION

When characterizing a microwave Field-Effect-Transistor (FET) by its S-parameters, the FET is usually mounted in a microstrip test fixture. An electrical network model of such a fixture is shown in Figure 5.1.

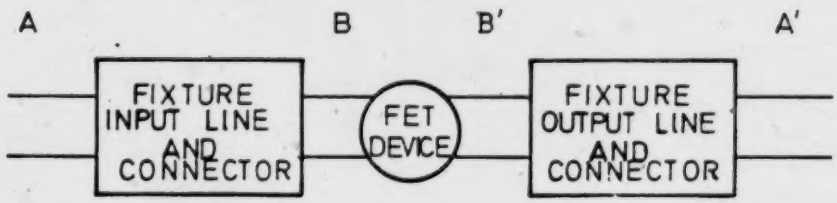

Figure 5.1 Network Model of a Device Embedded in a Test Fixture.

All ANA system measurements of the S-parameters are actually made at reference planes A and A'. Therefore, the S-parameters of the FET must be de-embedded by subtracting the effects of the fixture from the measured S-parameters. Various de-embedding methods have been used but the method developed in this project is based on the signal flowgraph.

The equivalent circuit model of an HP test fixture[30] is first found. The parameters of the input port and output port of the fixture are then computed and are subsequently stored in the disc memory. The technique used for extracting the corrected S-parameters from the error model is also used for de-embedding FET parameters from the test fixture. Details of the fixture modelling and the software involved in de-embedding FET parameters from the fixture will be discussed in this chapter. Furthermore, the ANA system together with the de-embedding software have been used for characterizing a few commercial low-noise microwave FETs and the results have been analysed. Thus, the performance of the ANA system for characterization of FET parameters is known. Further details are discussed below.

5.1 Methods for Characterization of FET Parameters

The characterization process involves both the measurement of the S-parameters at reference ports A and A' and the transformation of these same parameters to device ports B and B' (Figure 5.1). Various methods have been proposed for characterization of FET parameters. One method described by Ajose, Mathews and Aitchison [32] involved measurement of the input impedance at the connector ports by using open-circuit microstrip lines of different lengths. The scattering transfer matrix (T-matrix) of the input and output network were then computed and the device parameters

---

[30] HP 11608A test fixture

were obtained by matrix inversion. However, this excessively cumbersome method required changing the microstrip circuit eight times in order to minimize the error.

Another method was described by Cooper and Gupta [33]. In their method, the microstrip-to-coaxial transitions and the microstrip-to-device transitions were characterized. The first transition was characterized by placing a short circuit at its microstrip end, and by measuring the input reflection coefficient as a function of frequency. The parameters of the transition were then calculated to fit the measurement. The microstrip-to-device transition was characterized by placing a short where the device would be, and by then making similar measurements of the reflection coefficient. Having characterized the fixture, the S-parameters of the device were determined with the help of a network analysis computer program called MARTHA[3'] from the measured S-parameters at the test port of the analyser. Since details of the program MARTHA were not known, this method could not be used in this project.

A third method was proposed in the HP Application Note 117-1 [30]. In this method, the HP-11608A test fixture up to the planes of the FET mounting was represented by lengths of transmission lines. The lengths were compensated for by introducing equivalent line lengths in the reference channel of the network analyser. This method, though fast, was not accurate because of the excess reactance associated with

---

[3'] The MARTHA User's Manual is available at Massachusetts Institute Of Technology.

fixture discontinuities. Moreover, when the path length of the reference channel changed, the measurement reference plane would be shifted too. As a result, the reference plane as set for the error model calibration was no longer the same as that for device measurement. The corrected S-parameters obtained were, thus, invalid.

A fourth method proposed by Lane, Pollard, Maury and Fitzpatrick [34] was to design a universal test fixture for characterization of any packaged microwave transistor. The advantage of using this method was that the 12 coefficients of the error model could be computed up to the insert part of the fixture. Therefore, the only transition left to be modelled was the transition between the microstrip and the insert which could be modelled as a pi-network. However, this method required a double-ended 50 ohm load, a double-ended short circuit, a double-ended open circuit and a through insert for error model calibration. These calibrators are not easily fabricated and they were not yet available on the market at the time of writing of this thesis.

A fifth method named "A Two-Tier De-Embedding Technique" was described by Vaitkus and Scheitlin [35]. The de-embedding of the device parameters from the corrected measured values was based on the signal flowgraph. There were seven embedding terms in the signal flowgraph which were calculated by an iterative method from the measured S-parameters of the fixture inserted with 3 different

calibrators (a short, an open and a through). Once the embedding terms were determined, the de-embedded parameters of the device were obtained by solving a specific equation set derived by Vaitkus and Scheitlin [35]. These equations are the same equations as used for extracting the corrected S-parameters from a 10-term error model. This method avoided the need for fabricating an accurate 50 ohm matched calibrator at the insert of the fixture.

In this project, the method developed for FET characterization was based on the signal flowgraph as shown in Figure 5.2.

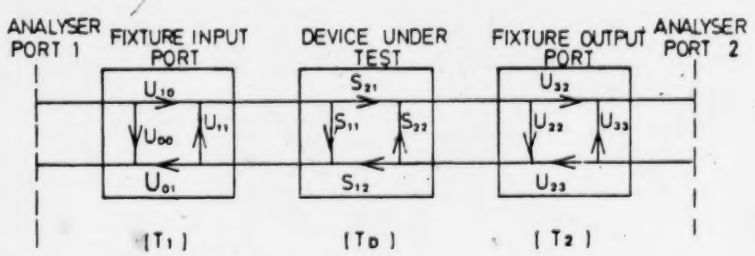

Figure 5.2 The Signal Flowgraph of a Device Embedded in a Test Fixture

The fixture network topology and all the initial values of the network elements were first determined. The equivalent circuit of the test fixture was obtained by least-squares fitting the fixture S-parameters to the measured

S-parameters using the computer program COMPACT.[33] The parameters of the input and output ports of the fixture were then computed from the modelled equivalent circuit using the same computer program. These parameters were the six embedded terms of the signal flowgraph shown in Figure 5.2 which could be treated as an 8-term error model. Hence, the technique used for extracting the corrected S-parameters of the test device from the error model was also used for de-embedding the FET parameters from the test fixture. Details of the developed de-embedding procedure will be described in section 5.23.

5.2 Fixture Modelling

The technique and procedure for modelling the HP-11608A test fixture are presented in this section. Although the network topology modelling and the calculations of the initial values are based on the HP fixture model, the principles can be applied equally well to any other test fixture.

5.2.1 Network Topology For Modelling the Test Fixture

The network topology for the overall fixture model is shown in Figure 5.3b. The input and output connectors of a test fixture were modelled as lengths of transmission lines

---

[33] Computerized Optimization of Microwave Passive and Active Circuits (COMPACT) was developed by the COMPACT Engineering Inc. to design linear circuits at R.F. or microwave frequencies.

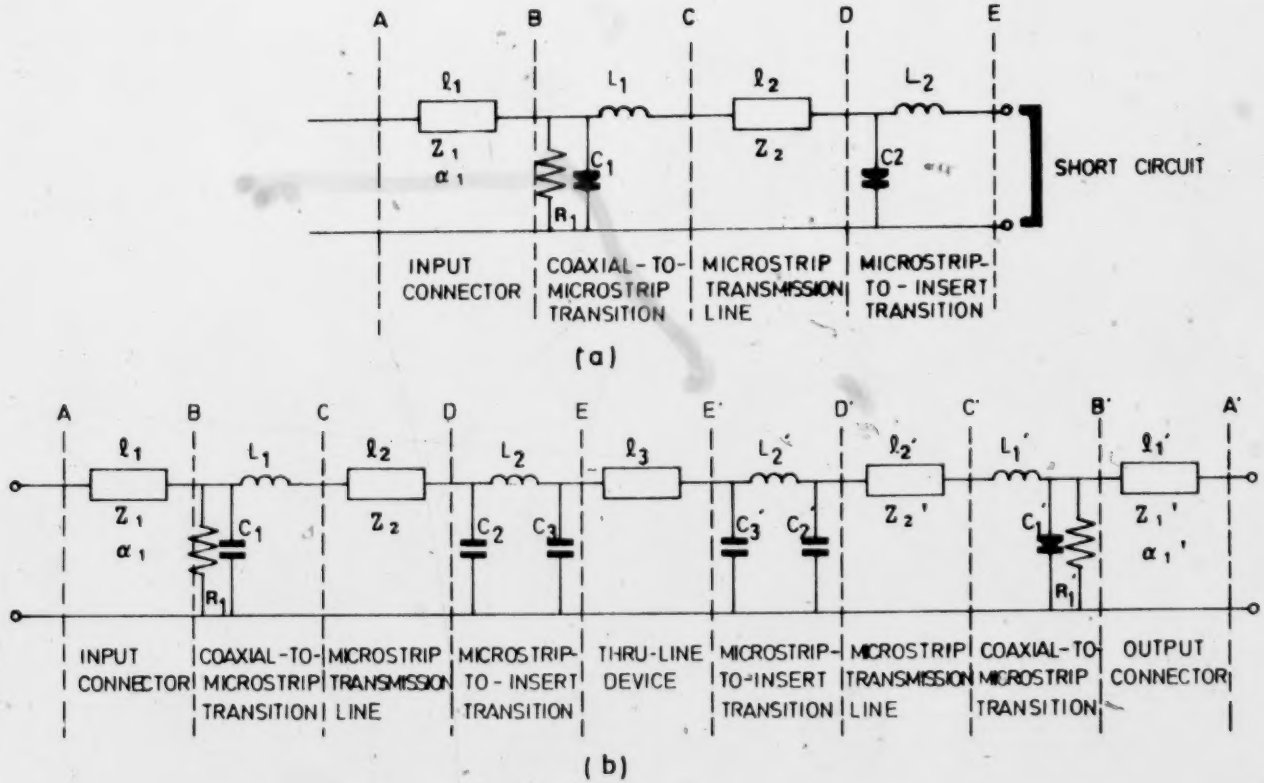

Figure 5.3 Network Topology for Modelling the Test Fixture
a) With a Short Inserted Calibrator
b) With a Through Inserted Calibrator

of impedances Z_1 and Z_1', lengths l_1 and l_1' and loss factors α_1 and α_1' respectively. The microstrip lines were modelled as lengths of transmission lines with Z_2, Z_2', l_2 and l_2'. The loss factors associated with the microstrip lines were assumed to be zero because the microstrip losses are relatively small and the microstrip lines are quite short. The modelling of the intermediate coaxial-to-microstrip transition has been studied by Wight, Jain, Chudobiak and Makios [36] who obtained a two element equivalent circuit model for a launcher transition. However, in modellling the HP-11608A test fixture, a resistor had to be added in parallel with the capacitor to account for the transition loss. Thus, the modelled launcher transitions at the input and output ports were represented by R_1, C_1, L_1 and R_1', C_1', L_1' respectively. Furthermore, the transitions between the microstrip and the device mounting at both ports were modelled as pi-networks [34] with C_2, L_2, C_3, C_2', L_2' and C_3'.

5.2.2 Calculation of the Initial Values of Elements

The HP test fixture was assumed to be symmetrical from either port to the center of the transistor mounting. Then

$$l_1=l_1';\ l_2=l_2';\ R_1=R_1';\ C_1=C_1'$$

$$C_2=C_2';\ C_3=C_3';\ L_1=L_1';\ L_2=L_2'$$

The required specifications for calculating the initial

value of each element of the network model were found from the HP11608A Operating Note [37] and were listed as follows:

a) The insertion loss from one port to the open end of the stripline: (one-half port-to-port)

0.15 dB + 0.04 x f (f in GHz)

b) Calibrator overall electrical length

Option 003 = 0.8 cm (through calibrator)

c) Physical length of microstrip : 1.046 cm (0.412 in)

d) Relative dielectric constant : 2.72 ±0.02

e) Dielectric thickness : 0.079 cm (0.031 in)

The steps for calculating the initial values of the elements are described as follows:

1) Calculation of l_2:

Physical length = 1.046 cm (0.412 in)

Electrical length = $1.046 \times \sqrt{2.72} = 1.72$ cm (0.679 in)

2) Calculation of l_1:

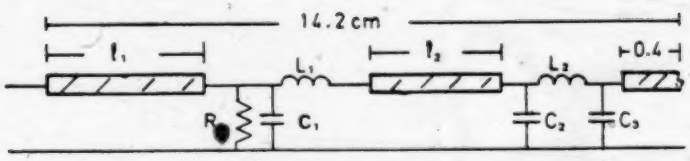

Figure 5.4 Equivalent Circuit of the Input Connector With a Through Line Inserted in the Fixture

Electrical length = $(14.2-0.4-l_2)$ cm

= (14.2-0.4-1.72) cm

= 12.08 cm (4.756 in)

3) Calculation of α_1 & R_1:

The total insertion loss of the fixture in reflection and transmission measurements is 2 x (0.15 + 0.04 x f) (dB)

$\therefore$ Total insertion loss = 0.3 + 0.08 x f (dB)

Let R_1 & α_1 account for the frequency-independent and frequency-dependent insertion losses respectively. Then, set the initial value of R_1 to be 1K ohms to account for 0.3 dB loss. Also set α_1 = 0.08 x f / l_1 (dB/cm).

For different frequencies, the corresponding values of α_1 are listed in the table below:

Frequency	Insertion Loss/Length(α_1)	
GHz	(dB/in)	(dB/cm)
1	0.0168	0.0066
2	0.0336	0.0132
8	0.135	0.0531

Table 5.1 The Insertion Loss Per Unit Length of the Input and Output lines of the Test Fixture , as a Function of Frequency.

4) Calculation of C_1 & L_1:

The parameters (L_1, C_1) of the launcher equivalent circuit of the HP fixture were obtained with the help of data[33] given by Wight [36]. ARM 2052-1124 SMA/Microstrip connectors were assumed to have been used at both input and output ports of the HP fixture since they were not identified specifically in the Operating Note. The parameters of the launcher equivalent circuit for various substrates at 10 GHz are listed in Table 5.2.

---

[33] The launcher equivalent circuit parameters for various launcher/substrate combinations at 10 GHz are presented in a table given by Wight [36].

Substrate			Launcher	
Dielectric	Substrate			
constant	thickness		ARM 2052-1124	
ϵ	h		ωL	ωC
	cm	in	ohm	mmho
23	0.00254	0.0010	31	14.5
9.9	0.00635	0.0025	50	7.0
9.9	0.00254	0.0010	60	8.0
2.72	0.00787	0.0031	12	13.0 * (HP fixture)

Table 5.2 The Launcher Equivalent Circuit Parameters for Various Substrates at 10 GHz.

The initial values of L_1 and C_1 were calculated from the last table entry as below:

$$\omega L_1 = 12$$

$$L_1 = 12 / 2\pi \times f$$

$$\therefore \quad L_1 = 12 / 2\pi \times 10^{10} = 0.19 \text{ nH}$$

$$\omega C_1 = 13 \times 10^{-3}$$

$$\therefore \quad C_1 = 13 \times 10^{-3} / 2\pi \times 10^{10} = 0.21 \text{ pF}$$

5) Values of C_2, C_3 and L_2:

From the suggested values given by Ajose [38], let the initial value of C_2 and C_3 be 0.03 pF and let L_2 be 0.2 nH.

6) Values of Z_1 and Z_2:

The initial values of line impedances Z_1 and Z_2 were chosen to be 50 ohms.

5.2.3 Actual Model of the Test Fixture

After the fixture network topology and all the initial values of the network elements were determined, the actual model of the fixture was obtained by least-square fitting the fixture model S-parameters to the measured S-parameters by means of the computer program COMPACT [39]. The COMPACT program computed the S-parameters of the model using the initial values of the circuit elements. The calculated S-parameters of the model were compared with the measured parameters and selected network elements were varied to minimize a predefined error function. For least-square fitting, the error function is defined in the following form

$$EF = \frac{1}{N} \sum_{F_1}^{F_n} W_1 \cdot |S_{11m} - S_{11c}|^2 + W_2 \cdot |S_{22m} - S_{22c}|^2 + W_3 \cdot |S_{21m} - S_{22c}|^2 + K|S_{12m} - S_{12c}|^2$$

where subscript m and c refer to the measured and calculated values of the S-parameters respectively and W_1, W_2, W_3 and W_4 are weighting factors.

The HP fixture was modelled in three discrete frequency bands: 1-2 GHz, 2-4 GHz and 8-12 GHz. Over each frequency band, two sets of corrected S-parameters of the fixture were measured using the ANA. One set corresponded to a short circuit calibrator inserted while the other corresponded to a through-connection calibrator inserted. These results were used for modelling the test fixture. The overall fixture model network in Figure 5.3b shows that there were more than 20 unknown elements whose values needed to be optimized. It was most unlikely that good optimization results would be obtained with many variables in the network. Therefore, the first set of S-parameters of the fixture with a short circuit calibrator inserted was first used for characterizing the coaxial-to-microstrip transition elements (R_1, C_1, L_1) and the transmission lines (l_1, l_2) of the network as shown in Figure 5.3a. Once the optimal values of these elements were found, the initial values were substituted in the overall fixture model network. The second set of S-parameters of the fixture with a through-connection calibrator inserted was then used for characterizing the rest of the elements and hence the final model of the fixture was obtained. Although the topology of the fixture remained the same throughout the 1 to 12 GHz range, the values of the elements were not the same for other frequency bands. Therefore, the fixture was modelled separately in three discrete frequency bands.

In characterizing the HP test fixture over three frequency bands, the difference between the measured and computed S-parameters using the COMPACT program was within ±0.07 in magnitude and less than ±4° in phase. The final values of all the elements in the 1-2 GHz frequency band are listed in Table 5.3. After the equivalent circuit of the test fixture model was found, the S-parameters (U_{00}, U_{11}, U_{10}, U_{01}, U_{22}, ...) of the fixture input and output ports shown in Figure 5.2 were computed with the aid of COMPACT.

5.3 De-Embedding Techniques

There are two schemes based on signal flowgraph methods for de-emdedding FET parameters from the fixture model. One method using matrix inversion was presented by Ajose [38]. In dealing with the cascade network as shown in Figure 5.2, the 2 x 2 scattering parameter matrix (S-matrix) is not the best network description because the resultant of two S-matrices in cascade cannot be obtained by simple multiplication. To overcome the difficulty, the scattering transfer matrix (T-matrix) was defined and obtained by rearranging the scattering relations[34] in order for the laws of matrix multiplication and inversion to be applicable. As a result, the following equation for the cascade network shown in Figure 5.2 can be set up:

$$[T_m] = [T_1]\,[T_d]\,[T_2]$$

Applying matrix multiplication and inversion, the above

---

[34] Details of the transformation from the S-matrix to the T-matrix can be found in [40].

Input and output coaxial connectors		Input circuit transition		Output circuit transition		microstrip transmission line
input	output	coaxial-to-microstrip	microstrip-to-insert	coaxial-to-microstrip	microstrip-to-insert	
Z_1=50 ohm	Z_1'=50 ohm	R_1=2.3K ohm	C_2=0.036 pF	R_1'=2.1K ohm	C_2'=0.037 pF	l_3 =0.677in
α_1=0.0114 dB/in (at 1 GHz)	α_1'=0.0117 dB/in (at 1 GHz)	C_1=0.228 pF	L_2=0.364 nH	C_1'=0.229 pF	L_2'=0.387 nH	l_3 =0.319in
		L_1=0.205 nH	C_3=0.035 pF	L_1'=0.212 nH	C_3'=0.037 pF	l_2'=0.677in
l_1=4.75in	l_1'=4.75in					Z_3=Z_2'=Z_3 =50 ohm

(All the above modelled values are specified in the frequency band of 1-2 GHz)

Table 5.3 Final Modelled Values of Elements in the Overall Fixture Model Network

equation can be rewritten as

$$[T_d] = [T_1]^{-1} [T_m] [T_2]^{-1}$$

The device matrix $[T_d]$ can be calculated if matrices $[T_1]$ and $[T_2]$ are known. Hence, the FET parameters can be obtained by re-transforming the result from the T-matrix to S-matrix format. The disadvantage of this method is that it requires extra work in transforming back and forth between the S and T matrices.

In this project, an alternate de-embedding method is used. It was simpler and easier when compared with the previous one. The technique used in this method is identical to the one used for extracting the corrected S-parameters from the ANA system error model. The signal flowgraph of the FET device embedded in the test fixture can be treated as an 8-term error model. If the Isolation Errors (E_{30}, E_{03}) and the Load Match Errors (E_{11}', E_{22}') are set to zero, the 12-term error model becomes an 8-term error model. Therefore, when eight terms of the error model (E_{00}, E_{11}, E_{22}, E_{33}, $E_{10}E_{01}$, $E_{32}E_{23}$, $E_{32}E_{10}$, $E_{23}E_{01}$) are replaced by the eight embedding terms of the fixture model (U_{00}, U_{11}, U_{22}, U_{33}, $U_{10}U_{01}$, $U_{32}U_{23}$, $U_{32}U_{10}$, $U_{23}U_{01}$), but with E_{30}, E_{03}, E_{11}' and E_{22}' set to zero, the same equations (3.25)-(3.28) and the same error correction subprogram can be used for obtaining the de-embedded FET parameters. Since there are now fewer error terms involved in the de-embedding, a simplified version of the error correction

subprogram can be used instead.

When de-embedding is required for characterizing FET parameters, a subprogram named "*DE-EMB-S" is called. The error model parameters in array E and the uncorrected measured S-parameters in array C are substituted automatically by the fixture model parameters[35] and the corrected embedded parameters[36] loaded from the disc memory. Then, the "*10CORR-S" subprogram, a simplified version of the "*12CORR-S" subprogram, is called to obtain the explicit solutions of the de-embedded FET parameters. The result will be printed and is also stored in the CXYRESDAT datafile.

5.4 Experimental Results

The measurement accuracy in de-embedding the S-parameters of a device from the modelled HP 11608A test fixture can be estimated by comparing the measurement results with the calculated results of a known characteristic standard device. A through-connection insert of 0.8 cm electrical length was used as the standard device in this project and the measurement results are listed in Table 5.4. By comparing the calculated and measured forward transmission coefficients (S_{21}), the measurement accuracy was found to be within ±0.034 in magnitude and ±5° in phase over the 8 to 12 GHz range. The result verified that the

---

[35] Fixture model parameters for three discrete frequency bands were stored in three seperate datafiles FIXD1-2G, FIXD2-4G and FIXD8-12G.

[36] These parameters are stored in rectangular co-ordinates in the CXCORDAT datafile and are used specifically for de-embedding purposes.

Device: A through-connection insert of 0.8 cm electrical length								
Freq	S11		S21		S12		S22	
GHz	Mag	Ang	Mag	Ang	Mag	Ang	Mag	Ang
1.0	.025	53.0	1.007	-9.5	.999	-9.5	.032	47.1
1.1	.019	52.8	.999	-10.4	.998	-10.4	.026	36.3
1.2	.020	31.8	1.005	-11.0	1.008	-11.0	.018	34.0
1.3	.023	47.5	1.002	-11.4	1.002	-11.4	.018	49.7
1.4	.025	43.2	.990	-12.1	.992	-12.1	.019	92.8
1.5	.032	53.9	.981	-13.0	.987	-13.0	.032	107.0
1.6	.041	75.3	1.003	-14.1	.998	-14.1	.044	100.5
1.7	.044	74.0	1.002	-14.5	.997	-14.5	.046	102.5
1.8	.039	69.2	.990	-15.9	.993	-15.9	.039	96.3
1.9	.027	78.3	.999	-17.5	.995	-17.5	.023	60.3
2.0	.024	63.4	.997	-18.2	1.004	-18.2	.026	28.7
8.0	.206	127.9	.995	-79.4	1.026	-79.9	.170	-113.3
8.5	.183	119.7	1.020	-81.0	1.010	-82.7	.181	-114.7
9.0	.147	87.7	1.009	-89.9	.987	-90.1	.089	-86.7
9.5	.232	132.8	.974	-92.4	.979	-92.7	.238	-146.0
10.0	.096	39.4	.982	-99.2	.987	-99.5	.106	-17.6
10.5	.200	141.0	.966	-102.7	.972	-103.4	.225	171.6
11.0	.095	79.3	.996	-110.2	.985	-109.6	.025	-62.0
11.5	.173	137.6	.972	-114.1	.972	-114.4	.196	134.0
12.0	.232	126.3	.971	-119.9	.971	-119.3	.260	153.3

Table 5.4 The Measurement Results of a Through-Connection Insert After De-Embedding From an HP Test Fixture.

test fixture was correctly modelled and the de-embedding software was logically right. Furthermore, the measurement accuracy in FET parameter characterization can also be estimated by comparing the measured parameters of several commercial FETs with the typical parameters[3] given by the manufacturers. However, the actual S-parameters of individual FETs, though of the same type, may vary from one to another. Moreover, the slot for mounting the device in the HP test fixture is too wide and is not adjustable in size. As a result, the FET device is not mounted right at the edge of the microstrip lines. The resulting extra lengths of transmission line between the device package and the microstrip lines cause an excess phase shift in the measured S-parameters. Therefore, discrepancy between the typical and measured S-parameters is expected to be large and to vary from device to device.

Three commercial low-noise FET devices embedded in the HP 11608A test fixture were characterized using the developed ANA system and de-embedding software. The first device was a 2-6 GHz range small signal ultra-low noise GaAs FET, AT-8110. The measurement results together with the given typical parameters are listed in Table 5.5. The magnitudes of the measured parameters of the device under test were very close to the given parameters over the 1-4 GHz frequency range. The variation in magnitude of the forward transmisson coefficients (forward transmission gain)

---

[3] All the given parameters were characterized for a packaged device.

Device 1: AT-8110 (2-6 GHz Ultra-Low Noise GaAs FET)								
Bias Condition: V_d=3 V ; I_g= 20 mA ; V_g= -0.56 V								
Measurement results:								
Freq GHz	S11		S21		S12		S22	
	Mag	Ang	Mag	Ang	Mag	Ang	Mag	Ang
1.0	.855	-55.2	5.061	127.5	.059	67.9	.456	-22.5
1.5	.677	-85.2	4.418	106.4	.077	60.4	.353	-32.4
2.0	.618	-117.2	3.875	84.2	.092	48.8	.354	-57.6
2.6	.606	-147.7	3.104	59.2	.104	39.8	.099	49.5
3.0	.596	-159.0	3.156	55.7	.125	45.2	.103	-83.8
3.6	.728	-171.4	2.859	40.3	.149	43.1	.045	-46.9
4.0	.515	140.7	2.887	1.6	.170	31.7	.227	-172.7
Given Typical S-Parameters:								
1.0	.877	-56.1	5.07	134.7	.052	48.0	.464	-40.2
1.5	.834	-80.7	4.571	117.5	.069	36.3	.416	-56.7
2.0	.797	-102.6	4.062	100.6	.080	24.7	.376	-71.3
2.5	.774	-122.9	3.640	86.2	.087	14.5	.345	-85.8
3.0	.758	-140.2	3.247	71.9	.092	5.6	.327	-99.3
3.5	.737	-155.3	2.924	58.6	.095	-2.3	.307	-110.5
4.0	.727	-168.4	2.663	47.2	.095	-8.9	.290	-120.6

Table 5.5 The Measurement Results and the Given Typical S-parameters of an AT-8110 FET

was found to be within ±5 % which was reasonably good. The measurement results for the second device (NE-218) and the third device (MGF-1412) are listed in Table 5.6 and Table 5.7 respectively. The measured forward transmission gains of both test devices were found to be higher than the given typical values in the range of 1 to 4 GHz. Within the 1 to 4 GHz frequency range, the measurement results of all three devices appeared to be well-behaved and consistent with the given typical parameters.

For some FET devices, only one set of S-parameters at one test frequency was given by the manufacturer. A designer would find it very difficult to design a high quality LNA just based on the given S-parameters. With the success of this project, it is now possible to predict and characterize the behaviour of each FET device by its S-parameters over a wide frequency range. As a result, better efficiency can be achieved in designing a Low-Noise Amplifier with the help of the developed ANA system.

Device 2: NE-218 FET (Low-Noise GaAs MESFET)								
Bias Condition: V_d= 3 V ; I_g= 10 mA ; V_g=-0.83 V								
Measured S-parameters:								
Freq GHz	S11		S21		S12		S22	
	Mag	Ang	Mag	Ang	Mag	Ang	Mag	Ang
1.0	.926	-37.0	3.734	140.6	.042	70.4	.717	-17.5
1.5	.781	-58.2	3.530	122.7	.055	62.5	.635	-26.4
2.0	.678	-77.1	3.341	105.4	.068	57.2	.613	-38.2
3.0	.604	-122.6	3.102	74.2	.082	52.0	.417	-51.9
4.0	.432	-173.6	3.098	20.0	.114	52.3	.397	-95.8
Given Typical S-parameters:								
2.0	.908	-55	3.029	128	.069	56	.653	-36
4.0	.781	-99	2.372	88	.097	27	.608	-69

Table 5.6 The Measurement Results and the Given Typical S-Parameters of a NE-218 FET

Device 3: MGF-1412 (Low-Noise GaAs FET)								
Bias Condition : V_d= 3 V ; I_g= 10 mA ; V_g= -0.56 V								
Measurement Results:								
Freq GHz	S11		S21		S12		S22	
	Mag	Ang	Mag	Ang	Mag	Ang	Mag	Ang
1.0	.956	-30.3	3.807	146.3	.027	75.4	.708	-13.2
1.1	.936	-33.3	3.760	141.7	.030	73.0	.696	-14.1
1.2	.905	-35.8	3.836	137.9	.033	70.4	.673	-15.5
1.3	.883	-39.9	3.898	135.4	.035	70.4	.658	-17.1
1.4	.867	-44.6	3.773	133.2	.036	69.9	.639	-18.6
1.5	.846	-48.5	3.676	130.5	.036	70.6	.629	-20.0
1.6	.814	-54.0	3.628	127.5	.038	69.2	.630	-21.6
1.7	.792	-59.6	3.516	124.3	.040	68.9	.625	-23.8
1.8	.735	-64.6	3.323	120.5	.041	68.7	.630	-26.0
1.9	.659	-66.2	3.333	119.8	.042	69.2	.634	-27.8
2.0	.701	-59.9	3.542	117.6	.045	68.3	.623	-29.8
2.2	.770	-76.8	3.633	103.7	.048	60.2	.628	-28.0
2.4	.760	-84.7	3.629	100.6	.050	63.5	.569	-21.4
2.6	.709	-92.9	3.415	88.3	.050	58.1	.345	-23.2
2.8	.686	-95.8	3.012	96.8	.049	74.3	.403	-8.2
3.0	.670	-103.3	3.443	86.7	.057	71.4	.442	-36.1
3.2	.640	-110.8	3.379	78.4	.060	71.1	.497	-43.9
3.4	.648	-114.6	3.290	75.8	.063	75.9	.507	-40.2
3.6	.721	-114.7	3.301	73.6	.069	81.0	.458	-37.5
3.8	.620	-137.3	3.855	73.8	.080	81.2	.369	-45.5
4.0	.516	-144.6	3.580	36.2	.090	78.6	.393	-67.3
Given Typical S-Parameters:								
4.0	0.853	-59.4	2.469	92.3	.065	21.3	.710	-62.6

Table 5.7 The Measurement Results and the Given Typical S-Parameters of a MGF-1412 FET

6. SUMMARY AND CONCLUSIONS

6.1 Summary and Conclusions

The objectives of this project were to convert the conventional network analyser system into an Automatic Network Analyser (ANA) system and to develope de-embedding software for characterizing any microwave Field-Effect-Transistor by its S-parameters using the ANA system. The project involved design of a Microprocessor-Controlled Data Acquisition System (MCDAS), modification of the old but still useful network analyser system, and development of both the ANA system program and the de-embedding software. The objectives were achieved for a cost of $3,000 which was less than one twentieth of the capital investment needed for purchasing a complete commercial ANA system.

The fully automatic control of the measurement procedure developed in this project makes the procedure simpler, easier and ten times faster than the conventional point-by-point measurement technique. In the new measurement procedure, the test set is not required to be calibrated before the measurement. As a result, the procedure has been simplified and the additional error caused by imprecise setting and resetting of the Reference Plane Extension has been eliminated. In calibrating the 12-term error model of the ANA system, the sequence for selecting the S-parameter switches and the I.F. gain is set in the system program. The operator is prompted to connect the appropriate calibrator.

When the S-parameters of the device under test are measured, the computer automatically searches for the optimal I.F. gain over the entire frequency band for each parameter. Thus, once the device is connected to the test set, the four S-parameters are measured, corrected and printed automatically without requiring any further attention from the operator.

Using the developed ANA system, tasks which would take several days to perform using manual point-by-point technique can now be completed within one to two hours. A minimal amount of technical skill or knowledge is required to operate the system so that precise measurements are consistently achieved on a routine basis and the operator errors (such as incorrectly setting instrument controls and erroneously reading the output display) are greatly reduced.

The developed ANA system has become a very useful system in the research laboratory for designing advanced microwave circuits. Particularly, the system cann be used for characterizing low-noise microwave FETs by their S-parameters as a function of frequency and bias conditions. As a result, the behaviour of a low-noise FET device at microwave frequencies can be predicted and this is an important factor for the successful design of a low-noise amplifier (LNA).

Furthermore, the designed MCDAS is significant in its low-cost, versatility, flexibility and compatibility. It is

not restricted to S-parameter measurement alone, but can be used for performing other measurements by simply making appropriate changes in the programs and in the physical equipment arrangement.

6.2 Recommendations for Further Research

The measurement accuracy of the present ANA system will be further improved if a phase-lock subsystem and a rectangular display unit housed in an HP8418A auxillary display holder are added. The phase-lock subsystem basically consists of a synthesizer and a synchronizer which provide frequency accuracy and repeatability. Therefore, the Harmonic Skip Error will be completely eliminated. If a rectangular display unit is used for acquiring the magnitude of the measured data, the Quadrature Error caused by the test-to-reference leakage of the polar display will be eliminated too. Although the measurement accuracy of the ANA system can be improved by adding these instruments, the total cost is approximately $22,000 which is rather expensive.

The speed of the ANA system can be improved by making use of the INS8073 microprocessor on the K-8073 microcomputer board. During S-parameter measurements, the INS8073 microprocessor is idle. The HP-85 acts as the only controller of the Microprocessor-Controlled Data Acqusition System (MCDAS) for both data acqusition and error correction. If the INS8073 microprocessor is programmed in

assembly code and used for acquiring data, the speed of the ANA system will be improved significantly. However, this requires: the re-writing of the data acquisition subprogram in assembly code, expansion of the EPROM to store the program, development of additional software to transfer the measured data to the HP-85 for error corrections.

Further improvement in speed, accuracy and versatility of the present ANA system can be achieved by integrating more processor modules such as an Arithmetic Processor Unit (APU) or another K-8073 microcomputer board into the MCDAS. Each processor would then be assigned to a particular job. The APU would be assigned particularly to error correction or to performing all of the required mathematical calculations. The other K-8073 microcomputer would be used as a processor especially for data acquisition. As a result, the MCDAS would then become a multipurpose system with high accuracy and efficiency for controlling different measurement systems in the research laboratory.

REFERENCES

1. R.W.Anderson, *"S-Parameter Techniques for Faster, More Accurate Network Design"*, HP-Journal Vol.18, No.6, p13-22, Feb 1967.

2. F.Weinert, *"Scattering Parameters Speed Design of High Frequency Transistor Circuit"*, Electronic Vol.39, No.18, p78-88, September 1966.

3. G.Fredricks, *"How to use S-Parameters for Transistor Design"*, EEE Vol.14, No.12, p36-38,40, Dec 1966.

4. R.A. Hackborn, *"An Automatic Network Analyser System"*, Microwave J. Vol.2, p45-52, May 1968.

5. S.F.Adam, *"A New Precision Automatic Microwave Measurement System"*, IEEE Trans. IM-17, No.4, p308-313, Dec 1968.

6. V.G.Gelnovatch, *"A Computer Program For The Direct Calibration of Two Port Reflectometers For Automated Measurement"*, IEEE Trans. MTT-24, No.1, p45-47, Jan 1976.

7. V.G.Gelnovatch, " *A Non-iterative Computer Program For The Direct Calibration Of Non-ideal Two Port Reflectometers*", ECOM Fort Monmouth, N.J., Tech. Rep., 1975.

8. S.F.Adam, "*Automatic Microwave Network Measurements*", Proc.of the IEEE Vol.66, No.4, p384-391, April 1978.

9. R.W. Beatty, "*Methods for Automatically Measuring Network Parameters*", Microwave J. p45-48, April 1974.

10. F.L.Warner, "*Microwave Attenuation Measurement*", Peter Peregrinus Ltd., Chapter 11, Appendix 2, 1977.

11. "*Vanderbilt 8000 Series K-8073 Tiny Basic Microcomputer Hareware/Software User's Manual*", Transwave Corp., 1981.

12. William C Cummings, "*STD Bus: A Standard for the 80's*", Wescon/81, Session 27/1, p1-11, Sept 1981.

13. R.K Pandrangi, S.S. Stuchy, M. Barski, "*A Digital System for Measurement of Resonant Frequency and Q Factor*", IEEE Trans. IM-31, No.8, p18-21, March 1982.

14. C. Akyel, R.G. Bosisio, *"Wide-Range Dynamic Complex Dielectric Constant Measurements Using Microprocessor Control Techiques"*, IEEE Trans. IM-28, No.4, p272-278, Dec 1979.

15. H. Ikedar, S. Ohkawa, H. Yamamoto, *"Microprocessor-Controlled Time-Sharing Services Terminal With Interfaces For Instruments And Its Application to Precision Measurement of High VSWR"*, IEEE Trans. IM-28, No.4, p306-311, Dec 1979.

16. *"Sweep Oscillator 8620A"*, HP Operating and Service Manual May, 1971.

17. *"Network Analyser 8410A & Harmonic Frequency Converter 8411A"*, HP Operating and Service Manual p3-97,3-106, Dec 1971.

18. *"Polar Display 8414A"*, HP Operating and Service Manual p8-18,8-22,8-23, Jan 1970.

19. J.G.Evans, *"Measuring Frequency Characteristics of Linear Two-Port Networks Automatically"*, Bell System Technical Journal Vol.48, p1313-1338, May-June 1969.

20. B.P.Hand, *"Developing Accuracy Specifications For Automatic Network Analyser Systems"*, HP-Journal Vol.21, p16-19, Feb 1970.

21. W.Kruppa, K.F.Sodomsky, *"An Explicit Solution For The Scattering Parameters Of A Linear Two-port Measured With An Imperfect Test-Set"*, IEEE Trans. MTT-19, p122-123, Jan 1971.

22. S.Rehnmark, *"On The Calibration Process Of Automatic Network Analyser Systems"*, IEEE Trans. MTT-22, p457-458, April 1974.

23. D.Silver,M.McPhun, *"Calibration Of Microwave Network Analyser For Computer-corrected S-Parameter Measurements"*, Electronics Lett. Vol.9, No.6, p126-128, March 1973.

24. G.R.Cobb, *"New Software For Low Loss Two Port Measurements"*, Microwave Journal Vol.24, No.4, p63-68, April 1981.

25. *"Semi-Automatic Measurement Using The 8410B Microwave Network Analyser And The 9825A Desk-Top Computer"*, HP Application Note 221

26. *"Automating The HP-8410B Microwave Network Analyser"*, HP Application Note 221A, June 1980.

27. I.Kasa, *"Closed-form Mathematical Solutions To Some Network Analyser Calibration Equations"*, IEEE Trans. IM-23, No.4, p399-402, Dec 1974.

28. Dough Rytting, *"An Analysis of Vector Measurement Accuracy Enhancement Techniques"*, Hewlett Packard, p8, appendix 7

29. C.Ambrose & C.S.Aitchinson, *"The Fringing Capacitance of Reference Open Circuit Used in Network"*, Conf Proc Eur Microwave, Conf 10th, p273-277, 1980.

30. *"Microwave Network Analyser Applications"*, Hewlett Packard Application Note 117-1, June 1970.

31. I.Kasa, *"A Circle Fitting Procedure and its Error Analysis"*, IEEE IM p8-14, March 1976.

32. S.O.Ajose,N.A.Mathews ,C.S.Aitchison, *"Characterization Of Coaxial To Microstrip Connector Suitable For Evaluation Of Microstrip Two-port"*, Electronics Lett. Vol.12, p430-431, Aug 1976.

33. Cooper & Gupta, *"Microwave Characterisation of GaAs MESFET and the Verification of Device Model"*, IEEE Journal of Solid-State Circuit, p325-329, June, 1977.

34. R.Q.Lane,R.D.Pollard,M.A.Maury,J.K.Fitzpatrick, *"Broadband Fixture Characterizes Any Packaged Microwave Transistor"*, Microwave J., p95-109, Oct 1982.

35. R.Vaitkus & D.Scheitlin, *"A Two-Tier De-embedding Technique For Packaged Transistors"*, IEEE MTT-S Digest p328-330, 1982.

36. S.Wight,P.Jain,J.Chudobiak,V.Makios, *"Equivalent Circuits of Microstrip Impedance Discontinuities and Launchers"*, IEEE MTT p48-52, Jan 1974.

37. *"Transistor Fixture 11608A"*, Hewlett Packard Operating Note, March 1971.

38. S.O.Ajose, *"Modelling Technique For An FET Chip"*, Electronics Lett. Vol.13, No.17, p511-512, Aug 1977.

39. *"Compact User's Manual"*, Computing Service R127.0279, University of Alberta, Feb 1979.

40. J.L.Altman, *"Microwave Circuits"*, D. Van Nostrand Company, Ltd. 1964.

APPENDIX I-A The Schematic Diagram of the Digital Attenuator

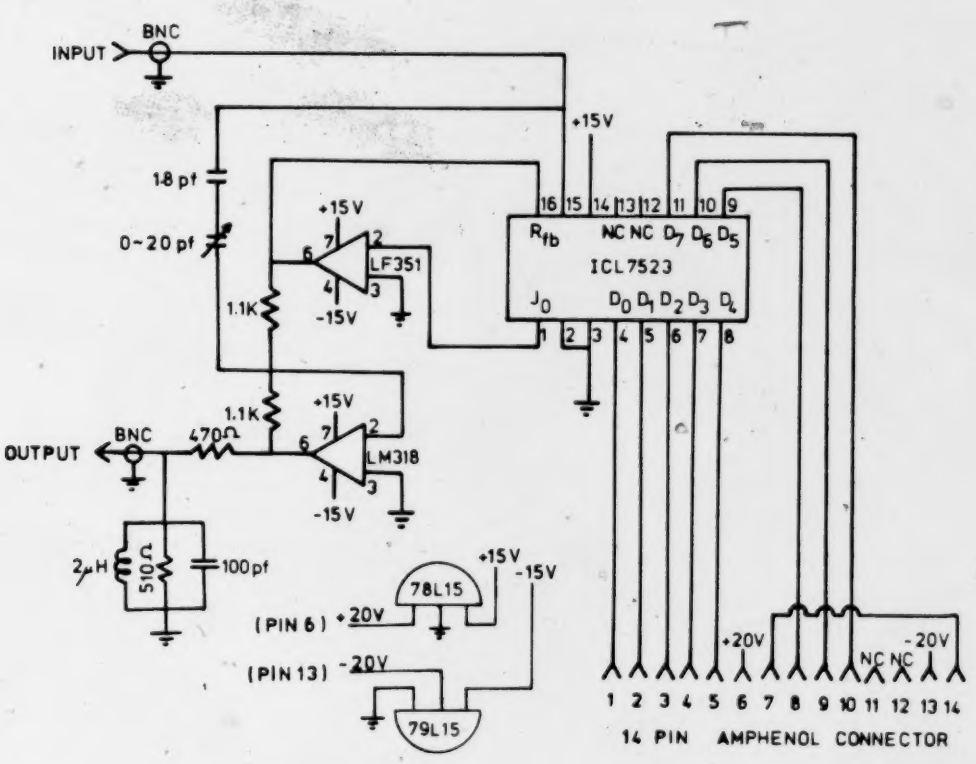

APPENDIX I-B The Modifications of the Connection Inside the Mainframe of the Netwrok Analyser

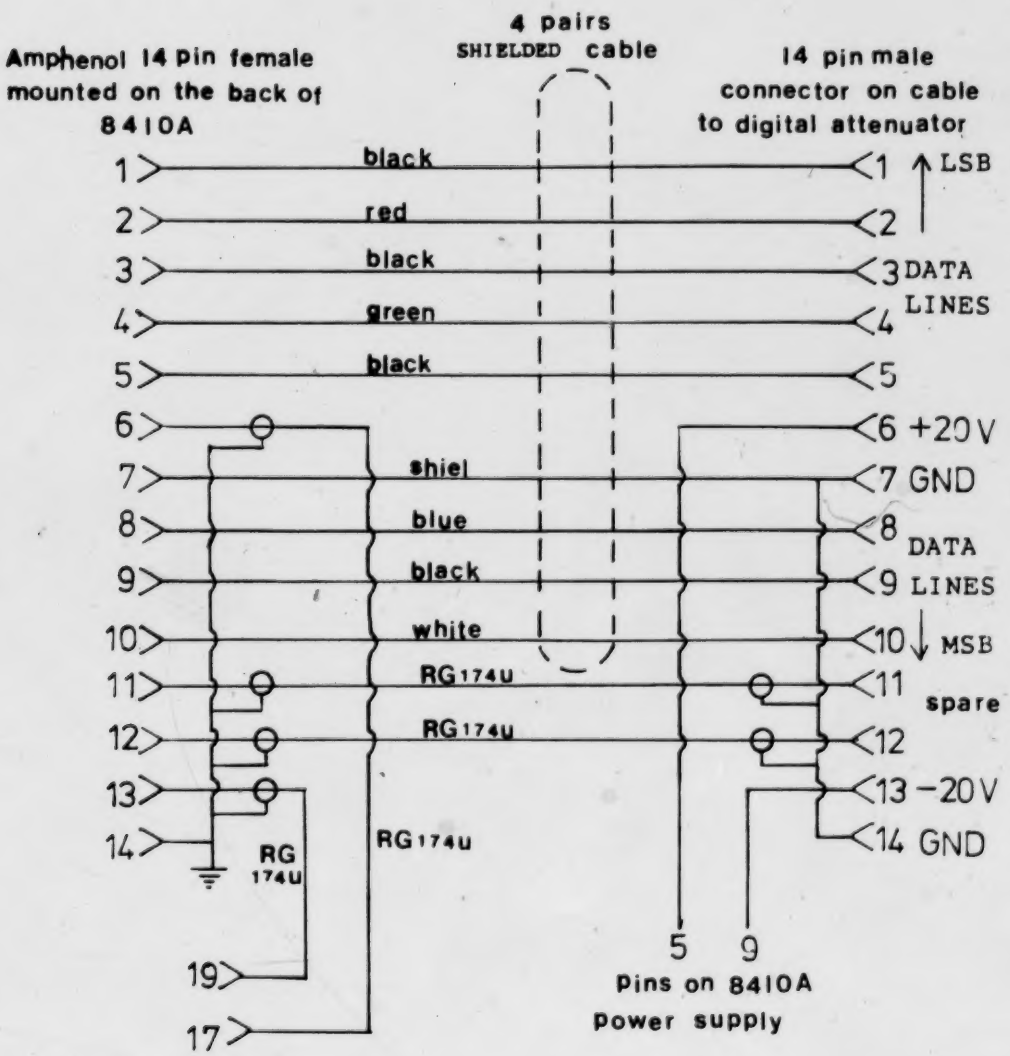

APPENDIX II S-parameter Measurement Instruction Manual

EQUIPMENT:

a. Source Locking Microwave Counter EIP575

b. Sweep Oscillator HP8620A

RF Section HP8621A (0.2-4 GHz)

RF Section HP8621B (5.9-9 GHz,8-12 GHz)

c. Test Set HP8746B (0.5-12.4 GHz)

d. Network Analyser HP8410A

e. Polar Display HP8414A

f. Microprocessor-Controlled Data Acquisition System (MCDAS)

g. HP-85 Desktop Computer

h. Disc Drive HP82901M, Printer HP82905B, Plotter HP7470A

Note : The diagram of the interconnection of all the instruments is shown in Figure A2.1 at the last page of the manual.

PROCEDURE:

41. **Power on :** Disc Drive, Printer, Plotter
HP-85 Desktop Computer
MCDAS
EIP575 Counter
HP8476B Test Set
HP8410A Network Analyser

42. **Insert disc "ANASYST" & "ANADATAFILE" into the disc drive "0" & "1" respectively.**

43. **Load the system program "*ANA-M" from the disc into the HP-85 computer.**
LOAD "*ANA-M" * PRESS RUN *

*** Follow the instructions on the CRT of the HP-85 computer ***

Attention:

If the gain of the test device is greater than 6 dB, the "Manual" mode for setting the I.F.gain has to be selected. (see procedure 7)

44. **Set sweeper mode:**
CAUTION: **Turn off the sweeper power first whenever you change the position of the switches at the rear panel, otherwise the fuse on the circuit**

board A4 or A5 may blow.

At rear panel of the modified sweeper 8620A

a. Switch AM Mod to "off" position

b. Set the "FM-AM" switch at the top of the rear panel to "FM" position.

At front panel

a. Set MODE to "EXT"

b. Set the desired frequency band by front panel control (start and stop button)

At RF section

a. For 1-2 GHz set ALC selection to INT

b. For 2-4 GHz set ALC selection to MTR

c. For 5.9-9 GHz set ALC selection to MTR

d. For 8-12 GHz set ALC to MTR

* NOW TURN THE SWEEPER POWER ON *

45. Set Network Analyser (8410A)

At rear panel of the modified Network Analyser 8410A

a. Set the switch to either the "REMOTE" or "MANUAL" position corresponding to remote or manual control of the I.F.Gain.

At the front panel

a. Set the range of the automatic tuning to the selected frequency range.

b. Adjust sweep stability so that the pointer of the REF CHANNEL LEVEL meter on the front panel stays

in the OPERATE region over the selected frequency band. However, in most cases, the best sweep stability can be achieved when the knob is turned fully anticlockwise.

46. **For best accuracy, let equipment warm up for two hours.**

47. **Calibration for S-parameter measurement:**

Remark: If "MANUAL" mode is selected,you need to set the I.F. gain manually according to the following table.

This is the table of the I.F. gain setting for the 12-term error model calibration.

S-PARAMETER	CALIBRATOR	I.F.GAIN (dB)	FREQUENCY (GHz)
S11,S21	matched load	60/54	1-8 / 8-12
S11,S21	sliding matched	54	1-12
S11	short	24	1-12
S11	open	24	1-12
S22,S12	matched load	54	1-12
S22,S12	sliding matched	54	1-12
S22	short	24	1-12
S22	open	24	1-12
S21,S12	through-line	24	1-12
S11,S22	thrpugh-line	48	1-12

* Follow the instructions on the CRT of the HP-85 computer *

48. Verification of the calibration data.

A standard device is first measured and the results are compared with the reference data listed at the back of this manual. The standard devices for one-port and two-port measurement are a direct short and a through-line connector respectively.

49. Measurement results:

Once the measurement of the first device is done, the error vector data is then stored in the files named "CXERRDAT" where X varies from 1 to 5. The results of the corrected S-parameters of each device is stored in files named "CXYRESDAT" where Y varies from 1 to 10. They are all named under the same set of calibration data and stored one after the other in ascending order of Y. When the value of Y reaches 10, it will reset to 1 automatically. The previous data will be overwritten.

50. When you finish the measurement, remove the disc from the disc drive and power off all instruments.

**********END**********

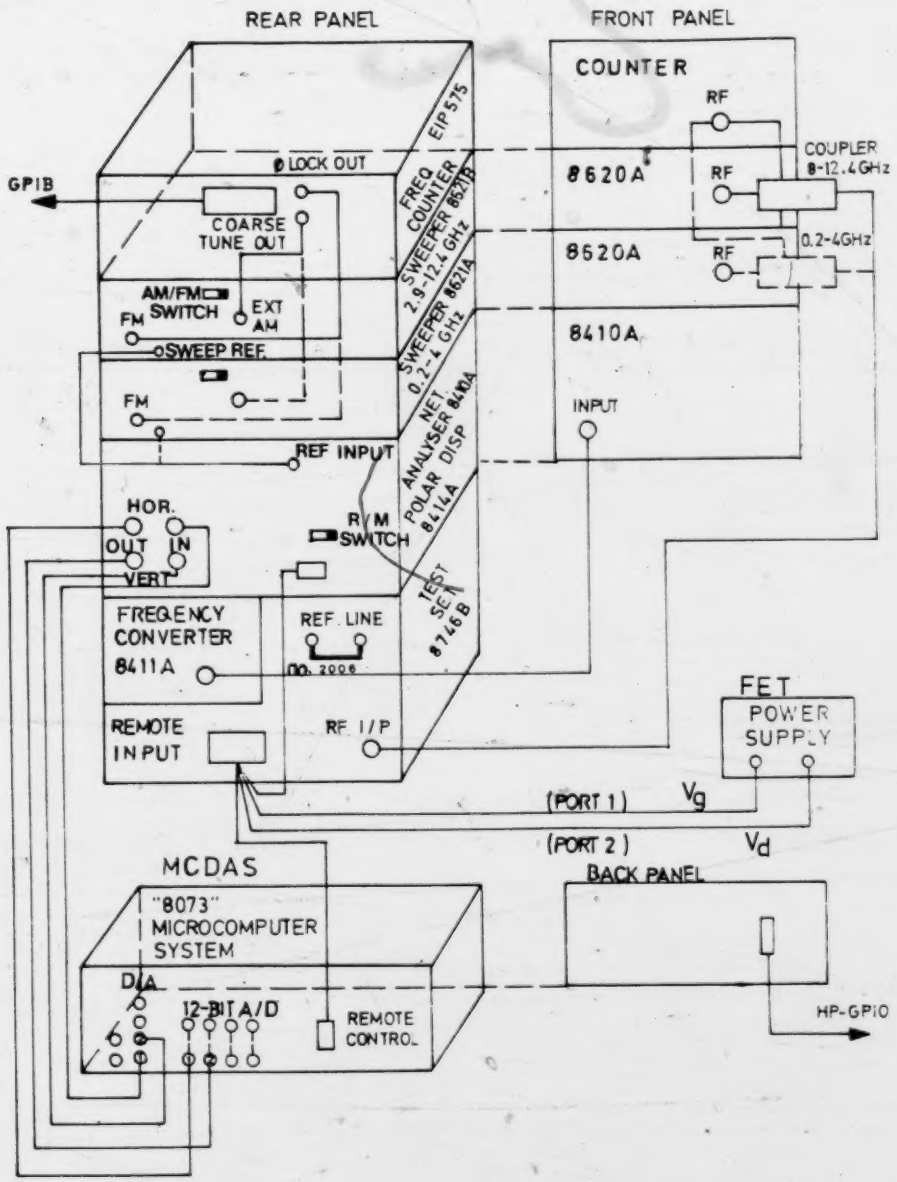

Figure A2-1 The Diagram of the Interconnections of all the instrument of the ANA System.

Reference Results for Verifying the calibration Data

Device : A direct short circuit						
Freq	S11		S11		Norm Imp	
	Mag	Ang	Real	Imag.	Real	Imag.
1.00	1.000	-179.92	-1.000	-.0014	.000	-.0007
1.10	1.011	-179.87	-1.011	-.0024	-.005	-.0012
1.20	1.001	-179.93	-1.001	-.0012	-.001	-.0006
1.30	1.001	-179.92	-1.001	-.0014	-.000	-.0007
1.40	1.000	-179.92	-1.000	-.0014	.000	-.0007
1.50	1.007	-179.58	-1.007	-.0075	-.004	-.0037
1.60	0.999	-179.88	-0.999	-.0020	.000	-.0010
1.70	1.001	-179.94	-1.001	-.0010	-.001	-.0005
1.80	1.001	-179.92	-1.000	-.0015	-.000	-.0007
1.90	1.000	-179.91	-1.000	-.0016	-.000	-.0008
2.00	1.001	-179.93	-1.001	-.0013	-.000	-.0006
8.00	0.997	-179.97	-0.997	-.0005	.002	-.0002
8.50	1.000	179.97	-1.000	.0005	.000	.0002
9.00	0.997	-179.89	-0.997	-.0018	.001	-.0009
9.50	1.002	179.94	-1.002	.0011	.001	.0005
10.0	0.998	-179.96	-0.998	-.0007	.001	-.0003
10.5	1.001	179.97	-1.001	.0006	.000	.0003
11.0	0.999	-179.95	-0.999	-.0008	.001	-.0004
11.5	1.001	-179.99	-1.001	-.0002	-.000	-.0001
12.0	0.999	-179.90	-0.999	-.0018	.000	-.0009

Device : A Thru-line (length = 56.44 cm)								
Freq	S11		S21		S12		S22	
	Mag	Ang	Mag	Ang	Mag	Ang	Mag	Ang
1.00	.006	34.03	.989	42.17	.991	42.10	.005	7.77
1.10	.014	-109.02	.996	-25.59	.987	-25.65	.013	-95.99
1.20	.022	155.20	.987	-93.54	.978	-93.21	.021	-179.33
1.30	.019	68.77	.992	-161.35	.994	-161.49	.021	105.76
1.40	.006	23.38	.994	131.67	.997	131.56	.013	33.76
1.50	.011	69.25	.986	63.34	.993	63.55	.006	-5.38
1.60	.013	-18.82	.990	-3.76	.986	-3.99	.007	-20.44
1.70	.004	-158.01	.996	-70.04	.995	-69.93	.010	-84.16
1.80	.014	33.22	.974	-138.40	.989	-138.85	.011	-138.52
1.90	.020	-85.57	.979	153.15	.987	152.99	.014	156.55
2.00	.024	152.11	.978	84.41	.977	84.34	.015	88.25
8.00	.045	178.60	.978	-20.15	.969	-20.14	.013	118.28
8.50	.023	-105.78	.962	2.60	.964	3.07	.017	140.50
9.00	.029	53.55	.969	22.45	.973	22.74	.051	154.08
9.50	.074	108.19	.966	45.45	.968	45.37	.072	153.16
10.0	.056	137.01	.968	65.23	.971	64.91	.028	161.10
10.5	.020	125.39	.956	88.00	.956	87.91	.033	-141.53
11.0	.019	-48.62	.962	108.52	.961	108.22	.022	155.17
11.5	.051	24.40	.952	131.21	.959	131.20	.012	-164.07
12.0	.130	49.59	.973	152.08	.973	151.47	.028	99.14

APPENDIX III Explicit Solution for 12-Term Error Model

The incident and the reflected wave modes are labelled with a_1-a_4 and b_1-b_4 respectively. In forward direction, a unit driving signal is introduced at port 1.

FORWARD DIRECTION

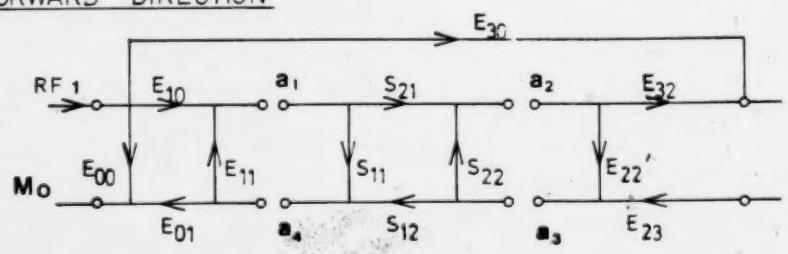

$$a_4 = S_{11}a_1 + S_{12}a_3 \quad \text{(A3.1)}$$

$$a_2 = S_{21}a_1 + S_{22}a_3 \quad \text{(A3.2)}$$

$$a_1 = E_{10} + E_{11}a_4 \quad \text{(A3.3)}$$

$$a_3 = E_{22}' a_2 \quad \text{(A3.4)}$$

$$S_{11m} = E_{00} + E_{01}a_4 \quad \text{(A3.5)}$$

$$S_{21m} = E_{32}a_2 + E_{30} \quad \text{(A3.6)}$$

Solving for the values of the a's from equations (A3.5)&(A3.6)

$$a_4 = \frac{(S_{11m}-E_{00})}{E_{01}} \quad \text{(A3.7)}$$

$$a_2 = \frac{(S_{21m}-E_{30})}{E_{32}} \quad \text{(A3.8)}$$

Substituting (A3.7) & (A3.8) into (A3.3) & (A3.4) respectively, we obtain

$$a_1 = E_{10} + \frac{E_{11}(S_{11m}-E_{00})}{E_{01}} \qquad \text{(A3.9)}$$

$$a_3 = \frac{E_{22}'\,(S_{21m}-E_{30})}{E_{32}} \qquad \text{(A3.10)}$$

In the reverse direction, a unit driving signal is introduced at port 2.

REVERSE DIRECTION

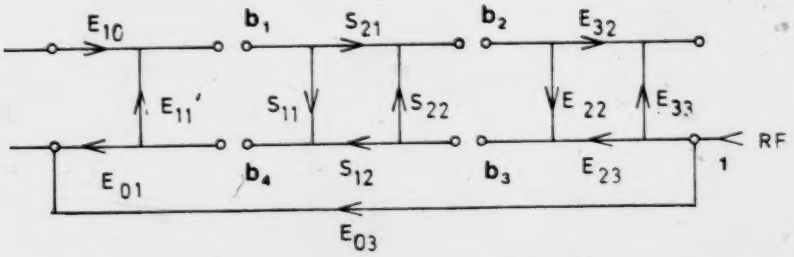

$$b_4 = S_{12}b_3 + S_{11}b_1 \qquad \text{(A3.11)}$$

$$b_2 = S_{22}b_3 + S_{21}b_1 \qquad \text{(A3.12)}$$

$$b_3 = E_{23} + E_{22}b_2 \qquad \text{(A3.13)}$$

$$b_1 = E_{11}'\,b_4 \qquad \text{(A3.14)}$$

$$S_{22m} = E_{33} + E_{32}b_2 \qquad \text{(A3.15)}$$

$$S_{12m} = E_{01}b_4 + E_{03} \qquad \text{(A3.16)}$$

Solving for the values of the b's from equations (A3.5) & (A3.6)

$$b_4 = \frac{(S_{12m}-E_{03})}{E_{01}} \qquad (A3.17)$$

$$b_2 = \frac{(S_{22m}-E_{33})}{E_{32}} \qquad (A3.18)$$

Substituting (A3.17) & (A3.18) into (A3.13) &(A3.14) respectively,we obtain

$$b_1 = \frac{E_{11}' (S_{12m}-E_{03})}{E_{01}} \qquad (A3.19)$$

$$b_3 = E_{23} + \frac{E_{22}(S_{22m}-E_{33})}{E_{32}} \qquad (A3.20)$$

Evaluate for S_{11}:

From equation (A3.1)

$$S_{12} = \frac{a_4-S_{11}a_1}{a_3} \qquad (A3.21)$$

If we substitute (A3.21) into (A3.11), we get

$$b_4 = \frac{(a_4-S_{11}a_1)b_3}{a_3} + S_{11}b_1 \qquad (A3.22)$$

Therefore , rearranging (A3.22),we get

$$S_{11} = \frac{a_4 b_3 - a_3 b_4}{a_1 b_3 - a_3 b_1} \qquad \text{(A3.23)}$$

Now substituting the values of the a's & b's from equations (A3.7)-(A3.10) & (A3.17-(A3.20) into equation (A3.23), we get

$$S_{11} = \frac{\left(\frac{S_{11m} - E_{00}}{E_{10}\,E_{01}}\right)\left[1 + \frac{E_{22}\left(\frac{S_{22m} - E_{33}}{E_{32}\,E_{23}}\right)}{}\right] - \frac{E_{22}'\left(\frac{S_{21m} - E_{30}}{E_{32}\,E_{10}}\right)\left(\frac{S_{12m} - E_{03}}{E_{01}\,E_{23}}\right)}{}}{\left[1 + \frac{E_{11}\left(\frac{S_{11m} - E_{00}}{E_{10}\,E_{01}}\right)}{}\right]\left[1 + \frac{E_{22}\left(\frac{S_{22m} - E_{33}}{E_{32}\,E_{23}}\right)}{}\right] - E_{11}'\,E_{22}'\left(\frac{S_{21m} - E_{30}}{E_{32}\,E_{10}}\right)\left(\frac{S_{12m} - E_{03}}{E_{01}\,E_{23}}\right)} \qquad \text{(A3.24)}$$

Similarly, evaluating S_{22} from equations (A3.12) & (A3.2), we get

$$S_{22} = \frac{a_1 b_2 - a_2 b_1}{a_1 b_3 - a_3 b_1} \qquad \text{(A3.25)}$$

Substituting the values of the a's & b's into equation (A3.24) we get

$$S_{22} = \frac{\left(\frac{S_{22m} - E_{33}}{E_{32}\,E_{23}}\right)\left[1 + \frac{E_{11}\left(\frac{S_{11m} - E_{00}}{E_{10}\,E_{01}}\right)}{}\right] - \frac{E_{11}'\left(\frac{S_{21m} - E_{30}}{E_{32}\,E_{10}}\right)\left(\frac{S_{12m} - E_{03}}{E_{01}\,E_{23}}\right)}{}}{\left[1 + \frac{E_{11}\left(\frac{S_{11m} - E_{00}}{E_{10}\,E_{01}}\right)}{}\right]\left[1 + \frac{E_{22}\left(\frac{S_{22m} - E_{33}}{E_{32}\,E_{23}}\right)}{}\right] - E_{11}'\,E_{22}'\left(\frac{S_{21m} - E_{30}}{E_{32}\,E_{10}}\right)\left(\frac{S_{12m} - E_{03}}{E_{01}\,E_{23}}\right)} \qquad \text{(A3.26)}$$

Then evaluate this for S_{21}

From equation (A3.12)

$$S_{22} = \frac{b_2 - S_{21} b_1}{b_3} \qquad \text{(A3.27)}$$

Substituting into equation (A3.2)

$$S_{21} = \frac{a_2 b_3 - a_3 b_2}{a_1 b_3 - a_3 b_1} \qquad \text{(A3.28)}$$

By substituting the values of the a's & b's into (A3.26), we get

$$S_{21} = \frac{\left[1 + \frac{(S_{22m} - E_{33})(E_{22} - E_{22}')}{E_{32}\,E_{23}}\right]\left[\frac{S_{21m} - E_{30}}{E_{32}\,E_{10}}\right]}{\left[1 + \frac{E_{11}(S_{11m} - E_{00})}{E_{10}\,E_{01}}\right]\left[1 + \frac{E_{22}(S_{22m} - E_{33})}{E_{32}\,E_{23}}\right] - \frac{E_{11}'E_{22}'(S_{21m} - E_{30})(S_{12m} - E_{03})}{E_{32}\,E_{10}\;E_{01}\,E_{23}}} \qquad \text{(A3.29)}$$

Similarly,

$$S_{12} = \frac{\left[1 + \frac{(S_{11m} - E_{00})(E_{11} - E_{11}')}{E_{10}\,E_{01}}\right]\left[\frac{S_{12m} - E_{03}}{E_{01}\,E_{23}}\right]}{\left[1 + \frac{E_{11}(S_{11m} - E_{00})}{E_{10}\,E_{01}}\right]\left[1 + \frac{E_{22}(S_{22m} - E_{33})}{E_{32}\,E_{23}}\right] - \frac{E_{11}'E_{22}'(S_{21m} - E_{30})(S_{12m} - E_{03})}{E_{32}\,E_{10}\;E_{01}\,E_{23}}} \qquad \text{(A3.30)}$$

APPENDIX IV The Flow Chart of the Developed ANA System Program for S-parameter Measurement

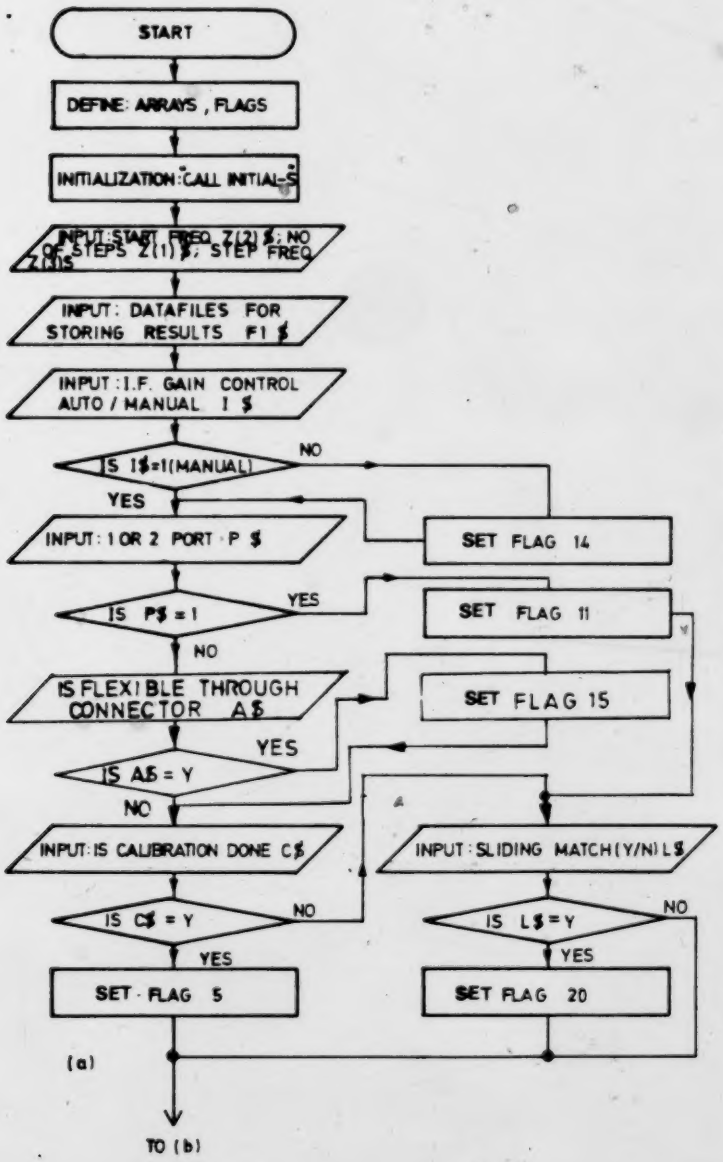

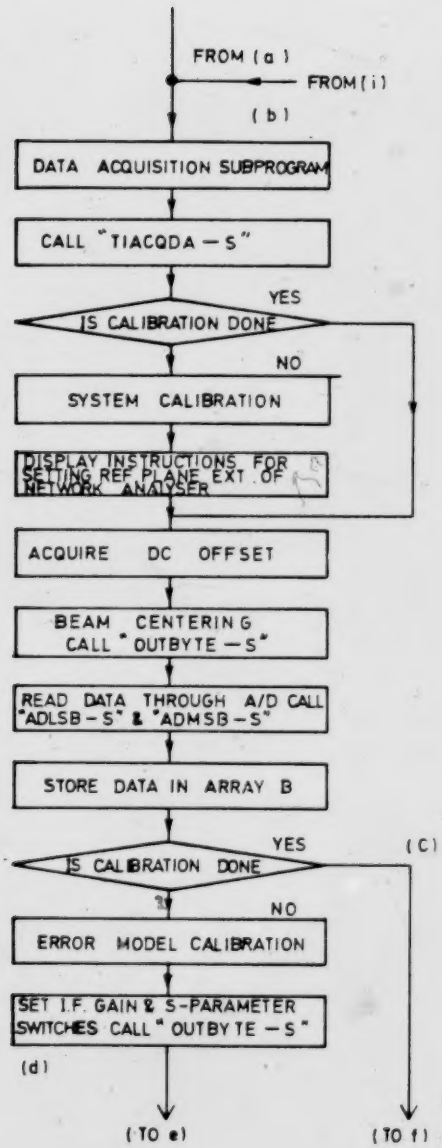
FROM (a)
FROM (i)
(b)
DATA ACQUISITION SUBPROGRAM
CALL "TIACQDA – S"
IS CALIBRATION DONE
YES
NO
SYSTEM CALIBRATION
DISPLAY INSTRUCTIONS FOR SETTING REF PLANE EXT. OF NETWORK ANALYSER
ACQUIRE DC OFFSET
BEAM CENTERING CALL "OUTBYTE – S"
READ DATA THROUGH A/D CALL "ADLSB – S" & "ADMSB – S"
STORE DATA IN ARRAY B
IS CALIBRATION DONE
YES
(C)
NO
ERROR MODEL CALIBRATION
SET I.F. GAIN & S-PARAMETER SWITCHES CALL "OUTBYTE – S"
(d)
(TO e)
(TO f)

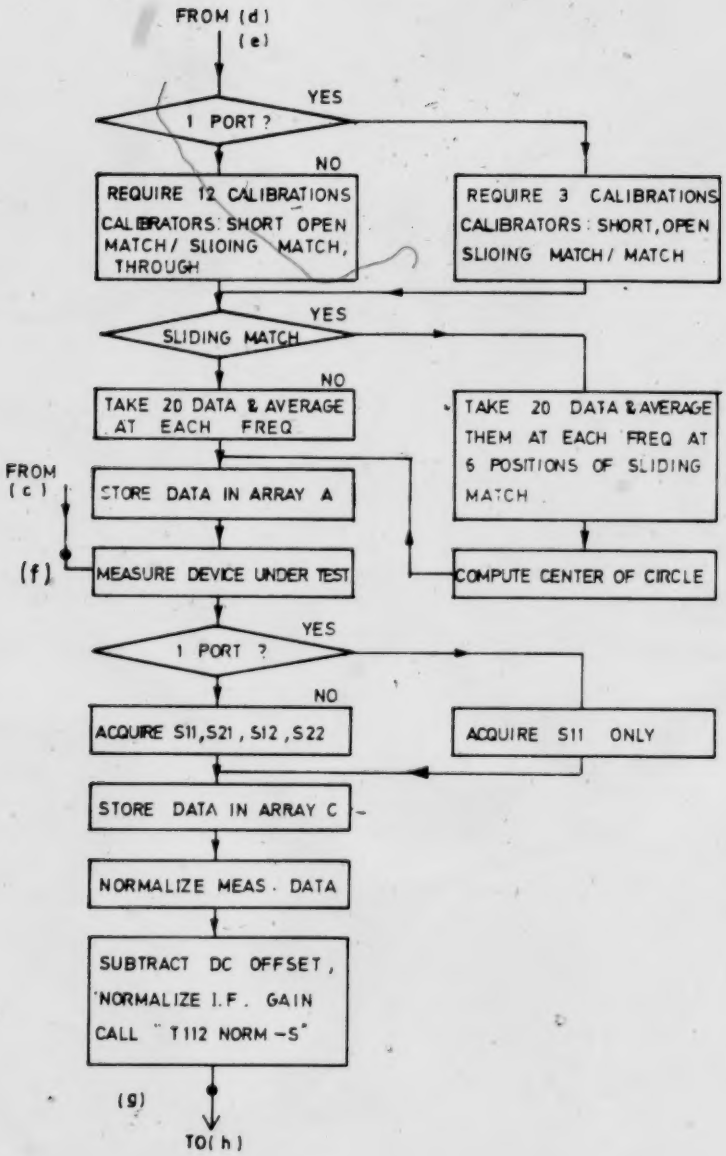
FROM (d)
(e)
1 PORT ?
YES
NO
REQUIRE 12 CALIBRATIONS
CALIBRATORS: SHORT OPEN
MATCH/ SLIOING MATCH,
THROUGH
REQUIRE 3 CALIBRATIONS
CALIBRATORS: SHORT, OPEN
SLIOING MATCH/ MATCH
SLIDING MATCH
YES
NO
TAKE 20 DATA & AVERAGE
AT EACH FREQ
TAKE 20 DATA & AVERAGE
THEM AT EACH FREQ AT
6 POSITIONS OF SLIDING
MATCH
FROM
(c)
STORE DATA IN ARRAY A
(f)
MEASURE DEVICE UNDER TEST
COMPUTE CENTER OF CIRCLE
1 PORT ?
YES
NO
ACQUIRE S11,S21, S12, S22
ACQUIRE S11 ONLY
STORE DATA IN ARRAY C
NORMALIZE MEAS. DATA
SUBTRACT DC OFFSET,
NORMALIZE I.F. GAIN
CALL "T112 NORM-S"
(g)
TO(h)

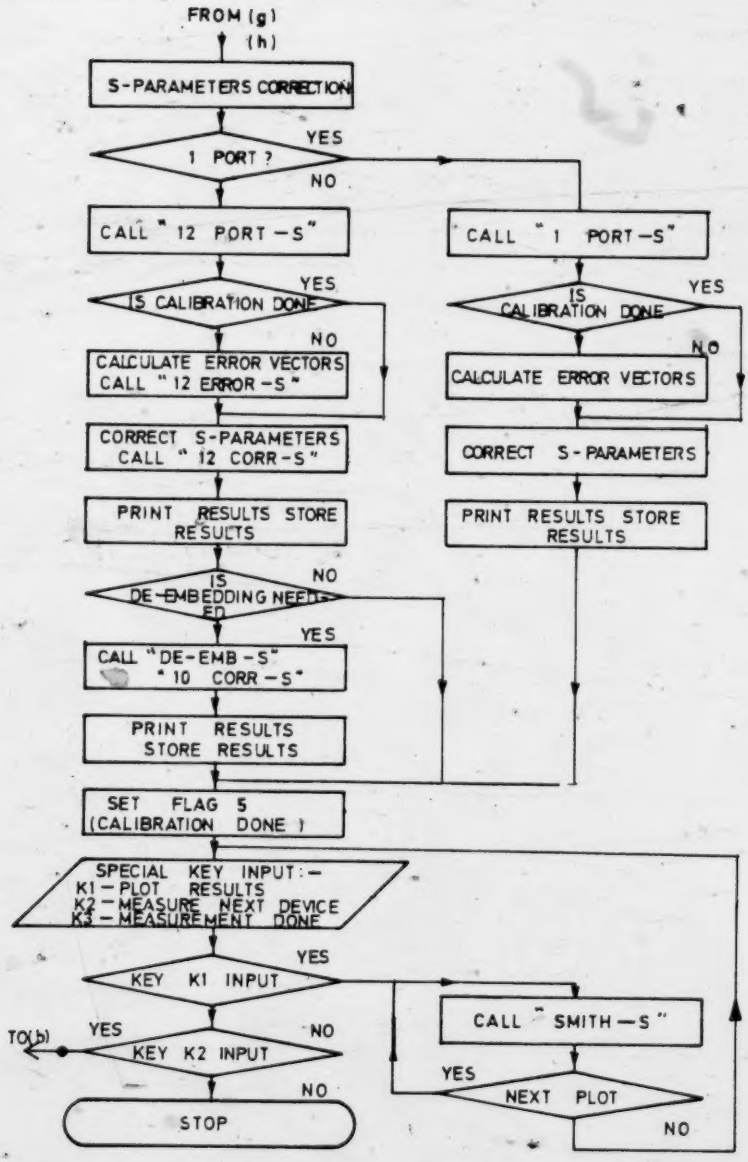
FROM (g)
(h)
S-PARAMETERS CORRECTION
1 PORT ?
YES
NO
CALL " 12 PORT-S"
CALL " 1 PORT-S"
IS CALIBRATION DONE
YES
NO
CALCULATE ERROR VECTORS
CALL " 12 ERROR-S "
CORRECT S-PARAMETERS
CALL " 12 CORR-S"
PRINT RESULTS STORE RESULTS
IS DE-EMBEDDING NEEDED
CALL "DE-EMB-S"
" 10 CORR-S"
SET FLAG 5
(CALIBRATION DONE)
SPECIAL KEY INPUT:-
K1 - PLOT RESULTS
K2 - MEASURE NEXT DEVICE
K3 - MEASUREMENT DONE
KEY K1 INPUT
KEY K2 INPUT
TO(b)
STOP
CALL " SMITH-S "
NEXT PLOT

APPENDIX V An Efficient Circle Fitting Method

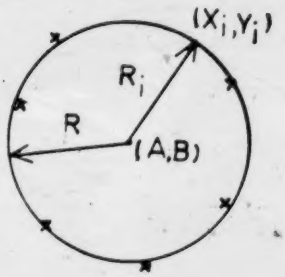

A modified least square error criterion for circle fitting is used by Kasa [31]. The criterion is

$$\sum_{i=1}^{N} (R_i^2 - R^2)^2 = \text{minimum} \qquad \text{(A-1)}$$

Where $R_i = \sqrt{(x_i - A)^2 + (y_i - B)^2}$

$C = R^2 - A^2 - B^2$

N = number of data points

This criterion is attractive because it is easy to handle analytically. As a result, a matrix equation (A-2) is obtained.

$$PQ = M \qquad \text{(A-2)}$$

Where
$$P = \begin{pmatrix} 2\Sigma x_i & 2\Sigma y_i & N \\ 2\Sigma x_i^2 & 2\Sigma x_i y_i & \Sigma x_i \\ 2\Sigma x_i y_i & 2\Sigma y_i^2 & \Sigma y_i \end{pmatrix}$$

$$M = \begin{pmatrix} \Sigma(x_i^2 + y_i^2) \\ \Sigma(x_i^3 + x_i y_i^2) \\ \Sigma(x_i^2 y_i + y_i^3) \end{pmatrix}$$

$$Q = \begin{pmatrix} A \\ B \\ C \end{pmatrix}$$

$$\therefore \quad Q = P^{-1} M \qquad \text{(A-3)}$$

Hence the center of the circle can be found.